Резонансная нанофотоника

Илья
Фрадкин

Наталия
Салахова

Сергей
Дьяков

Николай
Гиппиус

Skoltech
Skolkovo Institute of Science and Technology

ЛЕТНЯЯ ШКОЛА ФОНДА «БАЗИС»
СОВРЕМЕННЫЕ ПРОБЛЕМЫ ФИЗИКИ КОНДЕНСИРОВАННОГО СОСТОЯНИЯ
21 ИЮЛЯ — 1 АВГУСТА 2024

Группа Теоретической Нанофотоники
Центр Инженерной Физики

РНФ
Российский научный фонд

22-12-00351

План лекций

1. Резонансная нанофотоника
2. Резонансы в фотонно-кристаллических слоях: фундаментальные основы и применения
3. Гибридные резонансы в решетках плазмонных наночастиц

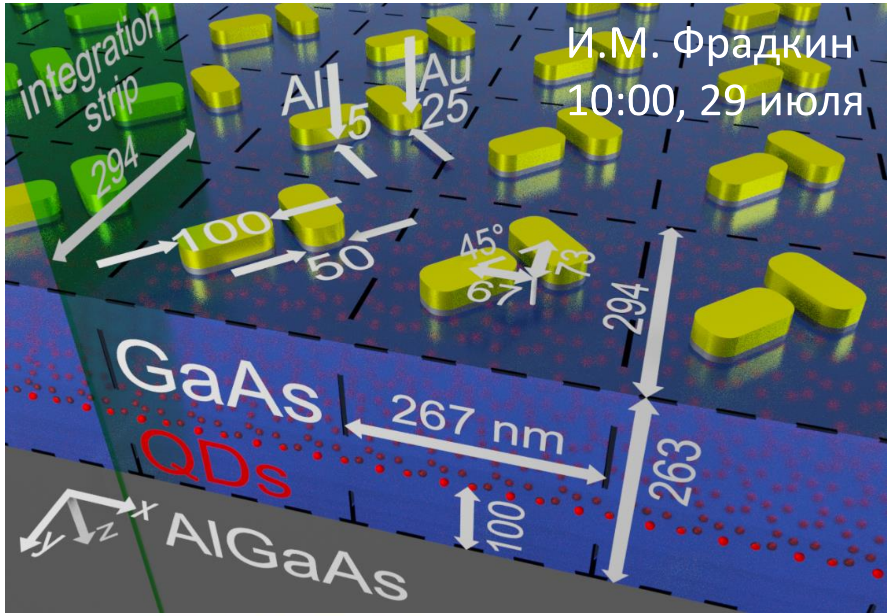

Н.А. Гиппиус, 10:00, 23 июля

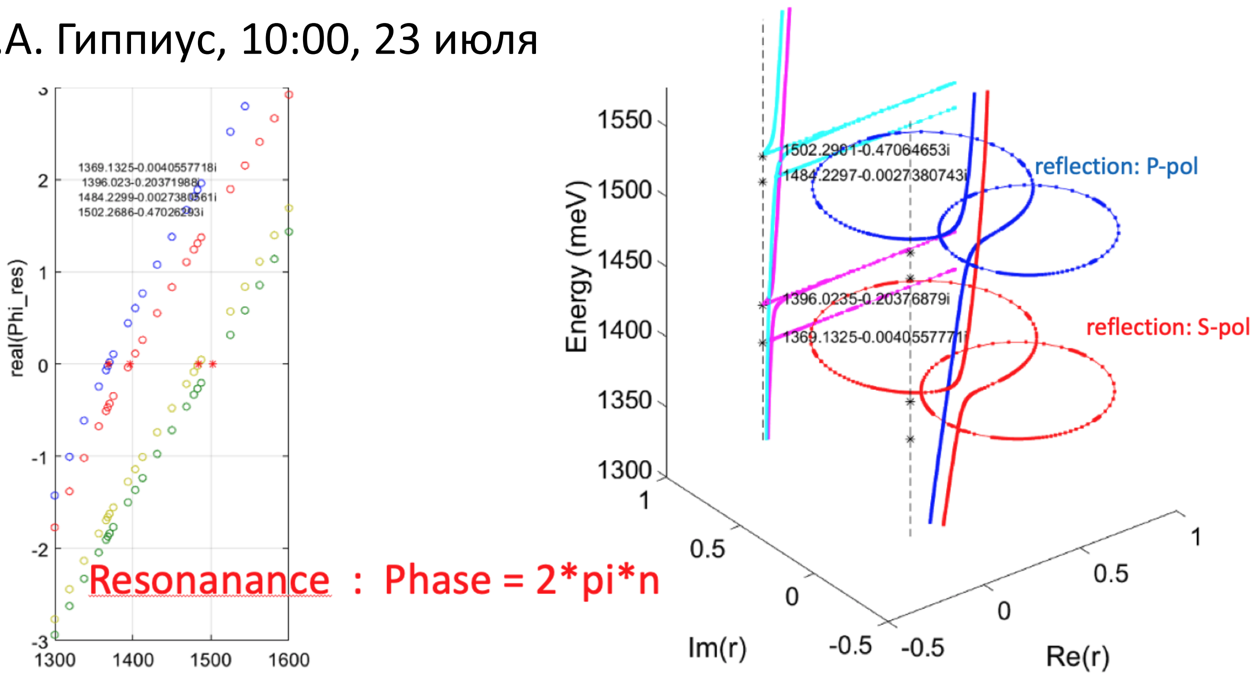

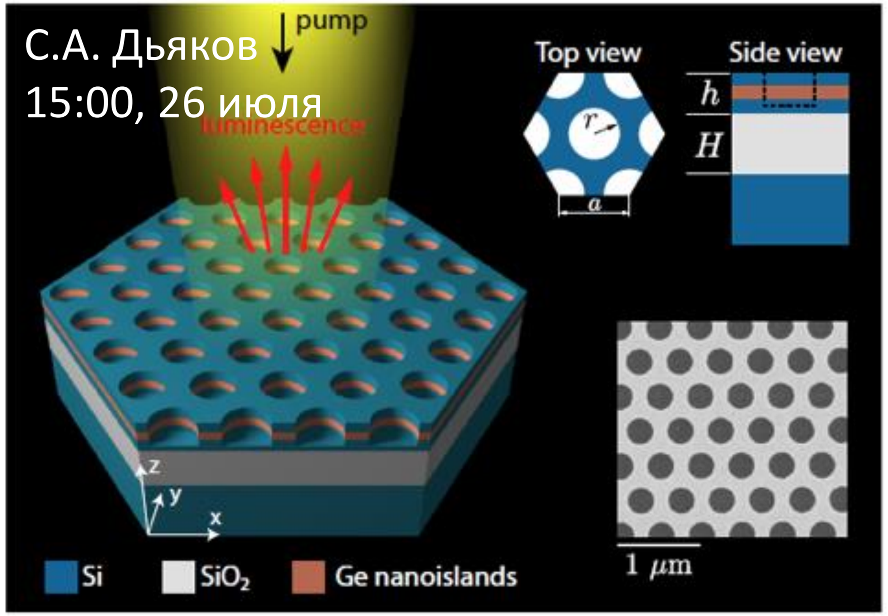

План этой лекции

1. Как поймать свет в решете?

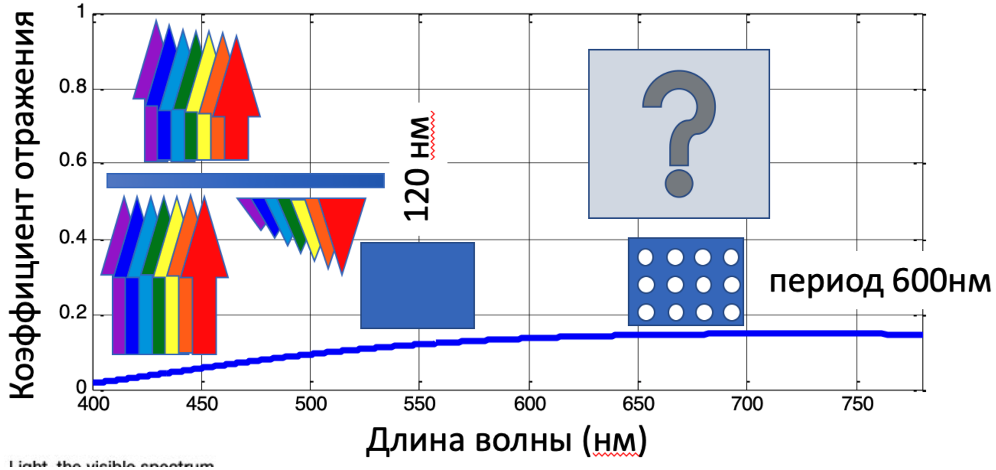

2. Сколько можно считать одно и тоже?!

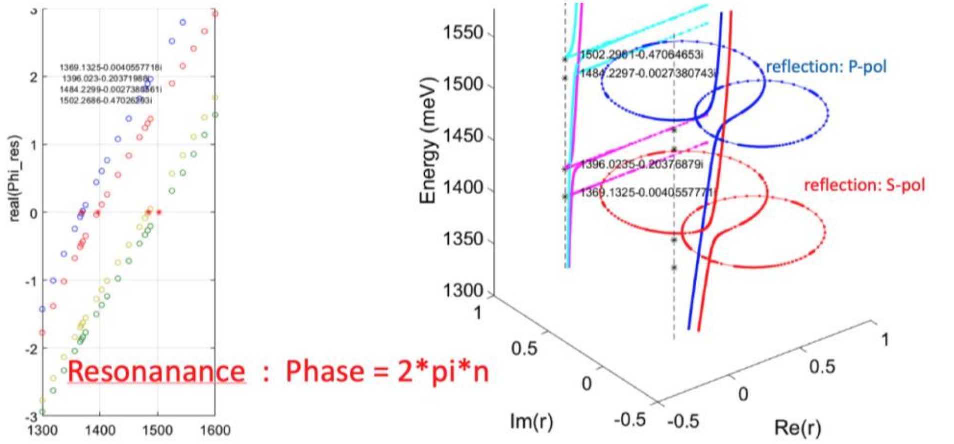

3. Как раскалываются резонансы?

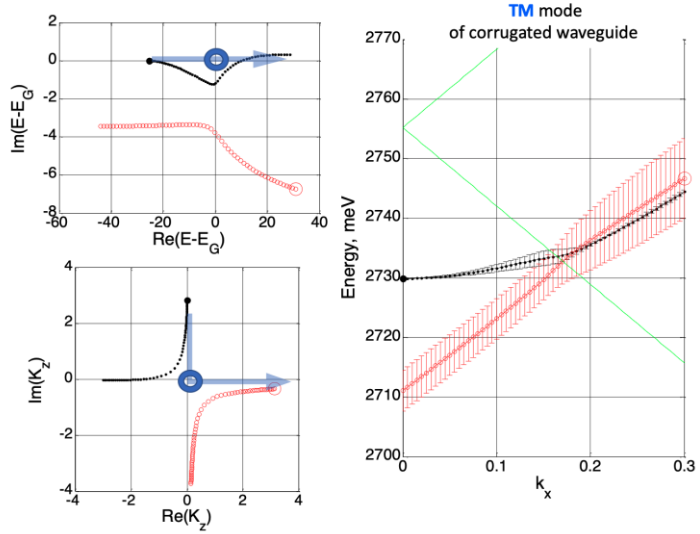

4. Как скрутить свет винтом?

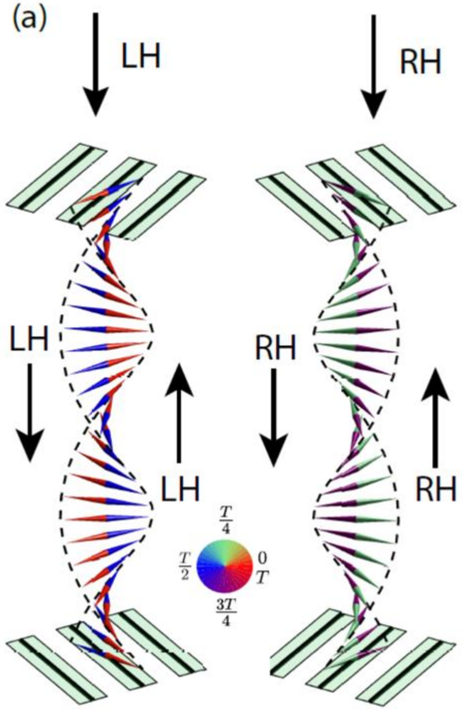

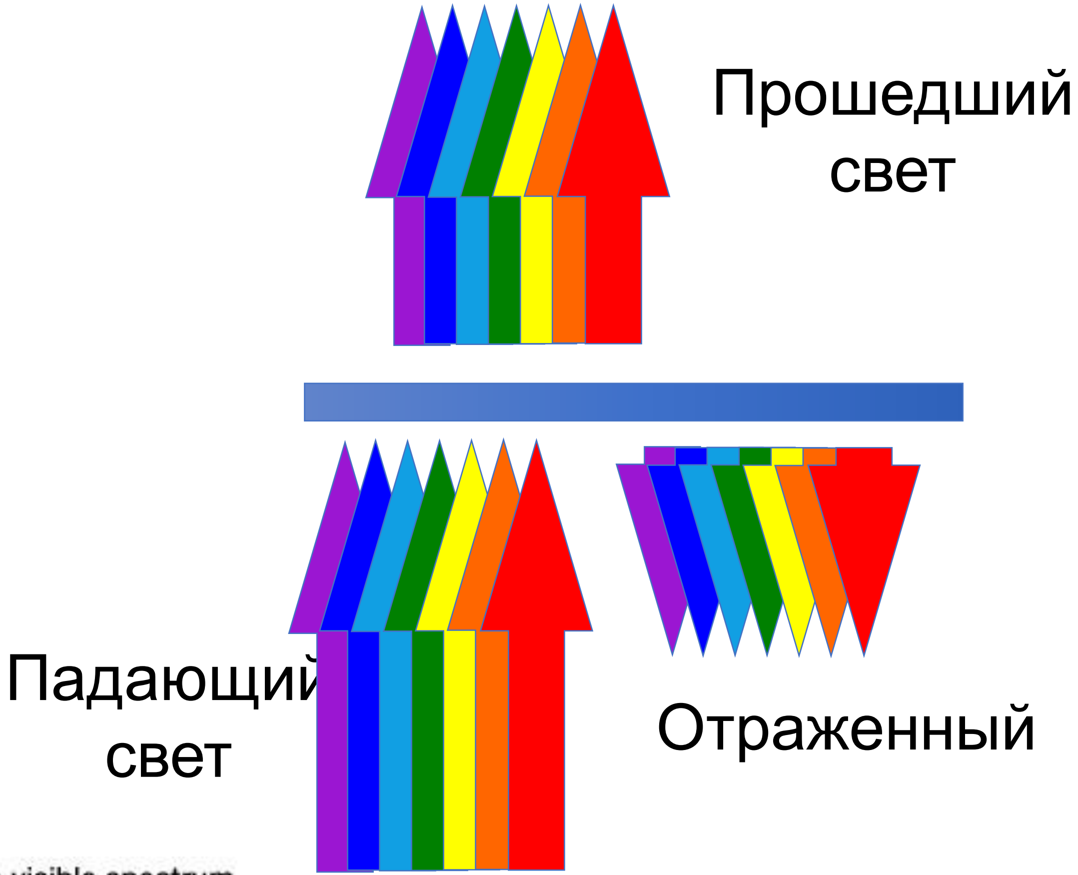
Прошедший свет
Падающий свет
Отраженный

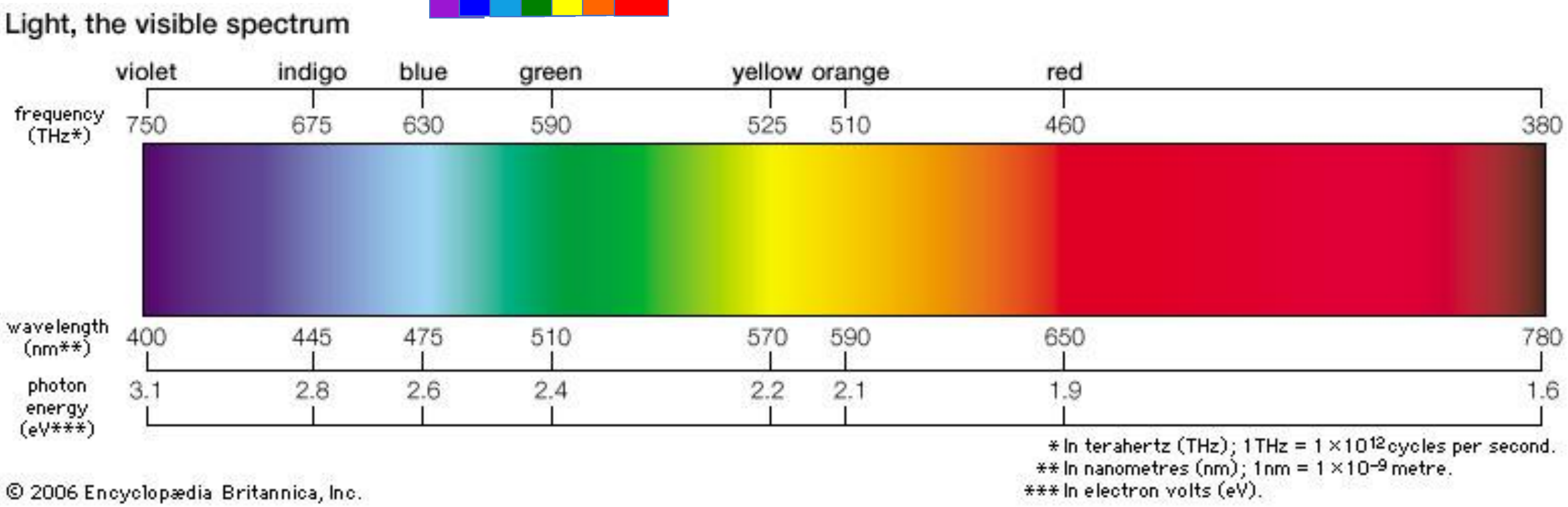
Light, the visible spectrum
violet
indigo
blue
green
yellow
orange
red
frequency (THz*)
750
675
630
590
525
510
460
380
wavelength (nm**)
400
445
475
510
570
590
650
780
photon energy (eV***)
3.1
2.8
2.6
2.4
2.2
2.1
1.9
1.6
* In terahertz (THz); 1 THz = 1 × 10[12] cycles per second.
** In nanometres (nm); 1 nm = 1 × 10[-9] metre.
*** In electron volts (eV).
© 2006 Encyclopædia Britannica, Inc.

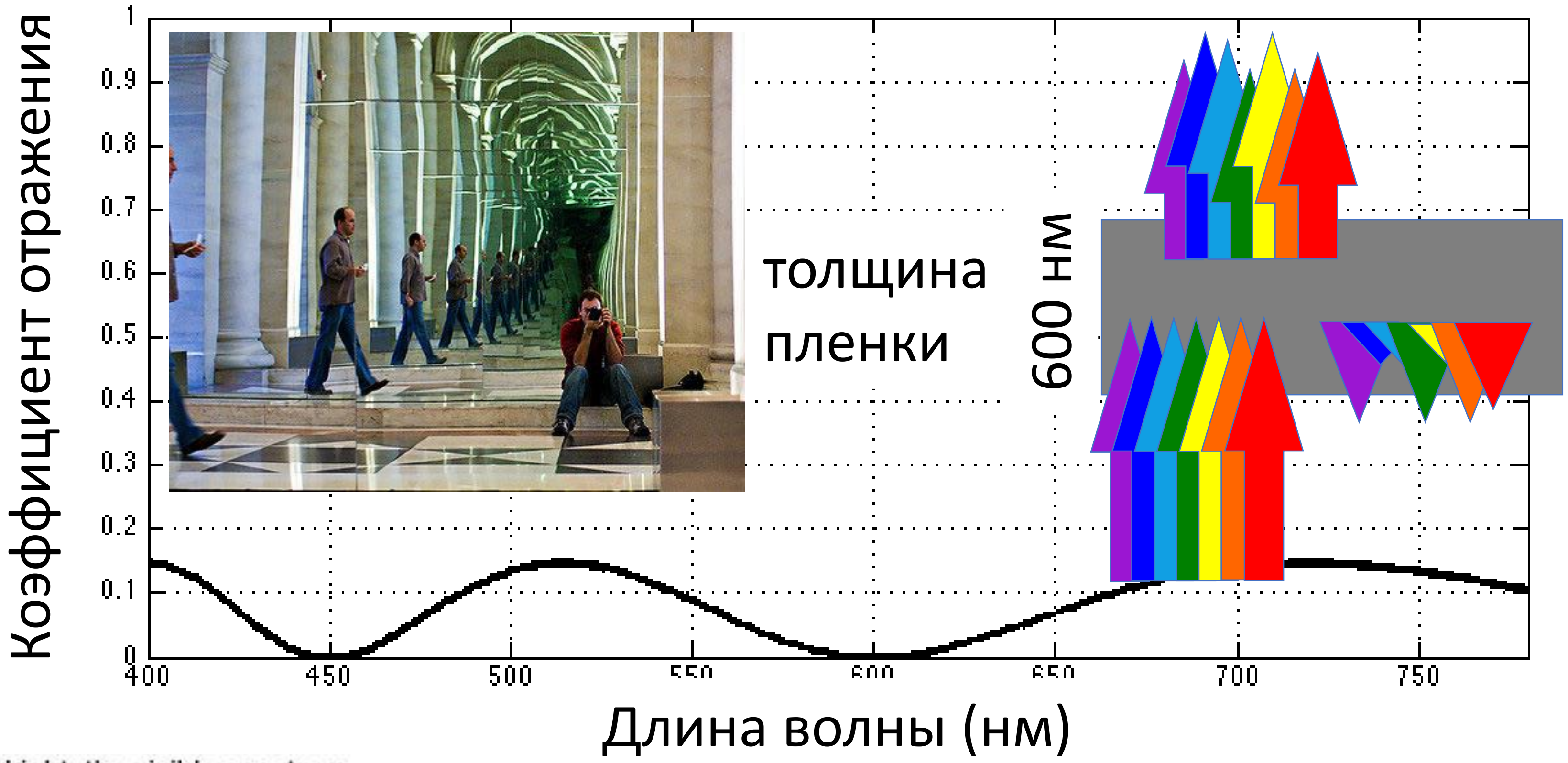
Коэффициент отражения
1
0.9
0.8
0.7
0.6
0.5
0.4
0.3
0.2
0.1
0
400
450
500
550
600
650
700
750
толщина
пленки
600 нм
Длина волны (нм)

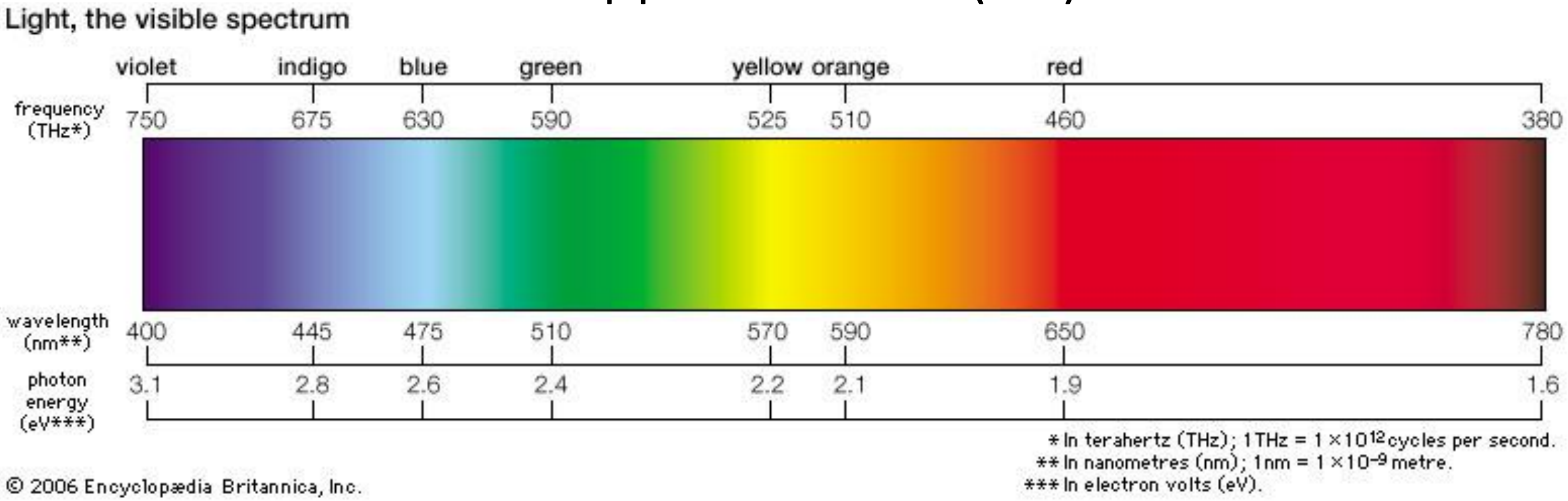
Light, the visible spectrum
violet
indigo
blue
green
yellow orange
red
frequency (THz*)
750 675 630 590 525 510 460 380
wavelength (nm**)
400 445 475 510 570 590 650 780
photon energy (eV***)
3.1 2.8 2.6 2.4 2.2 2.1 1.9 1.6
* In terahertz (THz); 1 THz = 1 × 10^12 cycles per second.
** In nanometres (nm); 1 nm = 1 × 10^-9 metre.
*** In electron volts (eV).
© 2006 Encyclopædia Britannica, Inc.

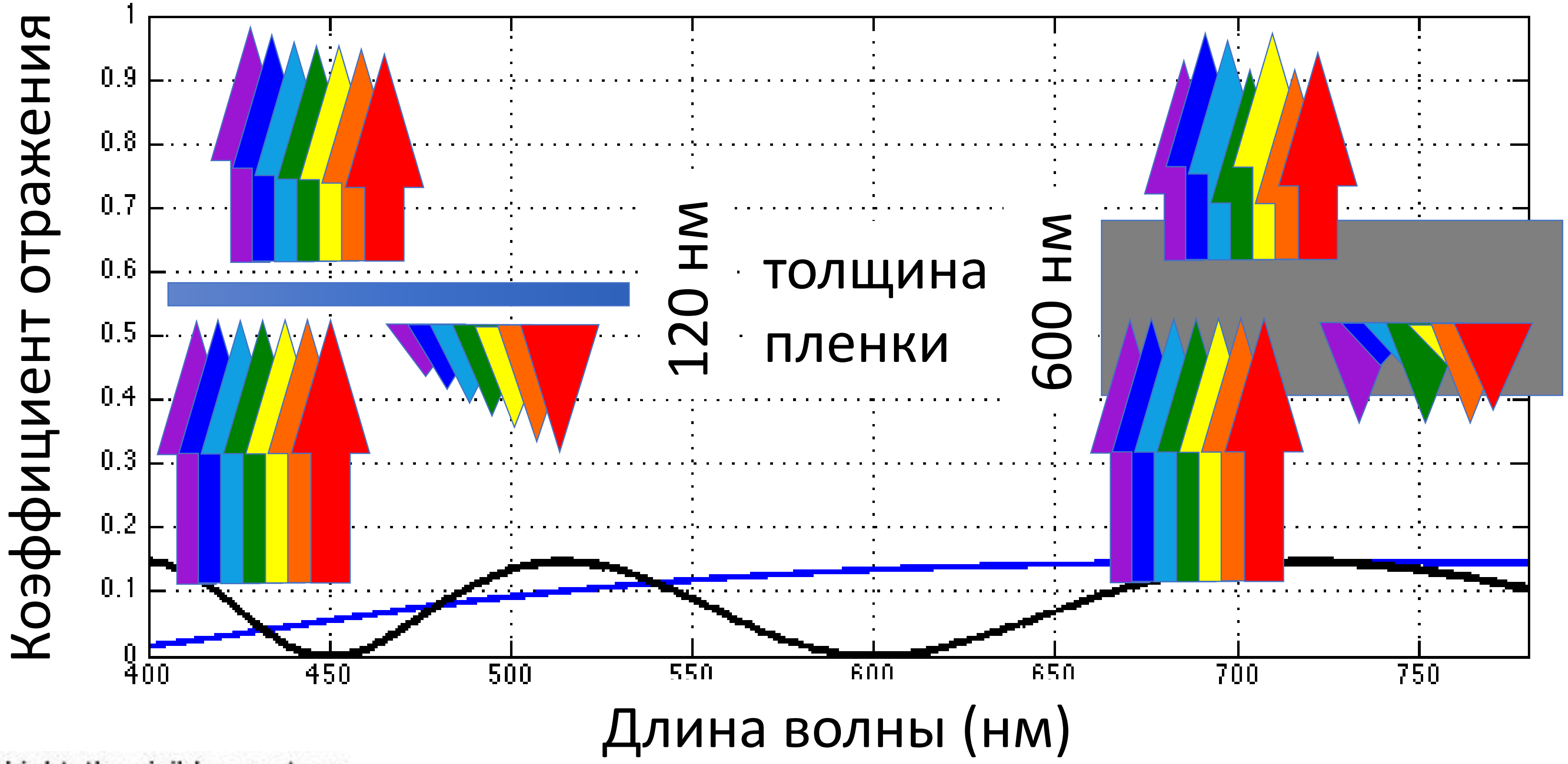
Коэффициент отражения
Длина волны (нм)
120 нм
толщина
пленки
600 нм
1
0.9
0.8
0.7
0.6
0.5
0.4
0.3
0.2
0.1
0
400
450
500
550
600
650
700
750

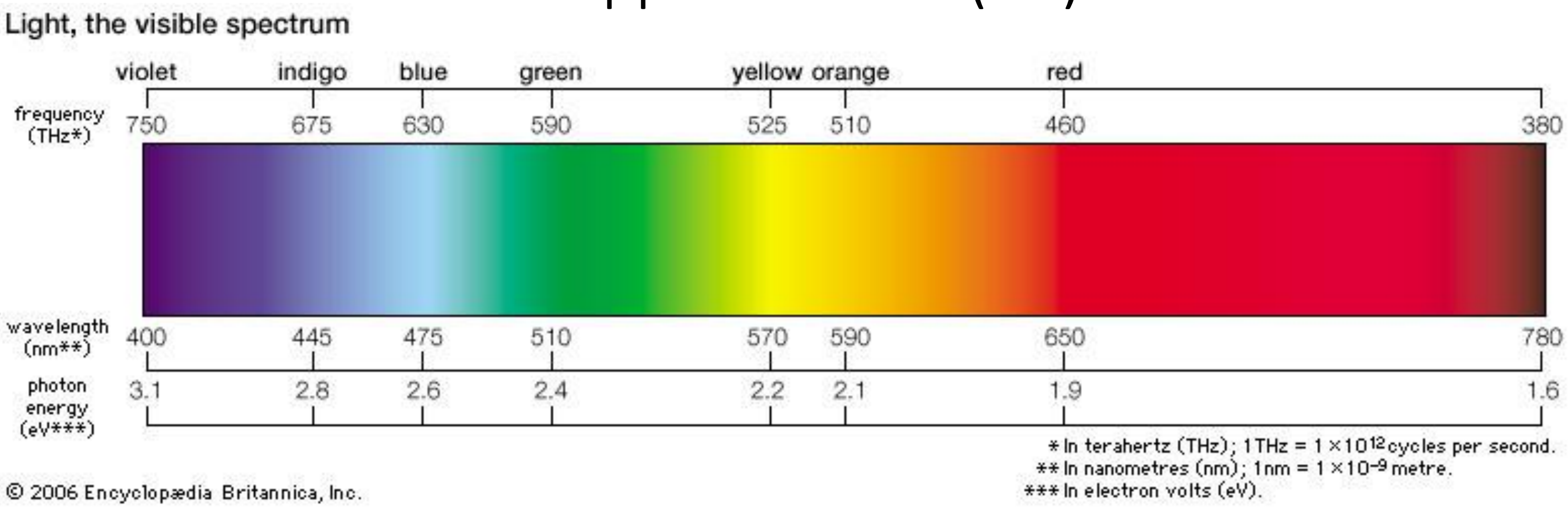
Light, the visible spectrum
violet
indigo
blue
green
yellow
orange
red
frequency (THz*)
750
675
630
590
525
510
460
380
wavelength (nm**)
400
445
475
510
570
590
650
780
photon energy (eV***)
3.1
2.8
2.6
2.4
2.2
2.1
1.9
1.6
* In terahertz (THz); 1 THz = 1 × 10¹² cycles per second.
** In nanometres (nm); 1 nm = 1 × 10⁻⁹ metre.
*** In electron volts (eV).
© 2006 Encyclopædia Britannica, Inc.

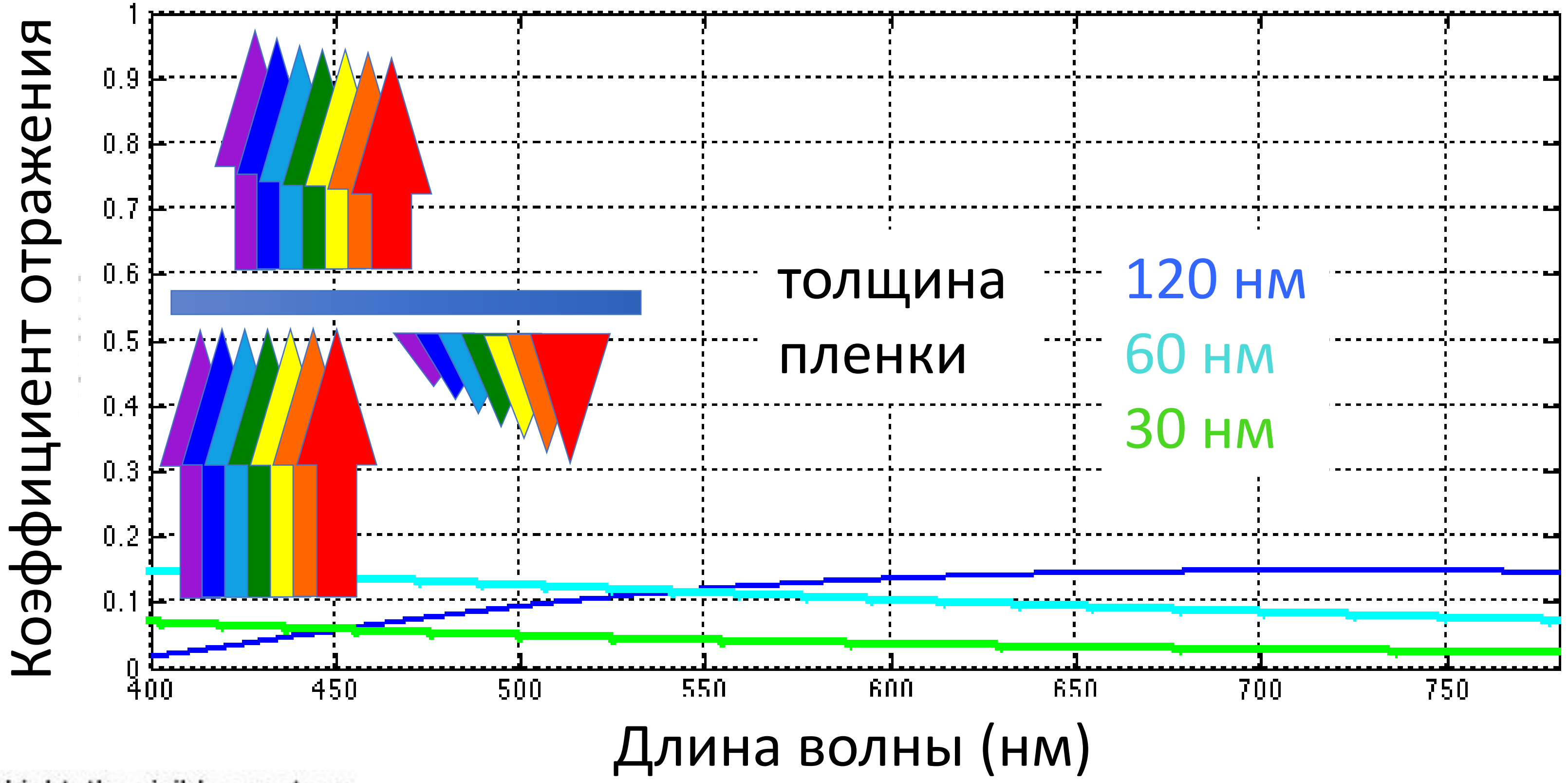
Коэффициент отражения
0
0.1
0.2
0.3
0.4
0.5
0.6
0.7
0.8
0.9
1
400
450
500
550
600
650
700
750
толщина
пленки
120 нм
60 нм
30 нм
Длина волны (нм)

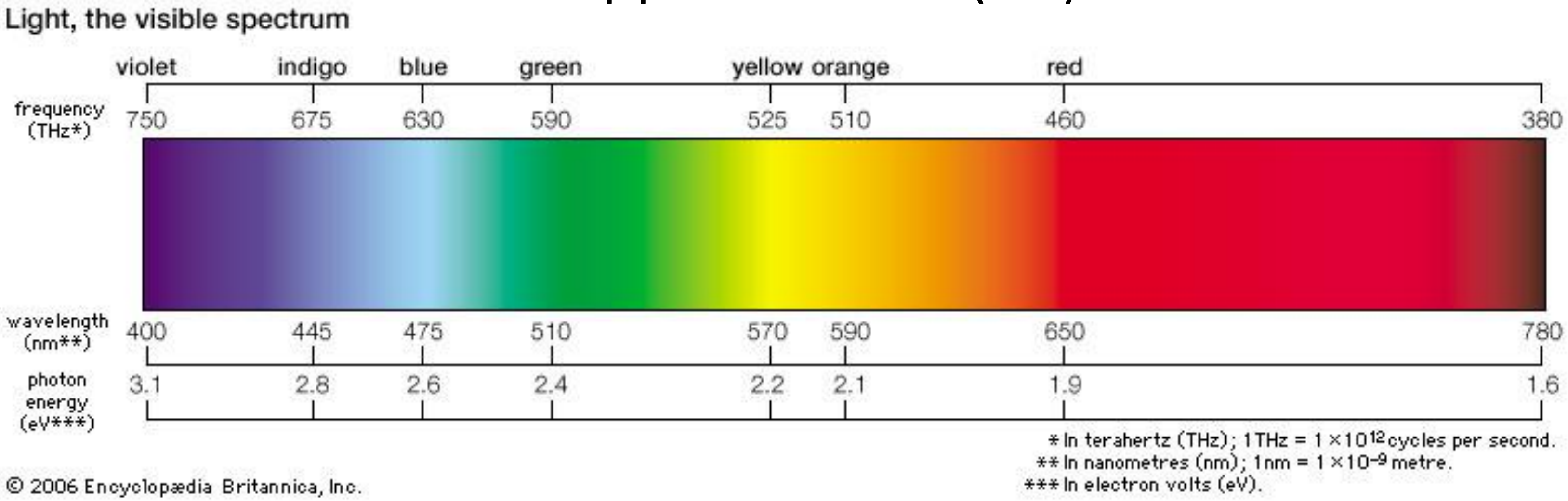
Light, the visible spectrum
violet
indigo
blue
green
yellow
orange
red
frequency (THz*)
750
675
630
590
525
510
460
380
wavelength (nm**)
400
445
475
510
570
590
650
780
photon energy (eV***)
3.1
2.8
2.6
2.4
2.2
2.1
1.9
1.6
* In terahertz (THz); 1 THz = 1 × 10^12 cycles per second.
** In nanometres (nm); 1 nm = 1 × 10^-9 metre.
*** In electron volts (eV).
© 2006 Encyclopædia Britannica, Inc.

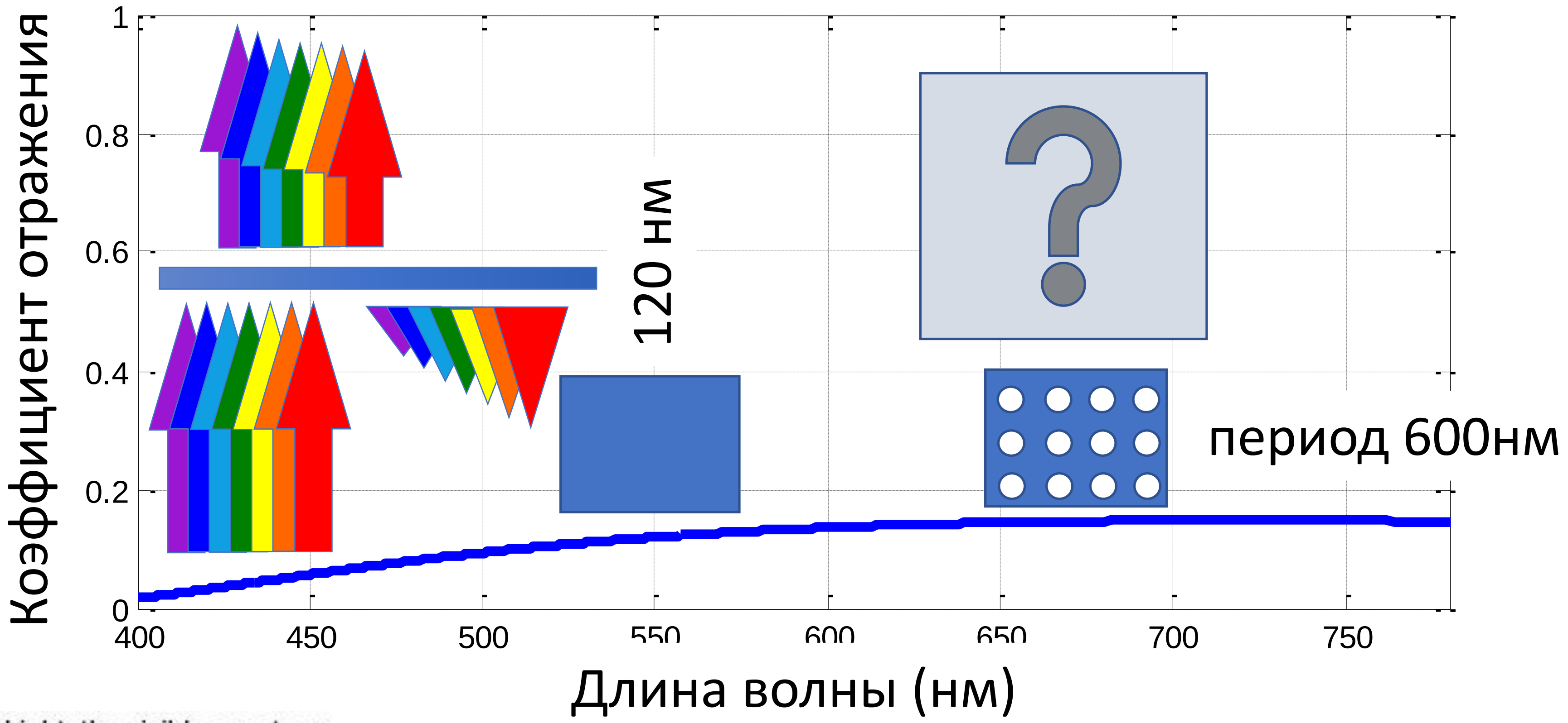

Коэффициент отражения
1
0.8
0.6
0.4
0.2
0
400
450
500
550
600
650
700
750
Длина волны (нм)
120 нм
период 600нм

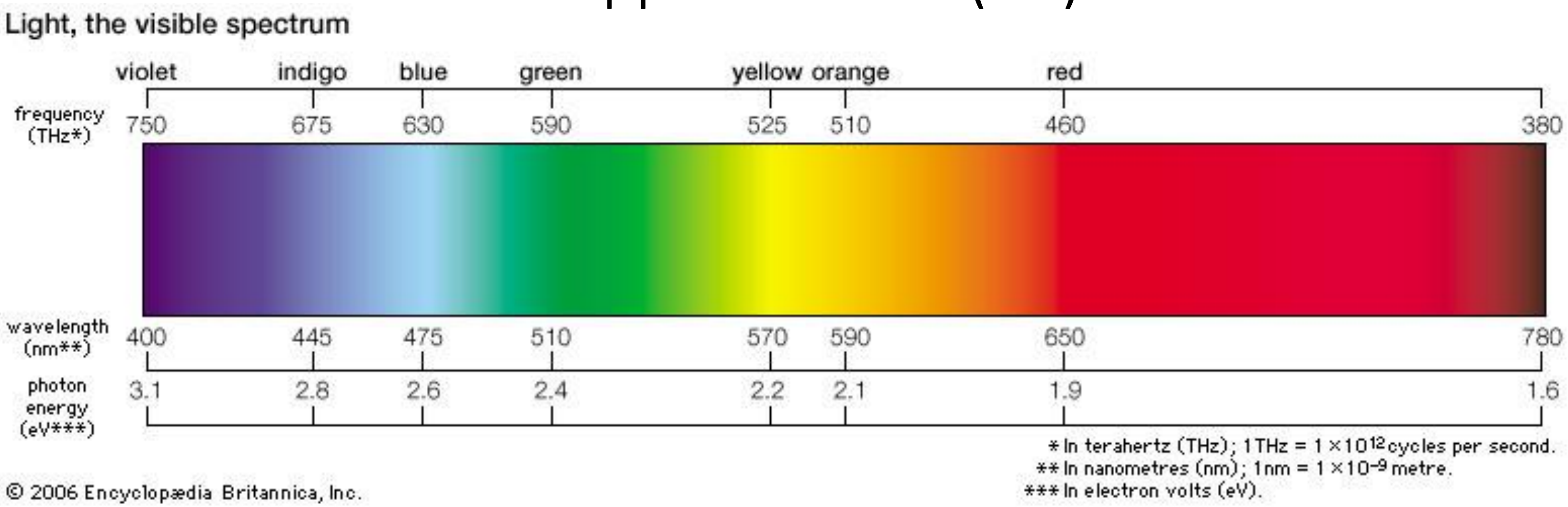

Light, the visible spectrum
violet
indigo
blue
green
yellow orange
red
frequency (THz*)
750
675
630
590
525
510
460
380
wavelength (nm**)
400
445
475
510
570
590
650
780
photon energy (eV***)
3.1
2.8
2.6
2.4
2.2
2.1
1.9
1.6
* In terahertz (THz); 1 THz = 1 × 10[12] cycles per second.
** In nanometres (nm); 1 nm = 1 × 10[-9] metre.
*** In electron volts (eV).
© 2006 Encyclopædia Britannica, Inc.

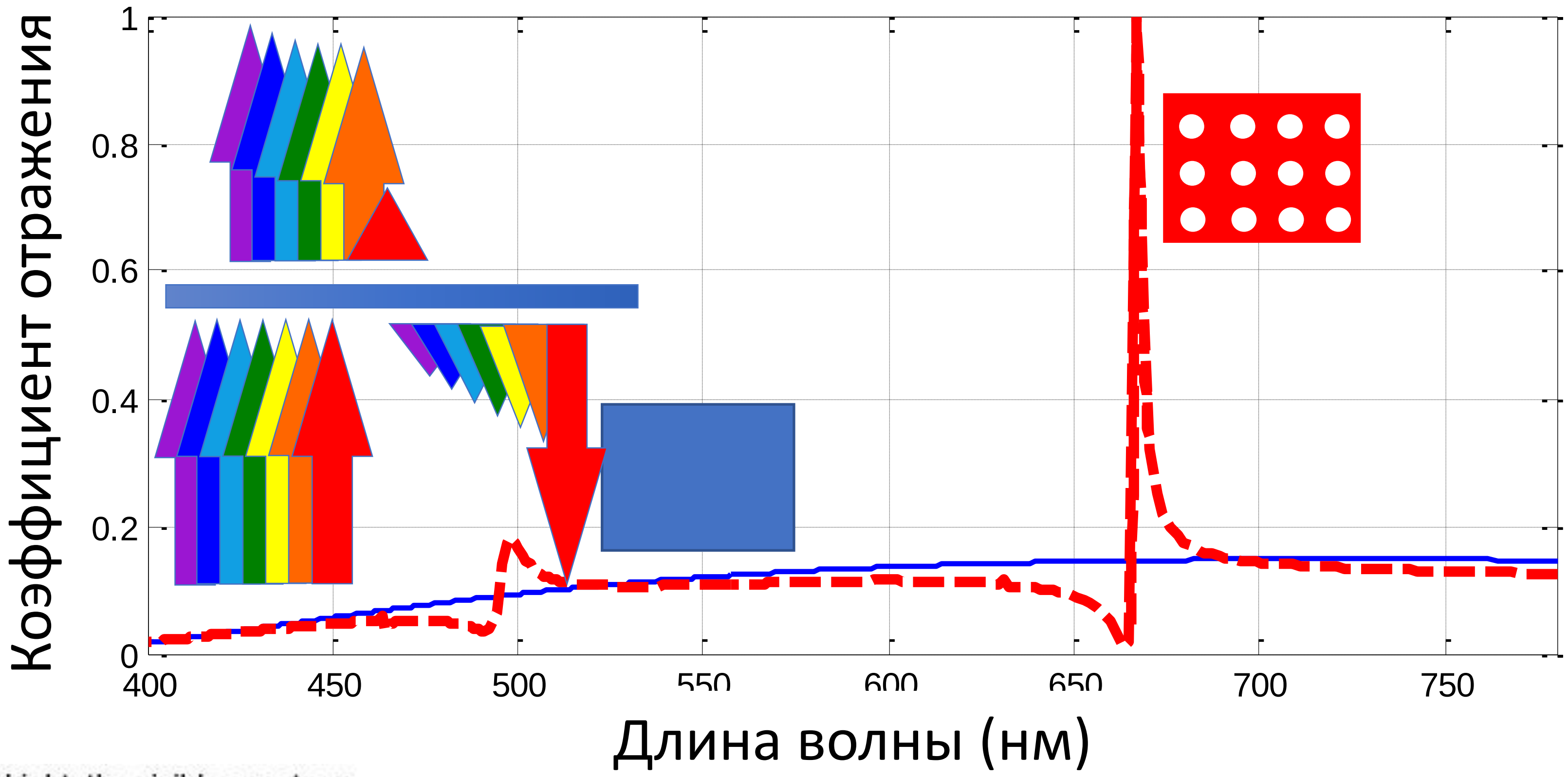
Коэффициент отражения
1
0.8
0.6
0.4
0.2
0
400
450
500
550
600
650
700
750
Длина волны (нм)

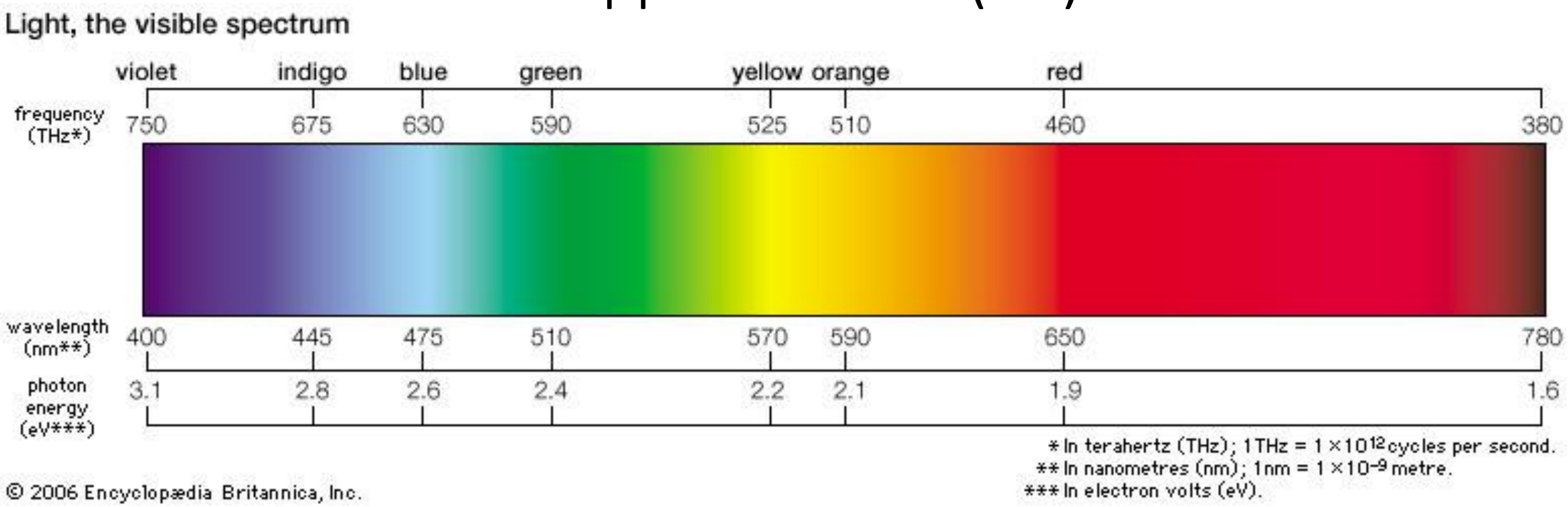
Light, the visible spectrum
violet
indigo
blue
green
yellow orange
red
frequency (THz*)
750 675 630 590 525 510 460 380
wavelength (nm**)
400 445 475 510 570 590 650 780
photon energy (eV***)
3.1 2.8 2.6 2.4 2.2 2.1 1.9 1.6
* In terahertz (THz); 1 THz = 1 × 10¹² cycles per second.
** In nanometres (nm); 1 nm = 1 × 10⁻⁹ metre.
*** In electron volts (eV).
© 2006 Encyclopædia Britannica, Inc.

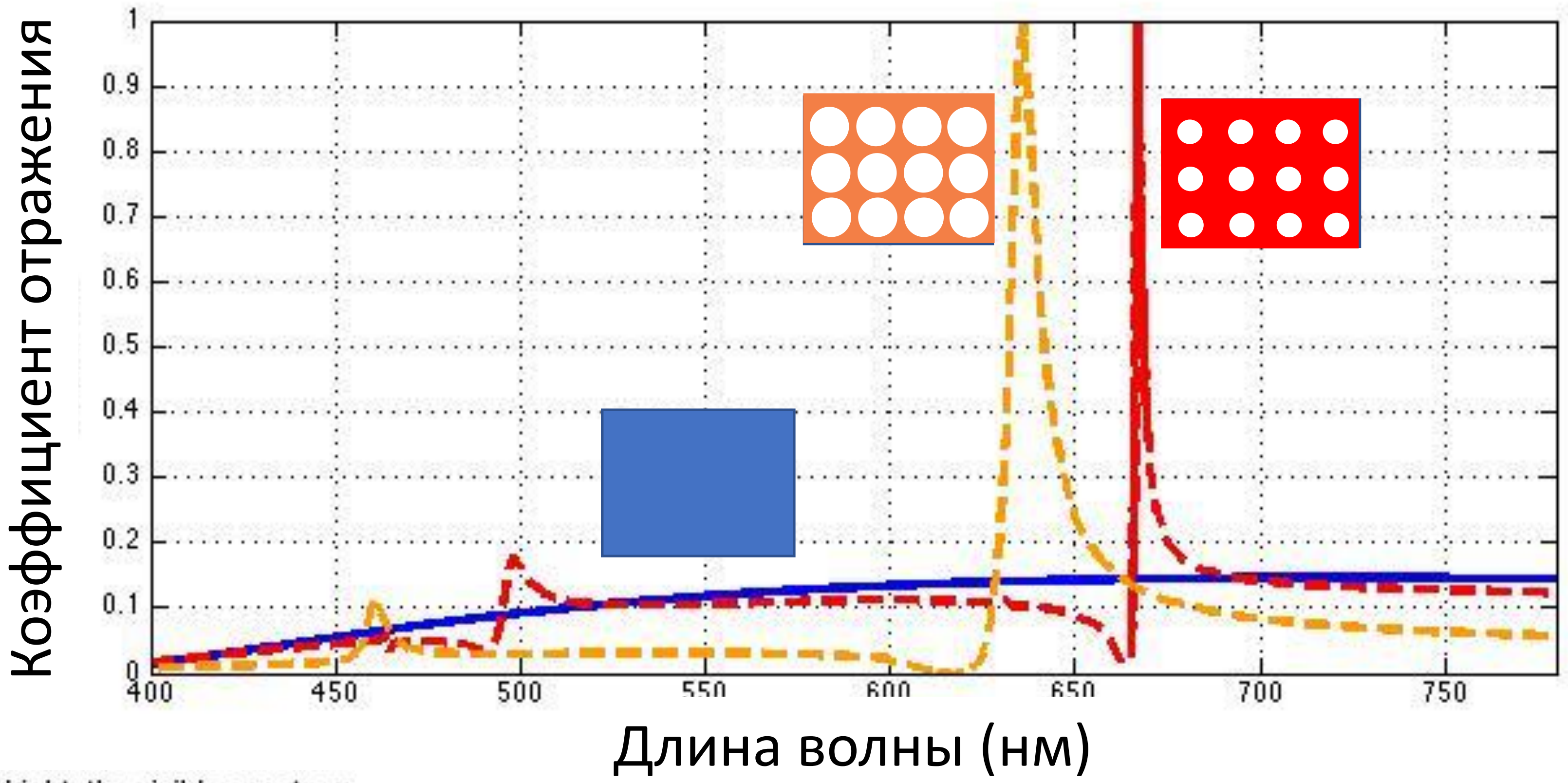
Коэффициент отражения
1
0.9
0.8
0.7
0.6
0.5
0.4
0.3
0.2
0.1
0
400
450
500
550
600
650
700
750
Длина волны (нм)

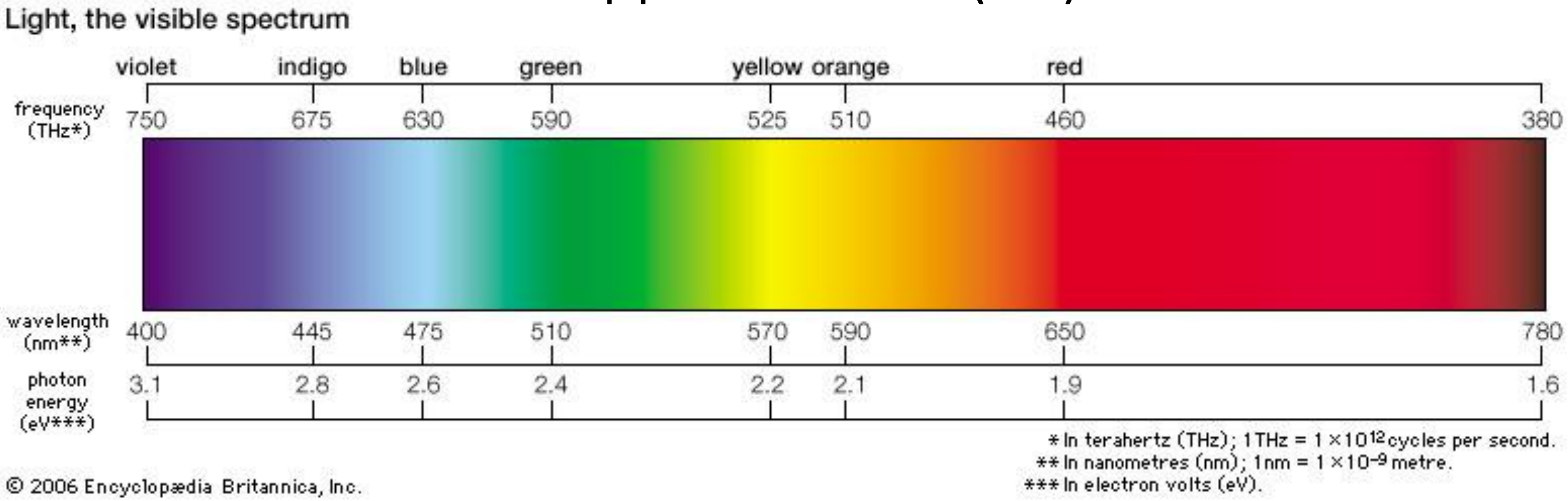
Light, the visible spectrum
violet
indigo
blue
green
yellow orange
red
frequency (THz*)
750 675 630 590 525 510 460 380
wavelength (nm**)
400 445 475 510 570 590 650 780
photon energy (eV***)
3.1 2.8 2.6 2.4 2.2 2.1 1.9 1.6
* In terahertz (THz); 1 THz = 1 × 10^12 cycles per second.
** In nanometres (nm); 1 nm = 1 × 10^-9 metre.
*** In electron volts (eV).
© 2006 Encyclopædia Britannica, Inc.

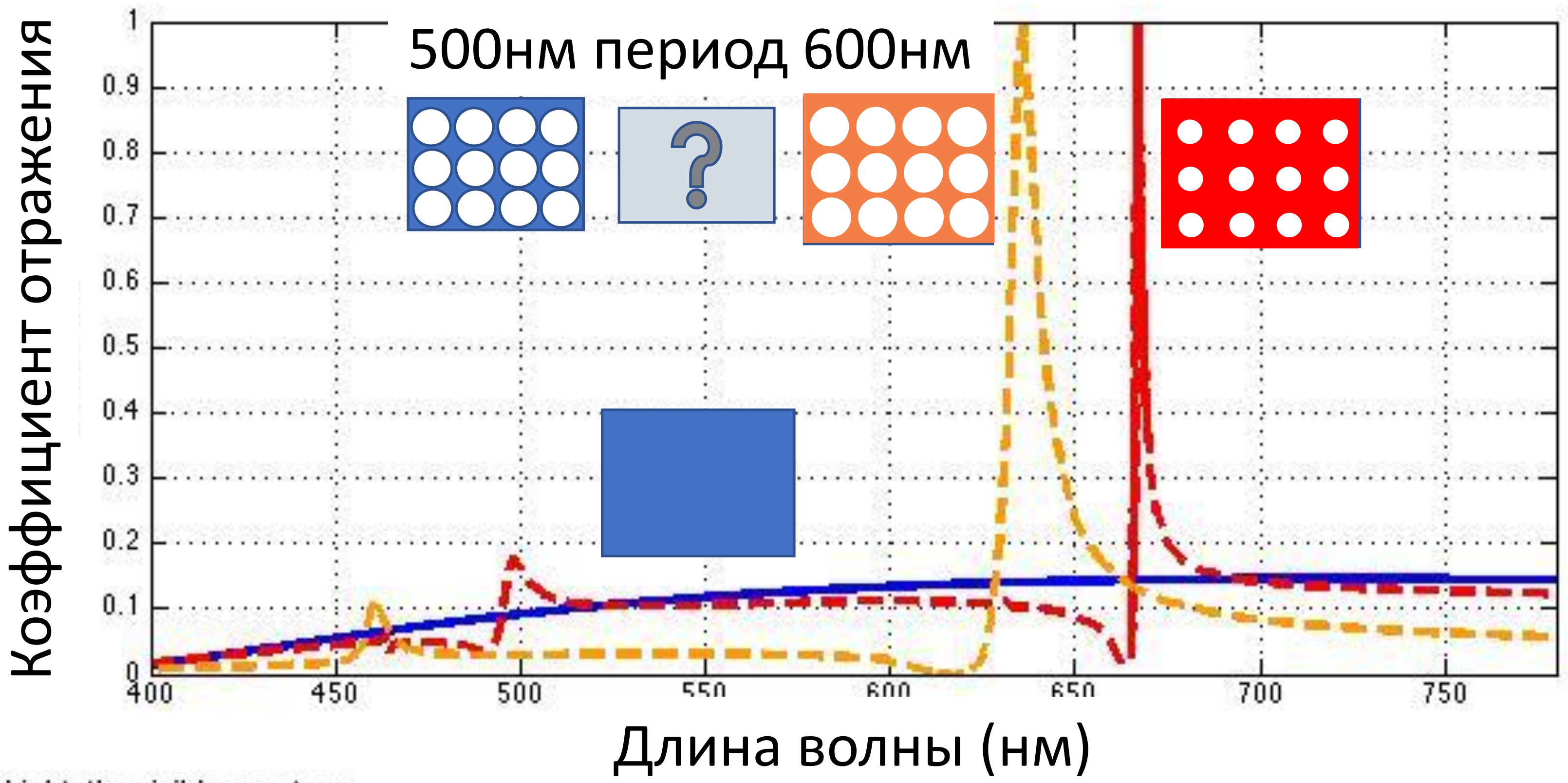
500нм период 600нм
?
Коэффициент отражения
1
0.9
0.8
0.7
0.6
0.5
0.4
0.3
0.2
0.1
0
400
450
500
550
600
650
700
750
Длина волны (нм)

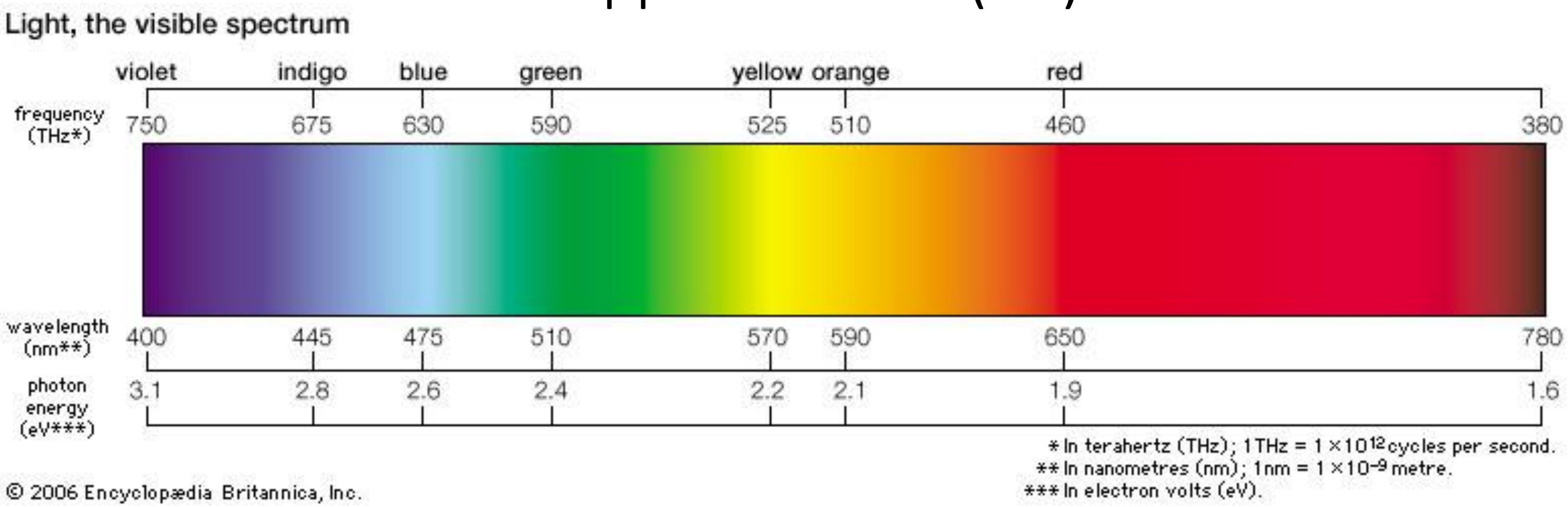
Light, the visible spectrum
violet
indigo
blue
green
yellow orange
red
frequency (THz*)
750
675
630
590
525
510
460
380
wavelength (nm**)
400
445
475
510
570
590
650
780
photon energy (eV***)
3.1
2.8
2.6
2.4
2.2
2.1
1.9
1.6
* In terahertz (THz); 1 THz = 1 × 10^12 cycles per second.
** In nanometres (nm); 1 nm = 1 × 10^-9 metre.
*** In electron volts (eV).
© 2006 Encyclopædia Britannica, Inc.

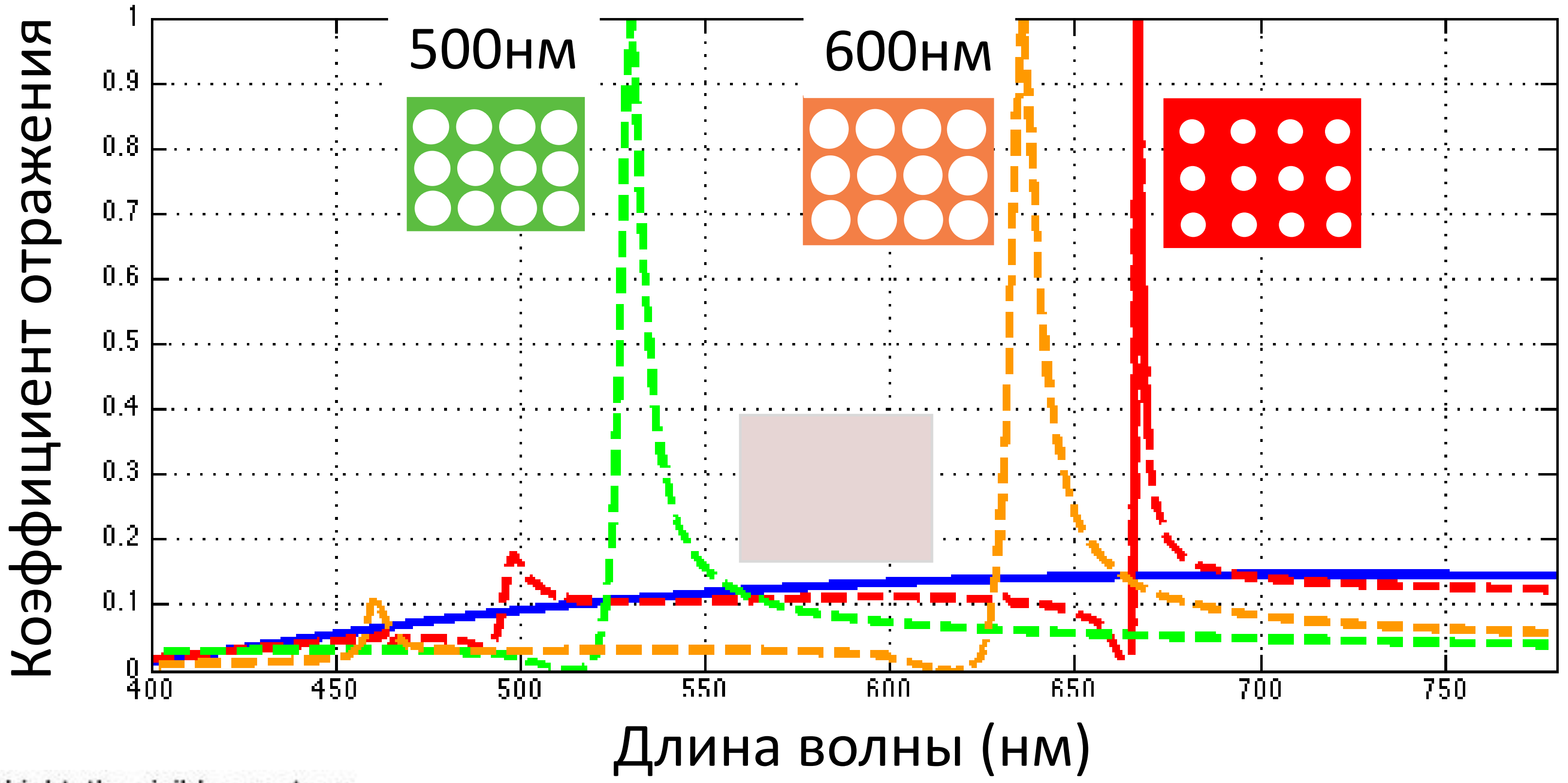
Коэффициент отражения
500нм
600нм
0
0.1
0.2
0.3
0.4
0.5
0.6
0.7
0.8
0.9
1
400
450
500
550
600
650
700
750
Длина волны (нм)

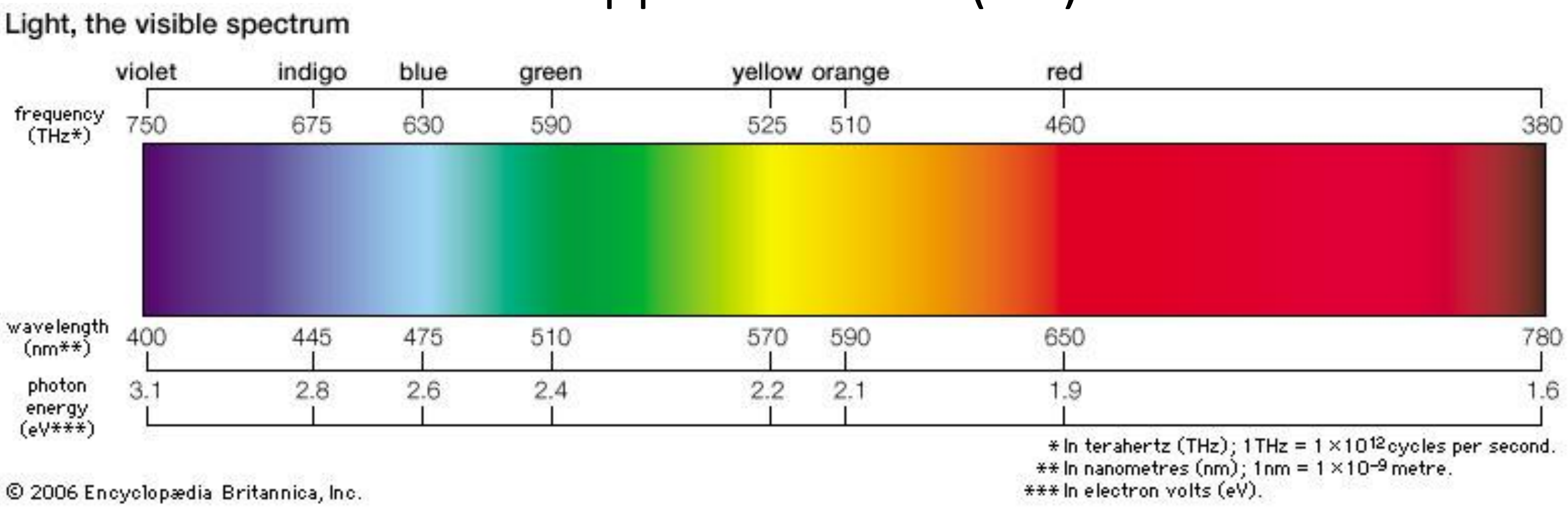
Light, the visible spectrum
violet
indigo
blue
green
yellow
orange
red
frequency (THz*)
750
675
630
590
525
510
460
380
wavelength (nm**)
400
445
475
510
570
590
650
780
photon energy (eV***)
3.1
2.8
2.6
2.4
2.2
2.1
1.9
1.6
* In terahertz (THz); 1 THz = 1 × 10¹² cycles per second.
** In nanometres (nm); 1 nm = 1 × 10⁻⁹ metre.
*** In electron volts (eV).
© 2006 Encyclopædia Britannica, Inc.

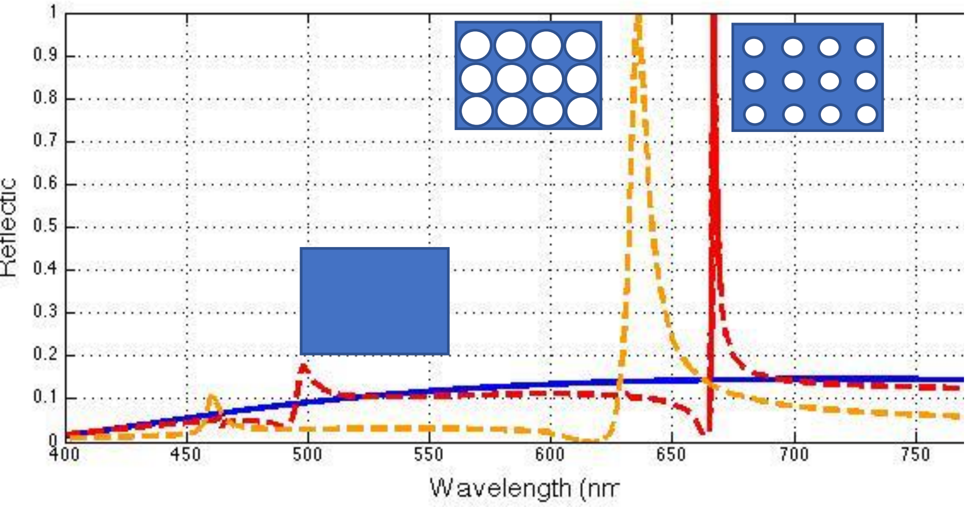

Свет иногда усиливается вблизи пленки с отверстиями

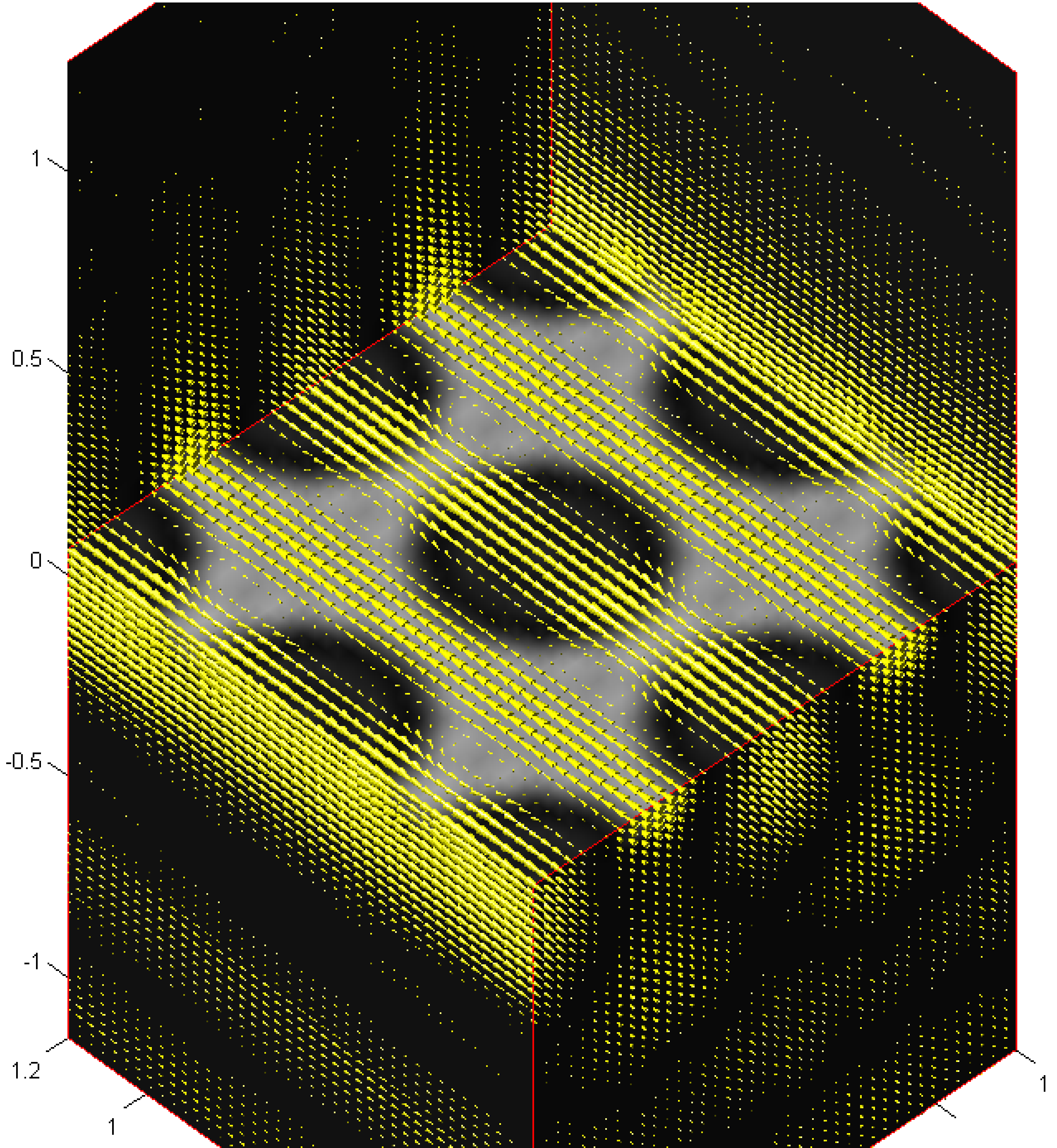

Фотонные кристаллы в природе

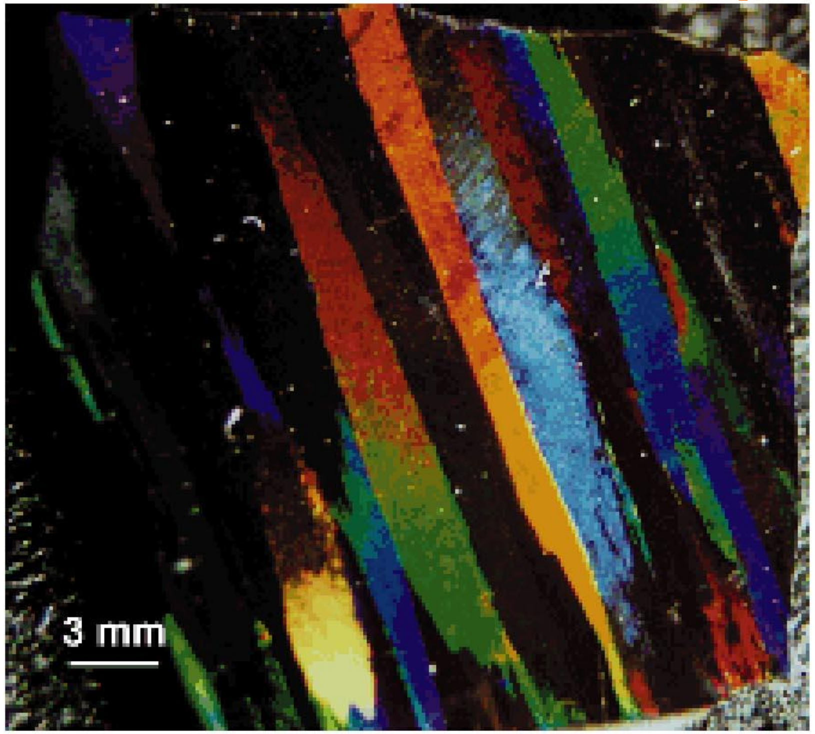

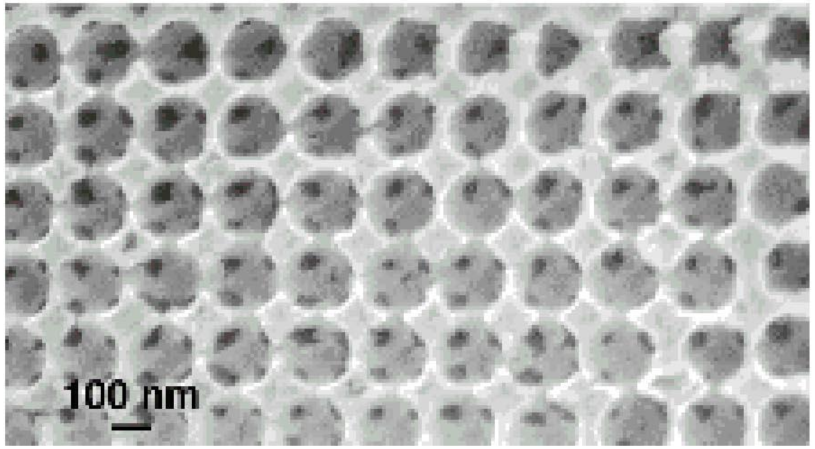

Опалы: естественные фотонные кристаллы, образованные слипшимися нано-шариками

На рисунке показаны искусственные опало-подобные структуры из фуллеренов (слева) и кварцевых наношариков (внизу)

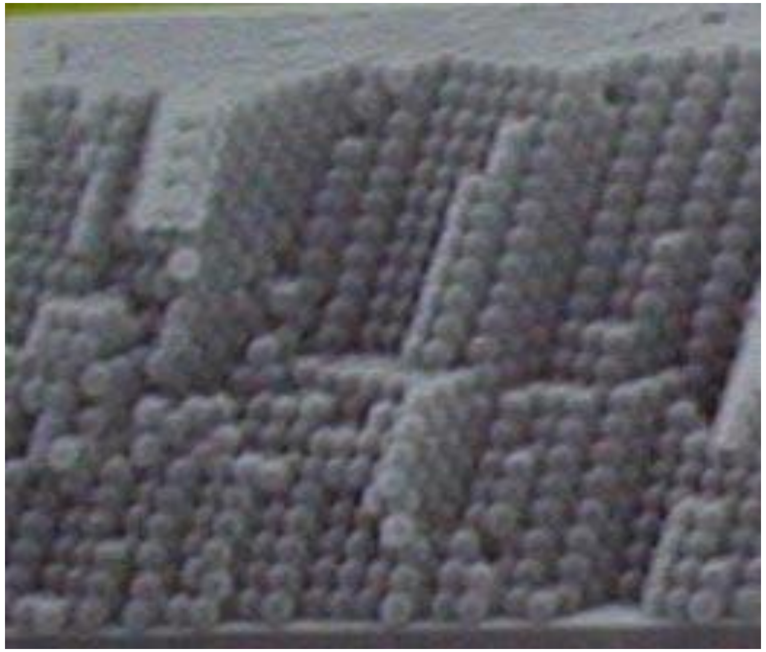

Окраска бабочки

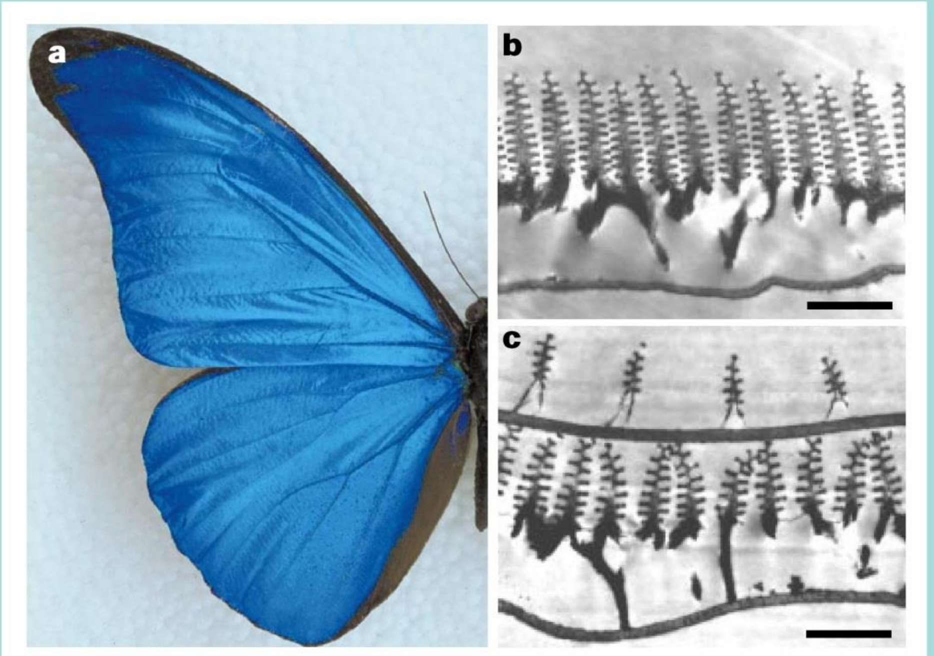

Figure 3 Iridescence in the butterfly *Morpho rhetenor*. **a**, Real colour image of the blue iridescence from a *M. rhetenor* wing. **b**, Transmission electron micrograph (TEM) images showing wing-scale cross-sections of *M. rhetenor*. **c**, TEM images of a wing-scale cross-section of the related species *M. didius* reveal its discretely configured multilayers. The high occupancy and high layer number of *M. rhetenor* in **b** creates an intense reflectivity that contrasts with the more diffusely coloured appearance of *M. didius*, in which an overlying second layer of scales effects strong diffraction[4]. Bars, **a**, 1 cm; **b**, 1.8 μm; **c**, 1.3 μm.

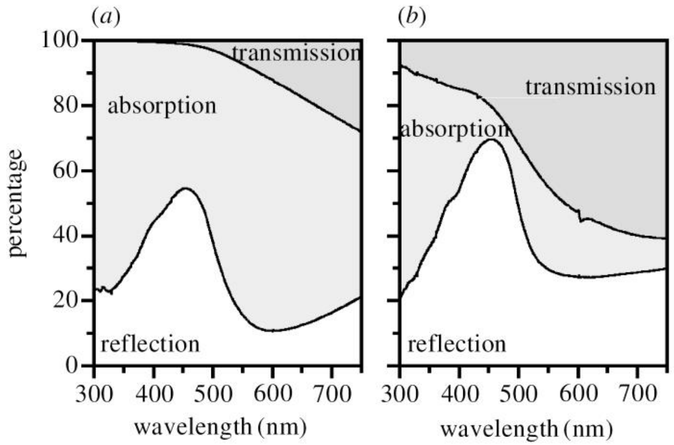

Figure 2. Percentages of transmission, absorption and reflection for the wings of (*a*) *Morpho didius* and (*b*) *Morpho sulkowskyi* measured by a spectrophotometer equipped with an integrated sphere.

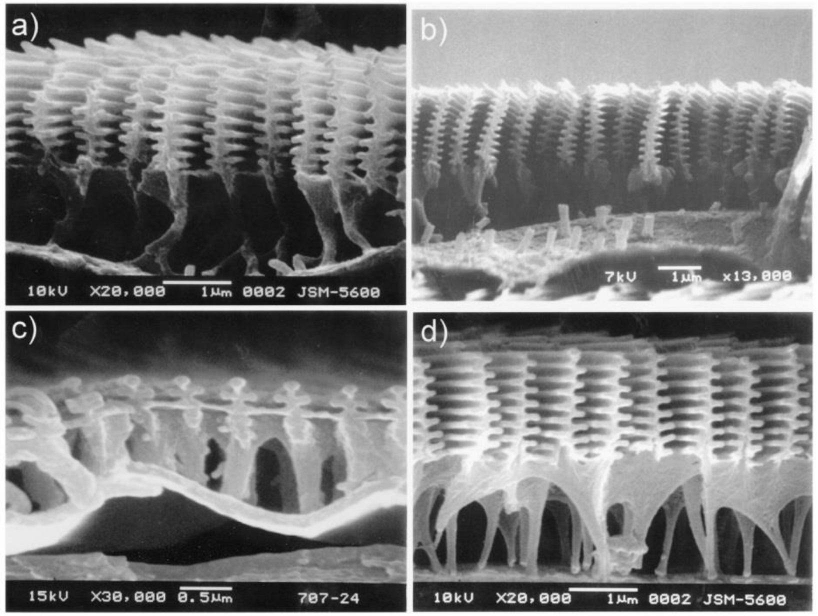

Fig. 3. Scanning electron microscope images of the cross sections of the iridescent scales of *Morpho* butterflies: (a) a ground scale of *M. didius*, (b) a scale of *M. rhetenor*, (c) a cover scale of *M. adonis* and (d) a scale of *M. sulkowskyi*.

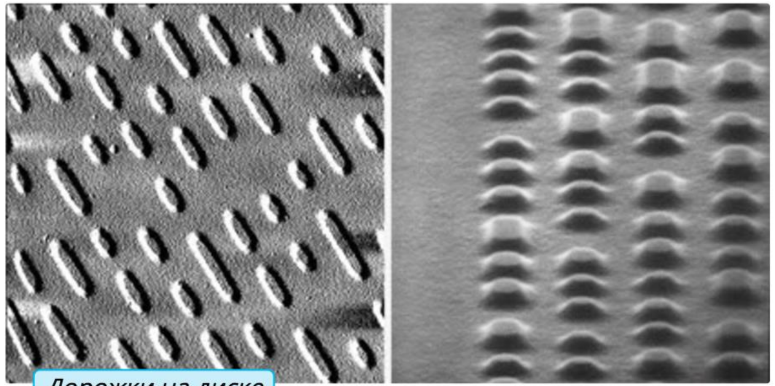

Дорожки на диске

	DVD	CD
размер штрихов	0.4	0.83
	(микрон)	
ширина дорожки	0.74	1.6

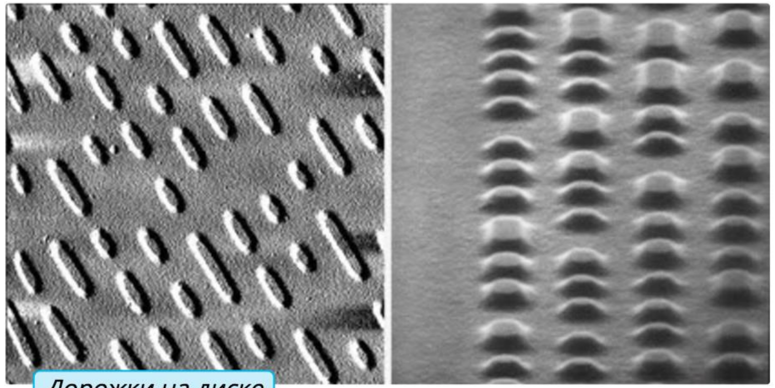

Дорожки на диске

	DVD	CD
размер штрихов	0.4	0.83
	(микрон)	
ширина дорожки	0.74	1.6

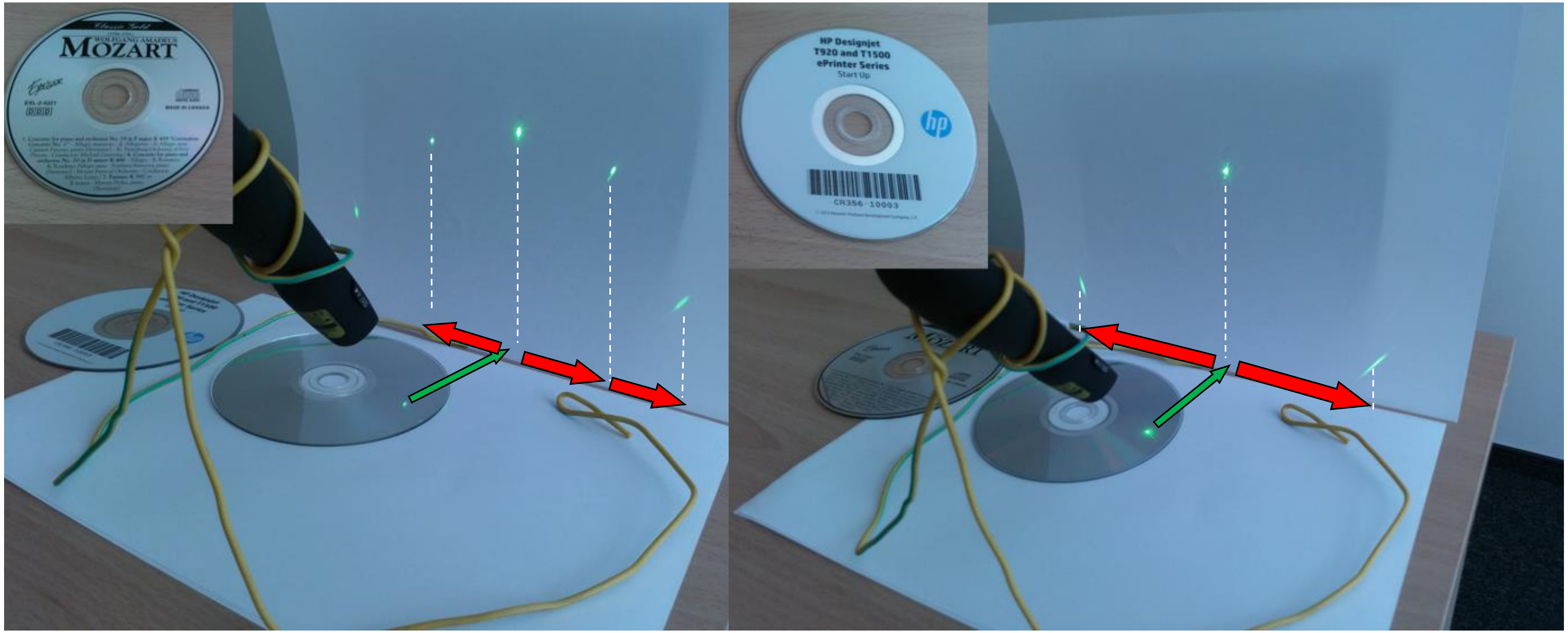

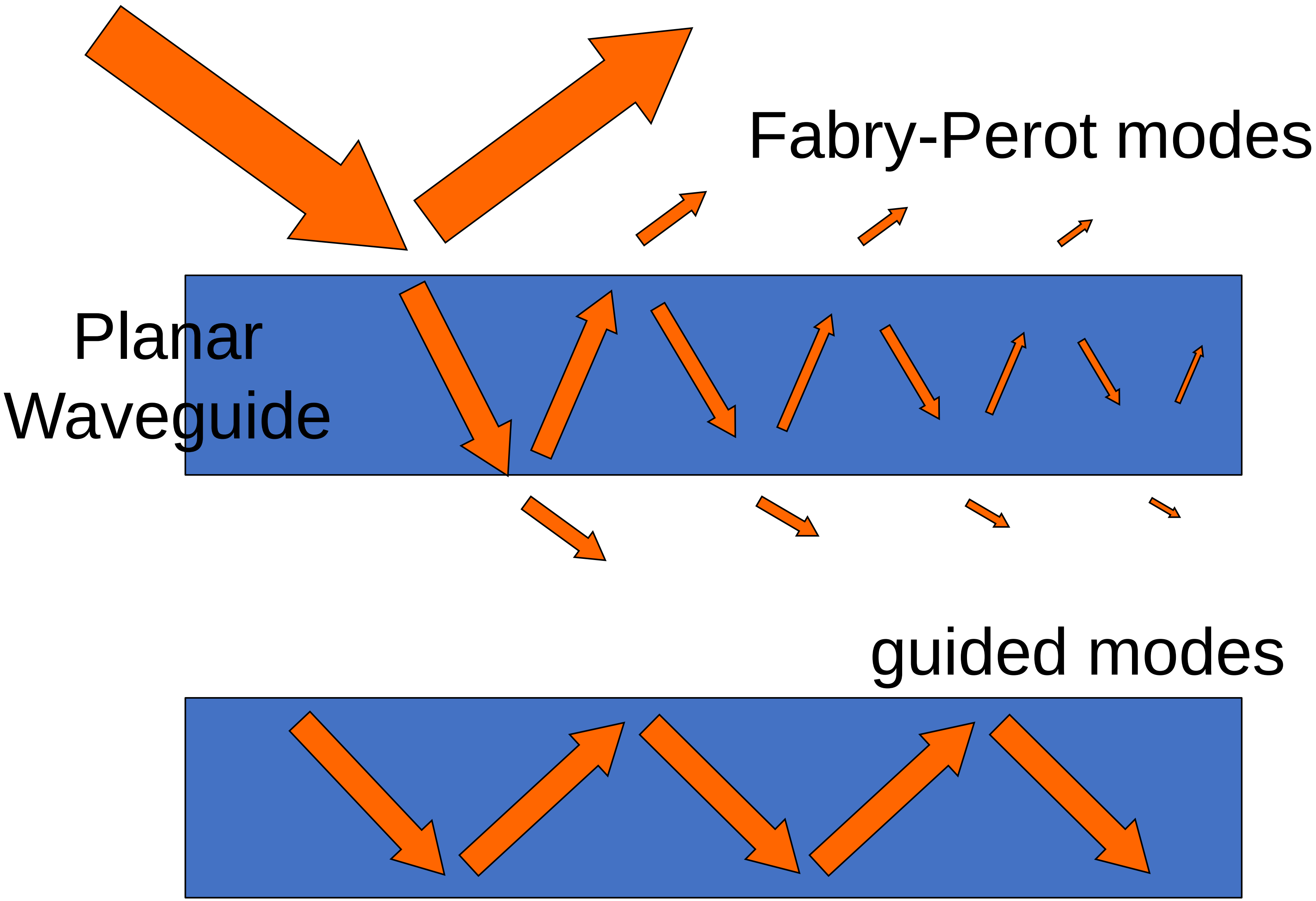
Fabry-Perot modes
Planar
Waveguide
guided modes

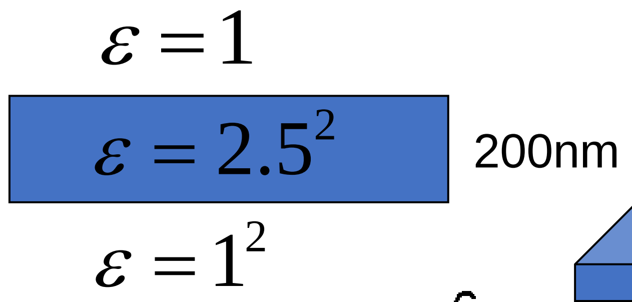

TE and **TM** modes of planar waveguide

circles: Re{E(k)}   bars: +/- Im{E(k)}

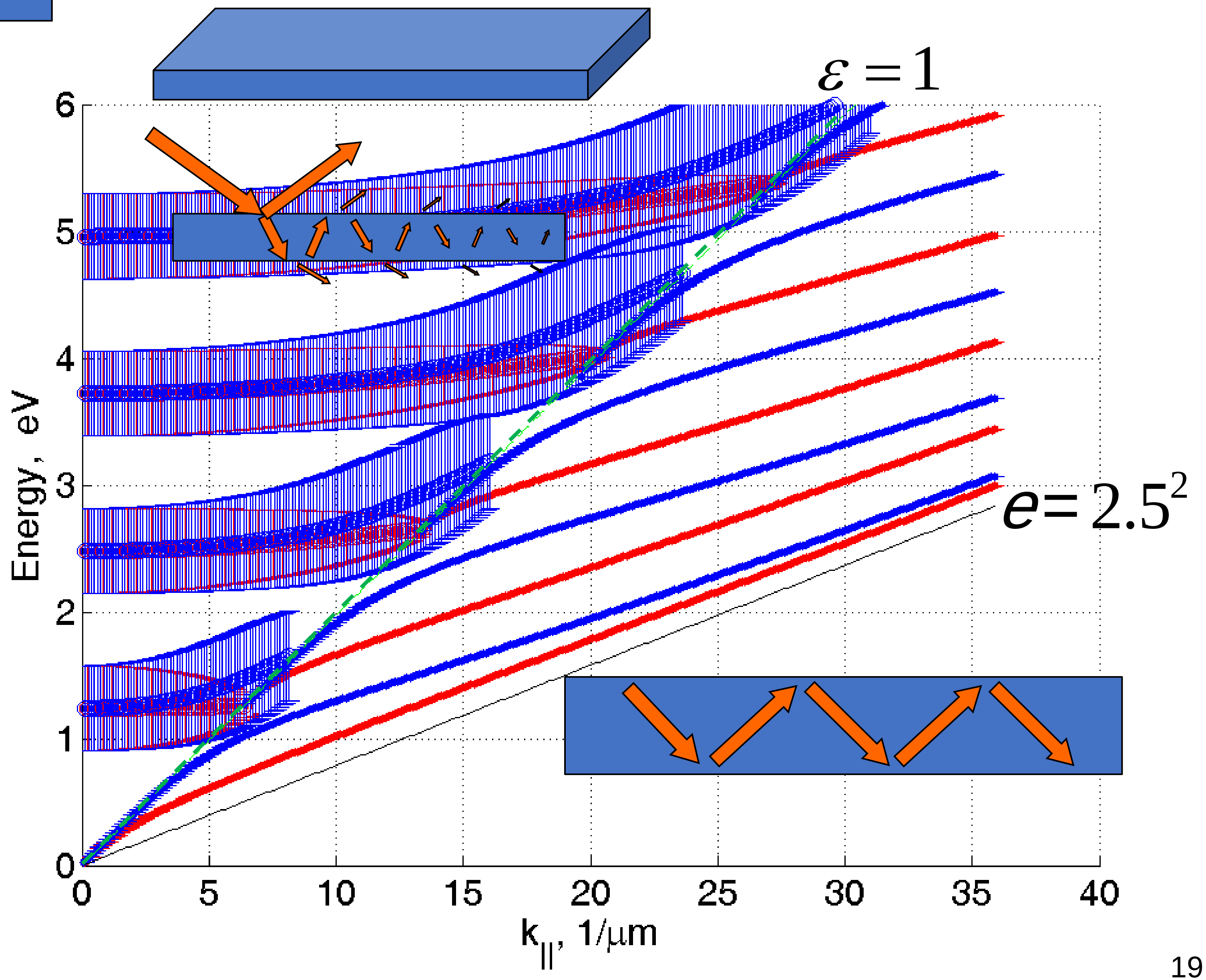

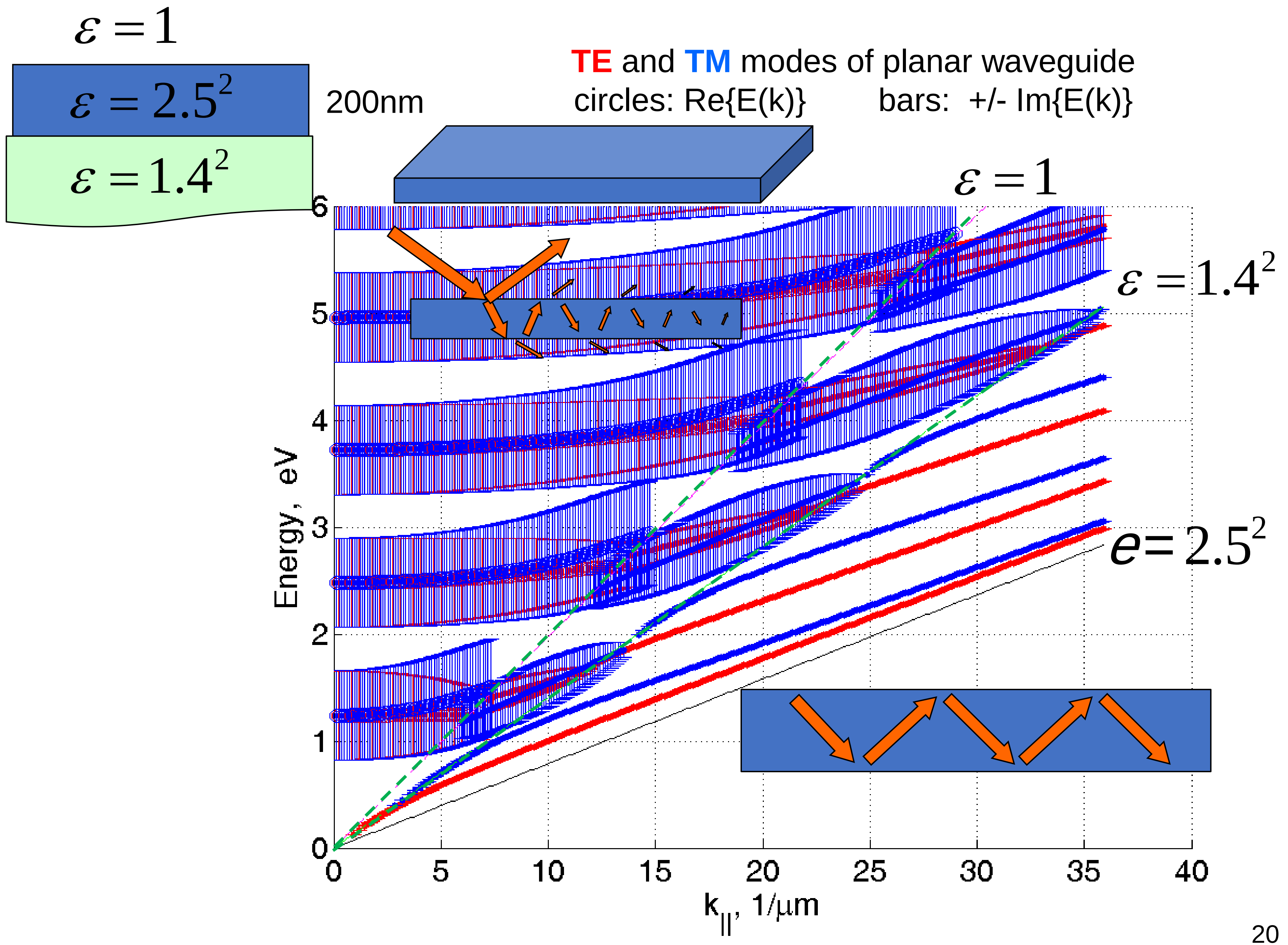

ε = 1
ε = 2.5²
ε = 1.4²
200nm
TE and TM modes of planar waveguide
circles: Re{E(k)}
bars: +/- Im{E(k)}
ε = 1
ε = 1.4²
e= 2.5²
Energy, eV
k||, 1/μm
0
1
2
3
4
5
6
0
5
10
15
20
25
30
35
40

Quasi-guided modes in *modulated* waveguide

$$k_z\left(G_x^n\right) = \sqrt{\frac{e_i}{c^2}w^2 - \left(k_x + G_x^n\right)^2}$$

$$E = \hbar\omega$$

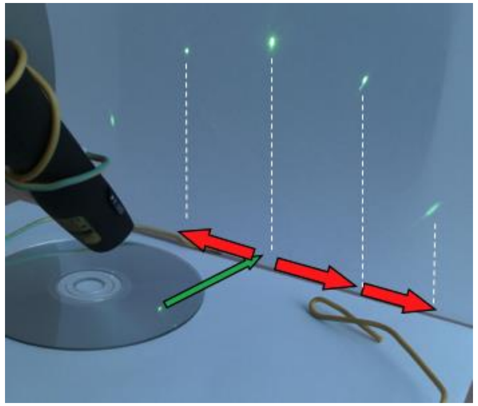

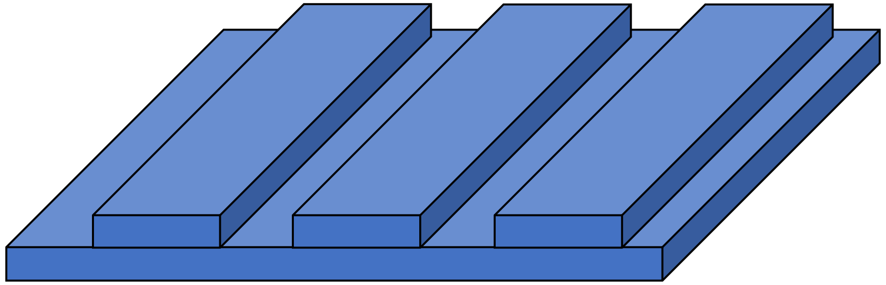

$$G_x^1 = \frac{2pi}{d}$$

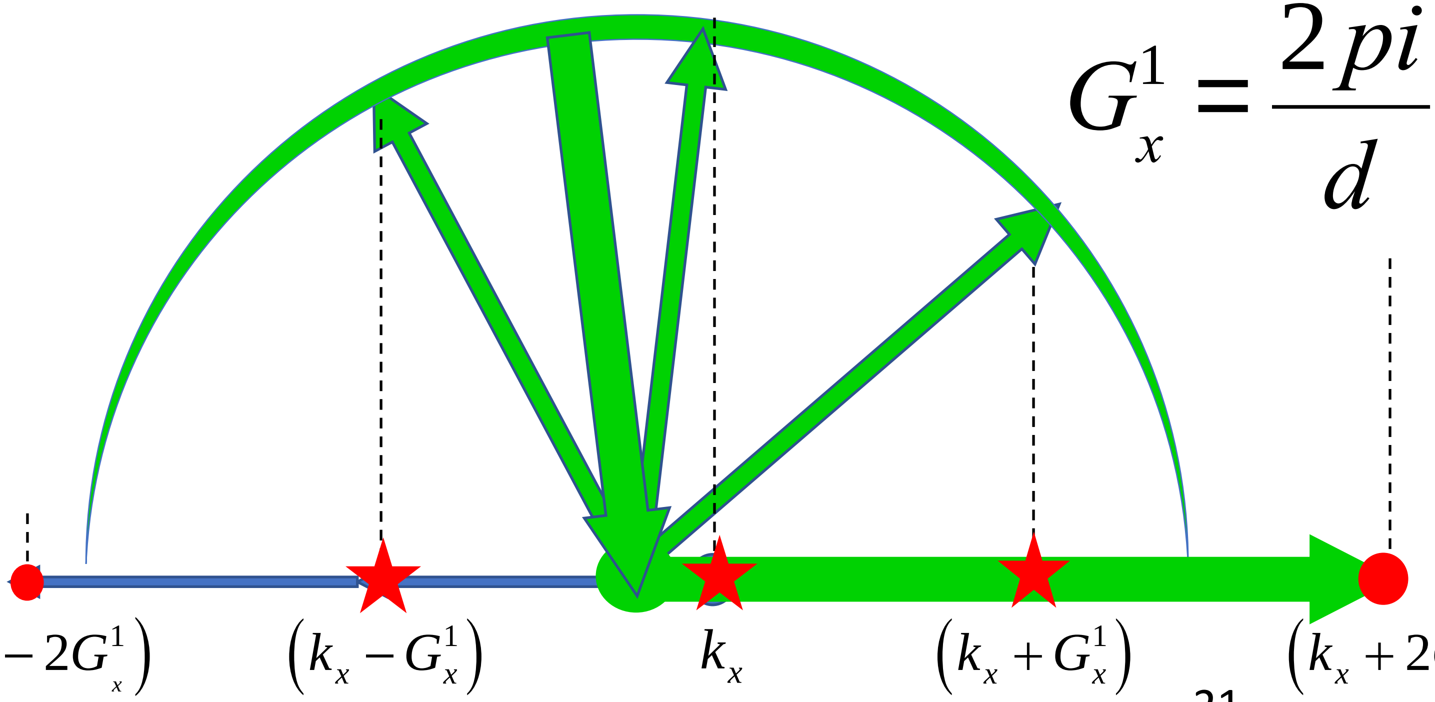

Quasi-guided modes in *modulated* waveguide

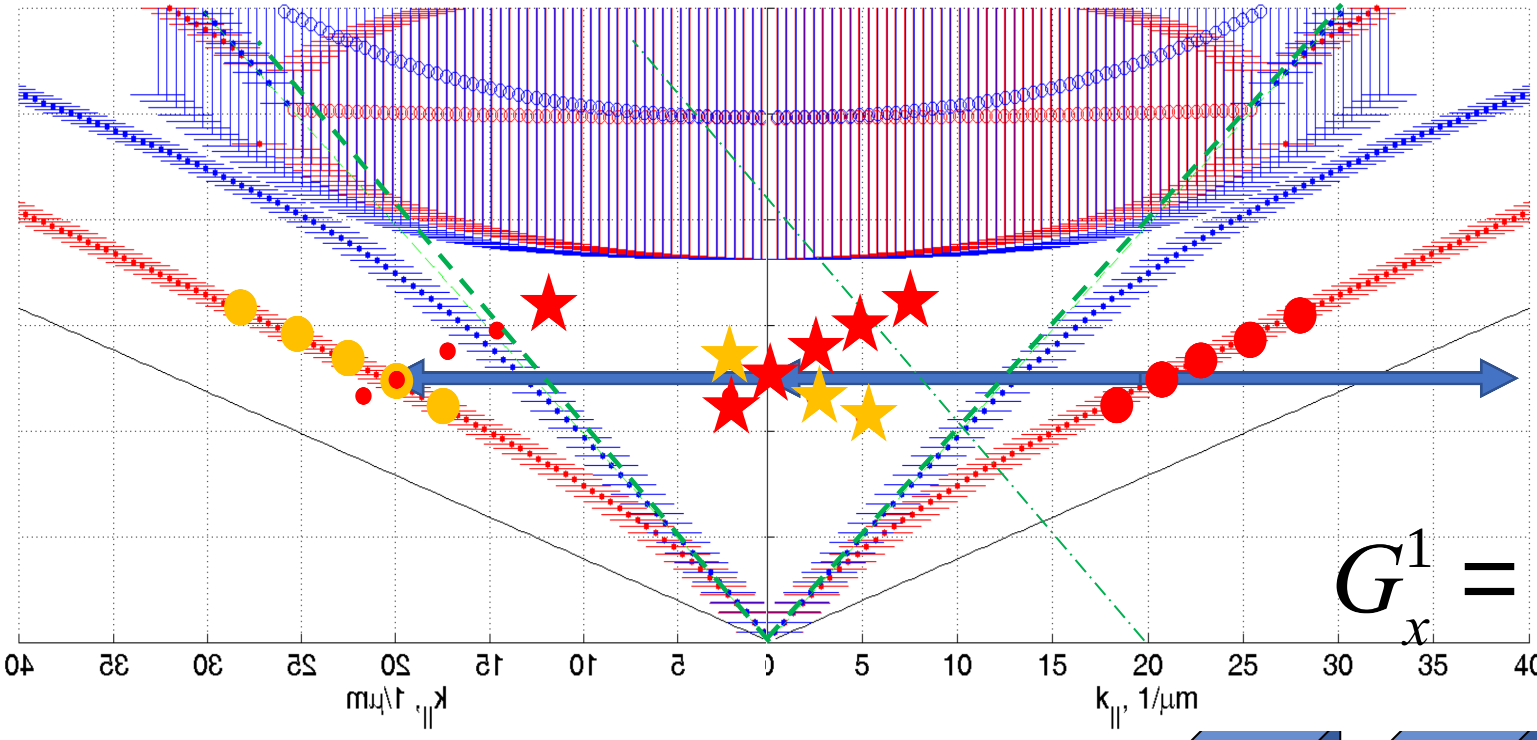

$$G_x^1 = \frac{2pi}{d}$$

$$k_z\left(G_x^n\right) = \sqrt{\frac{\varepsilon_i}{c^2}\omega^2 - \left(k_x + G_x^n\right)^2}$$

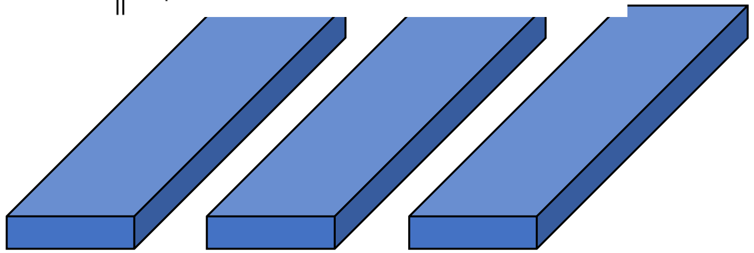

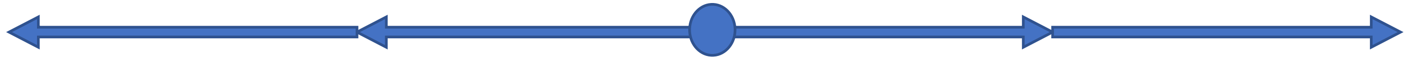

$\left(k_x - 2G_x^1\right)$ $\left(k_x - G_x^1\right)$ k_x $\left(k_x + G_x^1\right)$ $\left(k_x + 2G_x^1\right)$

Resonance is two S-matrix problem

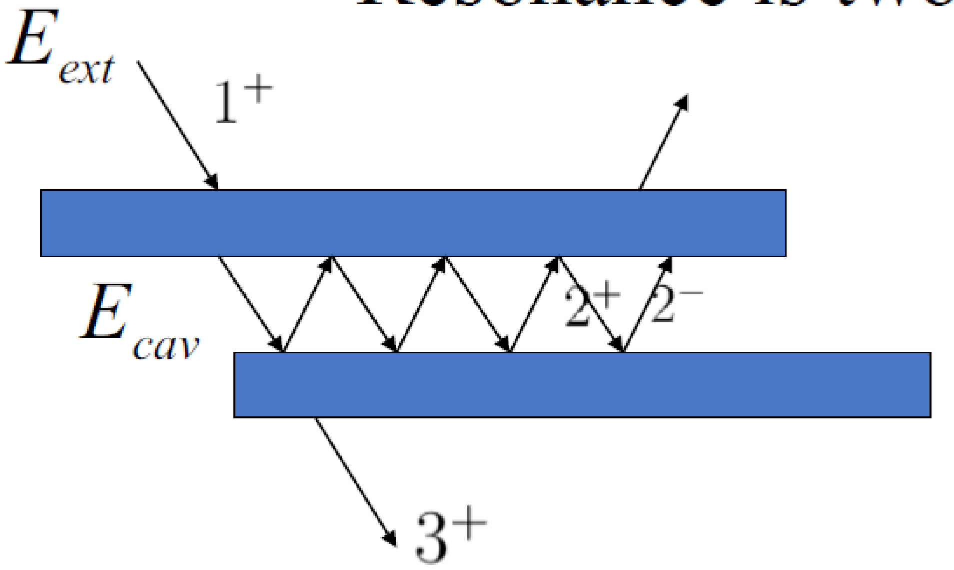

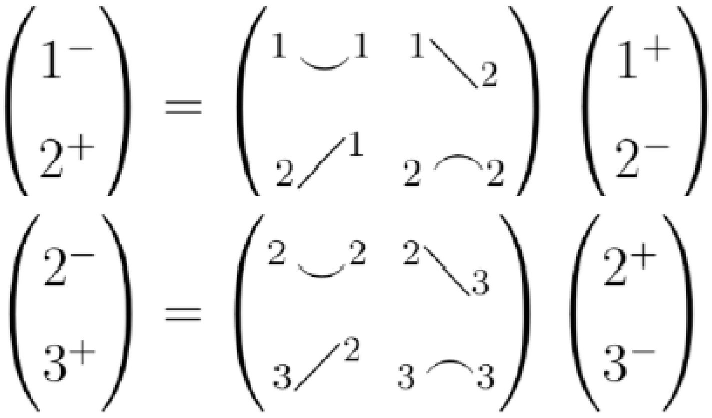

$$E_{cav} = \frac{1}{\omega - \omega_{cav}} \alpha E_{ext}$$

$$\omega_{cav} = \Omega_0 - i\gamma_0$$

PHYSICAL REVIEW B **66**, 045102 (2002)

Quasiguided modes and optical properties of photonic crystal slabs

S. G. Tikhodeev,[1] A. L. Yablonskii,[1] E. A. Muljarov,[1,2] N. A. Gippius,[1,2] and Teruya Ishihara[2]
[1]*General Physics Institute RAS, Vavilova 38, Moscow 119991, Russia*
[2]*Institute of Physical and Chemical Research (RIKEN), Wako 351-0198, Japan*
(Received 12 February 2002; published 8 July 2002)

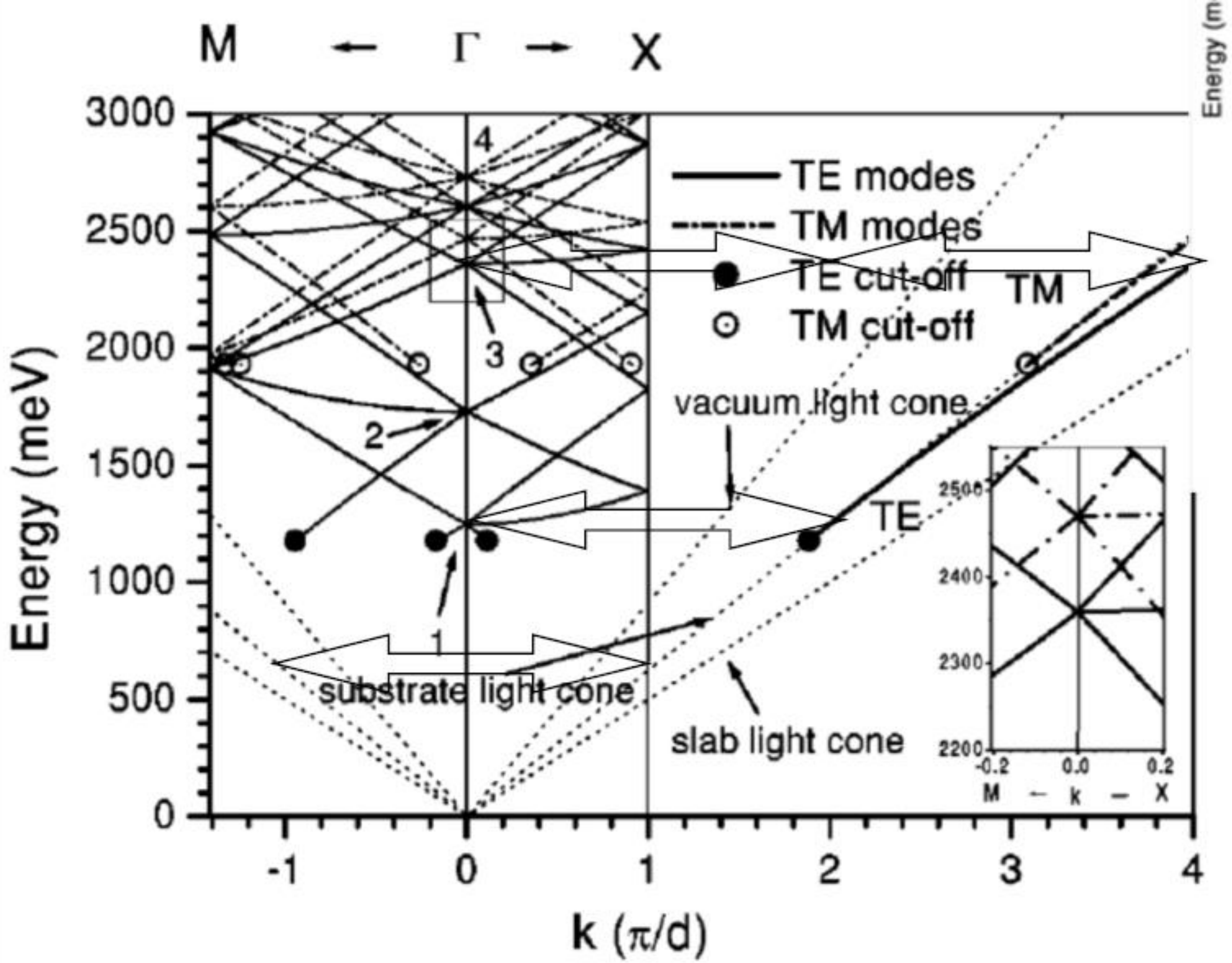

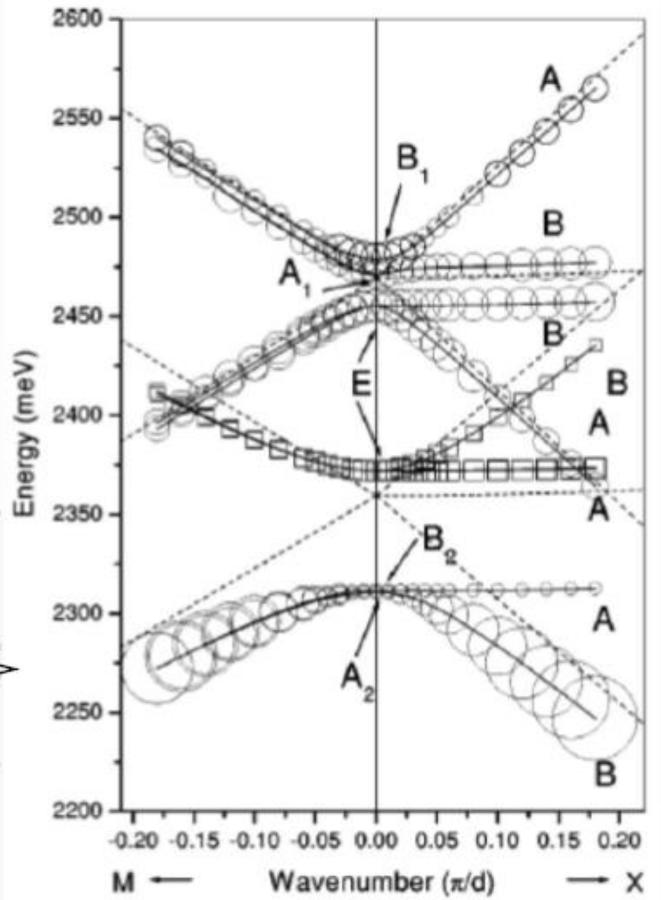

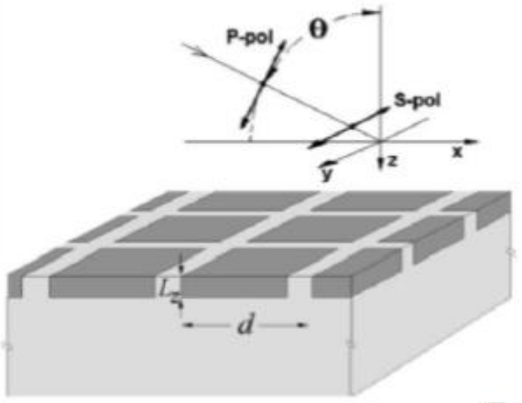

Resonant mode coupling of optical resonances in stacked nanostructures

Nikolay A. Gippius[1,2], Thomas Weiss[1,3]*,
Sergei G. Tikhodeev[2], and Harald Giessen[3]

[1] *LASMEA, University Blaise Pascal, 24 Avenue des Landais, 63177 Aubière Cedex, France*
[2] *A. M. Prokhorov General Physics Institute, RAS, Vavilova Street 38, Moscow 119991, Russia*
[3] *4th Physics Institute and Research Center SCOPE, University of Stuttgart, Pfaffenwaldring 57, 70550 Stuttgart, Germany*

*t.weiss@physik.uni-stuttgart.de

Received 4 Feb 2010; revised 24 Mar 2010; accepted 24 Mar 2010; published 26 Mar 2010
29 March 2010 / Vol. 18, No. 7 / OPTICS EXPRESS 7569

$$(\omega - \omega_n^{\mathrm{a}})\alpha_n = \sum_{m=1}^{N} \langle I_{u,n}^{\mathrm{a}} | \tilde{\mathrm{S}}_{ud}^{\mathrm{b}} | \mathbf{O}_{d,m}^{\mathrm{a}} \rangle \alpha_m + \sum_{m=1}^{M} \langle I_{u,n}^{\mathrm{a}} | \mathbf{O}_{u,m}^{\mathrm{b}} \rangle \beta_m$$

$$(\omega - \omega_n^{\mathrm{b}})\beta_n = \sum_{m=1}^{N} \langle I_{d,n}^{\mathrm{b}} | \mathbf{O}_{d,m}^{\mathrm{a}} \rangle \alpha_m + \sum_{m=1}^{M} \langle I_{d,n}^{\mathrm{b}} | \tilde{\mathrm{S}}_{du}^{\mathrm{a}} | \mathbf{O}_{u,m}^{\mathrm{b}} \rangle \beta_m$$

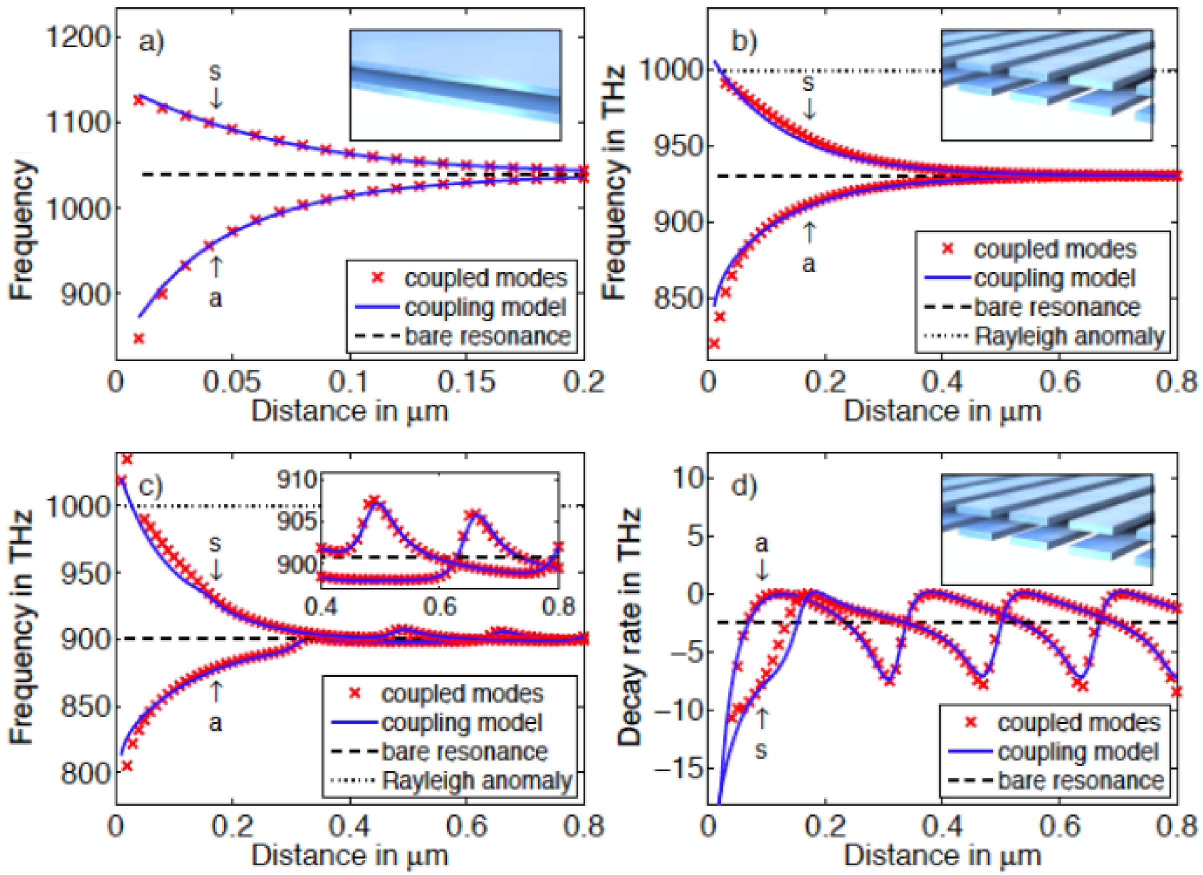

Bykov, Dmitry A.; Doskolovich, Leonid L. (2013). *Numerical Methods for Calculating Poles of the Scattering Matrix With Applications in Grating Theory. Journal of Lightwave Technology, 31(5), 793–801.* doi:10.1109/jlt.2012.2234723

$$1/\det S(\omega) = 0. \tag{10}$$

$$\omega_{n+1} = \omega_n - \min\operatorname{eig}\left(S^{-1}(\omega_n), \left.\frac{\mathrm{d}S^{-1}}{\mathrm{d}\omega}\right|_{\omega_n}\right), \tag{15}$$

$$\omega_{n+1} = \omega_n + 2\,\min\operatorname{eig}\left(U_r^{\dagger} S'(\omega_n) V_r \Sigma_r^{-1}\right). \tag{19}$$

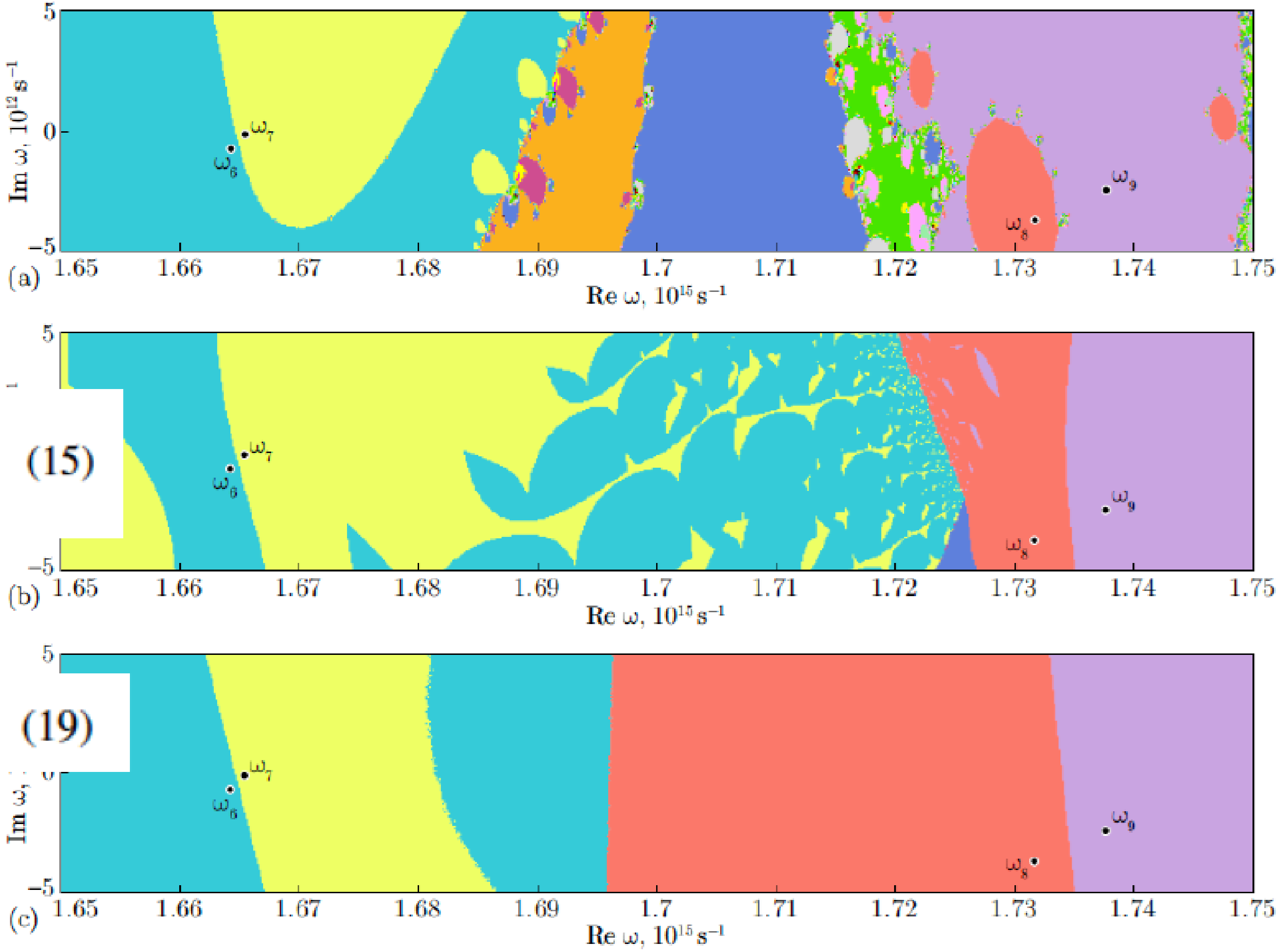

Fig. 2. (Color online) Basins of attraction (different colors denote different attraction poles): (a) Newton for Eq. (10); (b) Eq. (15); (c) Eq. (19).

2. Сколько можно считать одно и тоже ?!

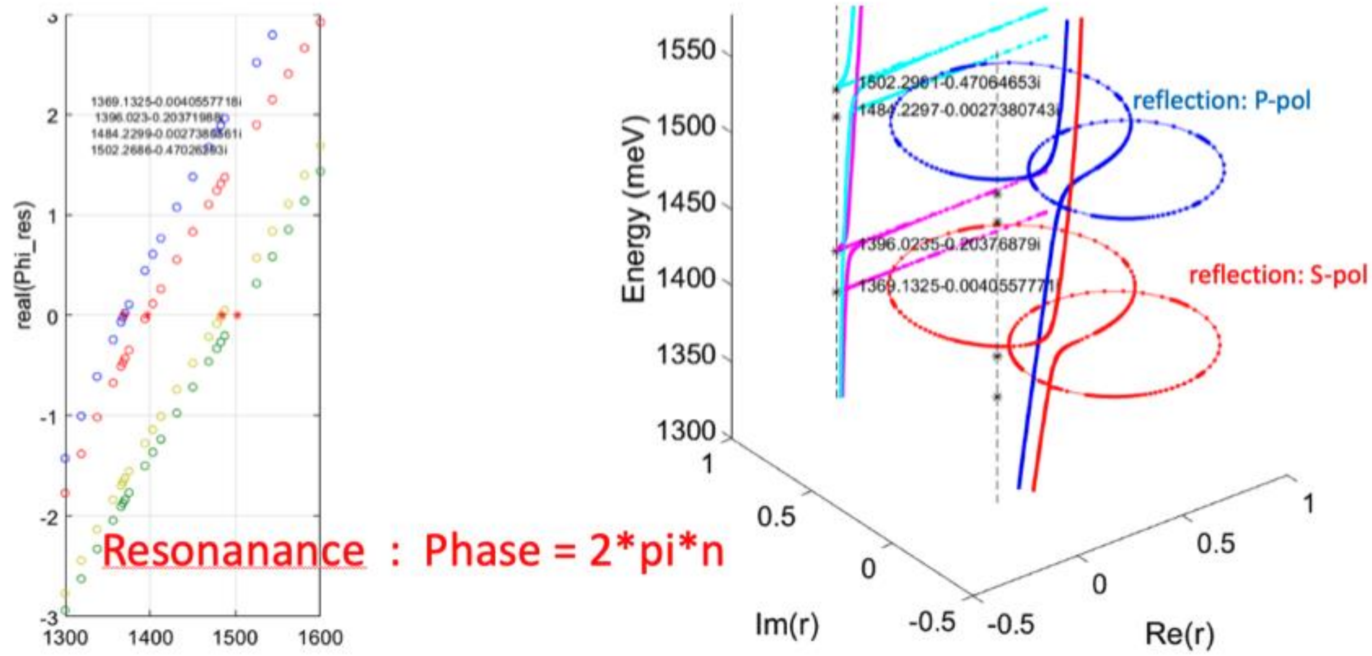

Resonance is two S-matrix problem

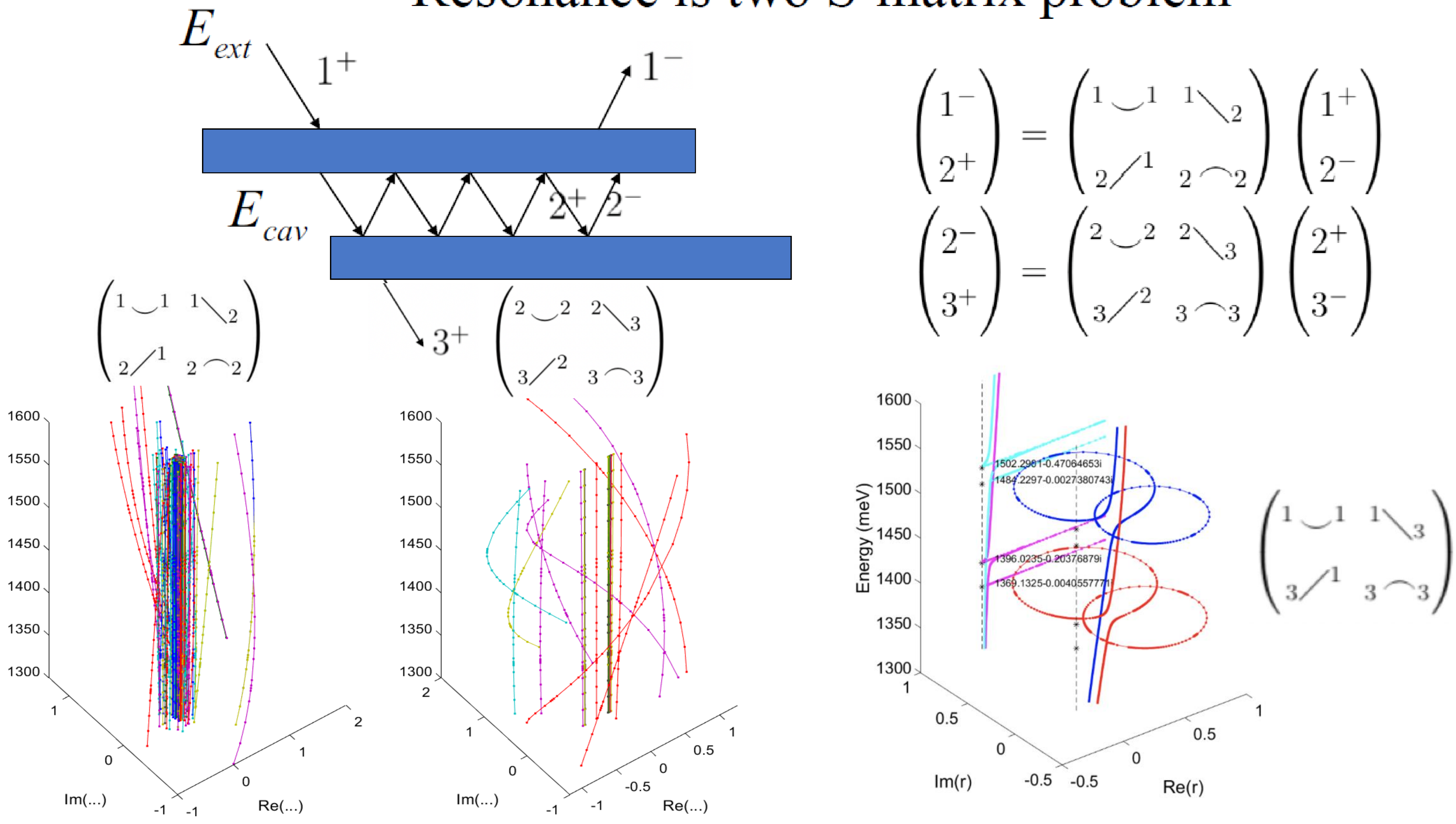

Resonances – two S-marix problem

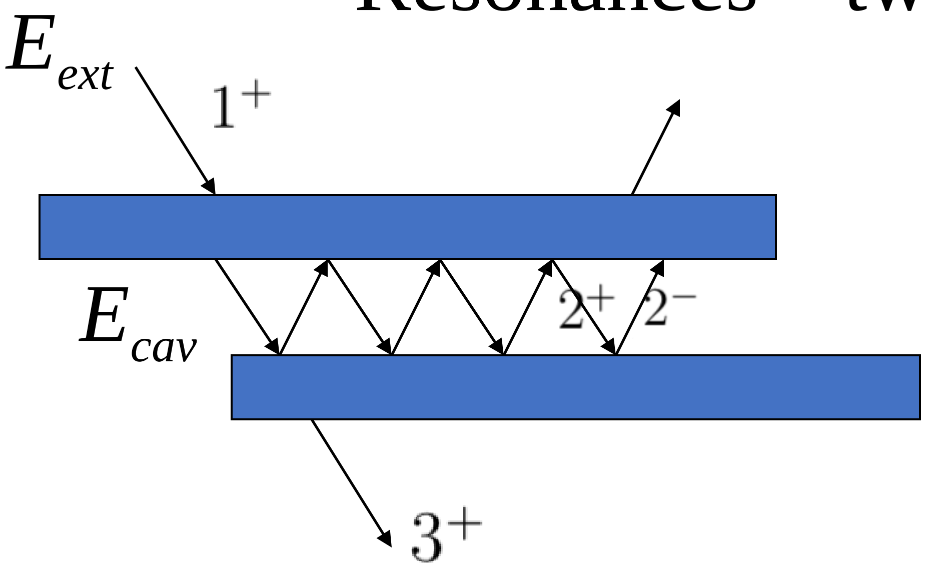

$$\begin{pmatrix} 1^- \\ 2^+ \end{pmatrix} = \begin{pmatrix} {}^1\smile^1 & {}^1\diagdown_2 \\ {}_2\diagup^1 & {}_2\frown_2 \end{pmatrix} \begin{pmatrix} 1^+ \\ 2^- \end{pmatrix}$$

$$\begin{pmatrix} 2^- \\ 3^+ \end{pmatrix} = \begin{pmatrix} {}^2\smile^2 & {}^2\diagdown_3 \\ {}_3\diagup^2 & {}_3\frown_3 \end{pmatrix} \begin{pmatrix} 2^+ \\ 3^- \end{pmatrix}$$

$$\begin{pmatrix} {}^1\smile^1 & {}^1\diagdown_3 \\ {}_3\diagup^1 & {}_3\frown_3 \end{pmatrix} = \begin{pmatrix} {}^1\smile^1 + {}^1\diagdown_2 {}^2\smile^2 {}_2\diagup^1 + \dots & {}^1\diagdown_2 {}^2\diagdown_3 + {}^1\diagdown_2 {}^2\smile^2 {}_2\frown_2 {}^2\diagdown_3 + \dots \\ {}_3\diagup^2 {}_2\diagup^1 + {}_3\diagup^2 {}_2\frown_2 {}^2\smile^2 {}_2\diagup^1 + \dots & {}_3\frown_3 + {}_3\diagup^2 {}_2\frown_2 {}^2\diagdown_3 + \dots \end{pmatrix}$$

$$[1 - {}^2\smile^2(E,\mathbf{k})\,{}_2\frown_2(E,\mathbf{k})]^{-1}$$

$$[1 - {}_2\frown_2(E,\mathbf{k})\,{}^2\smile^2(E,\mathbf{k})]^{-1}$$

$$S_1^{ab} t^b s_2^{ba} t^a X = X e^{i\Phi}, \quad \Phi = \Phi(k_0, k_{||})$$

Roundtrip phase of resonant mode

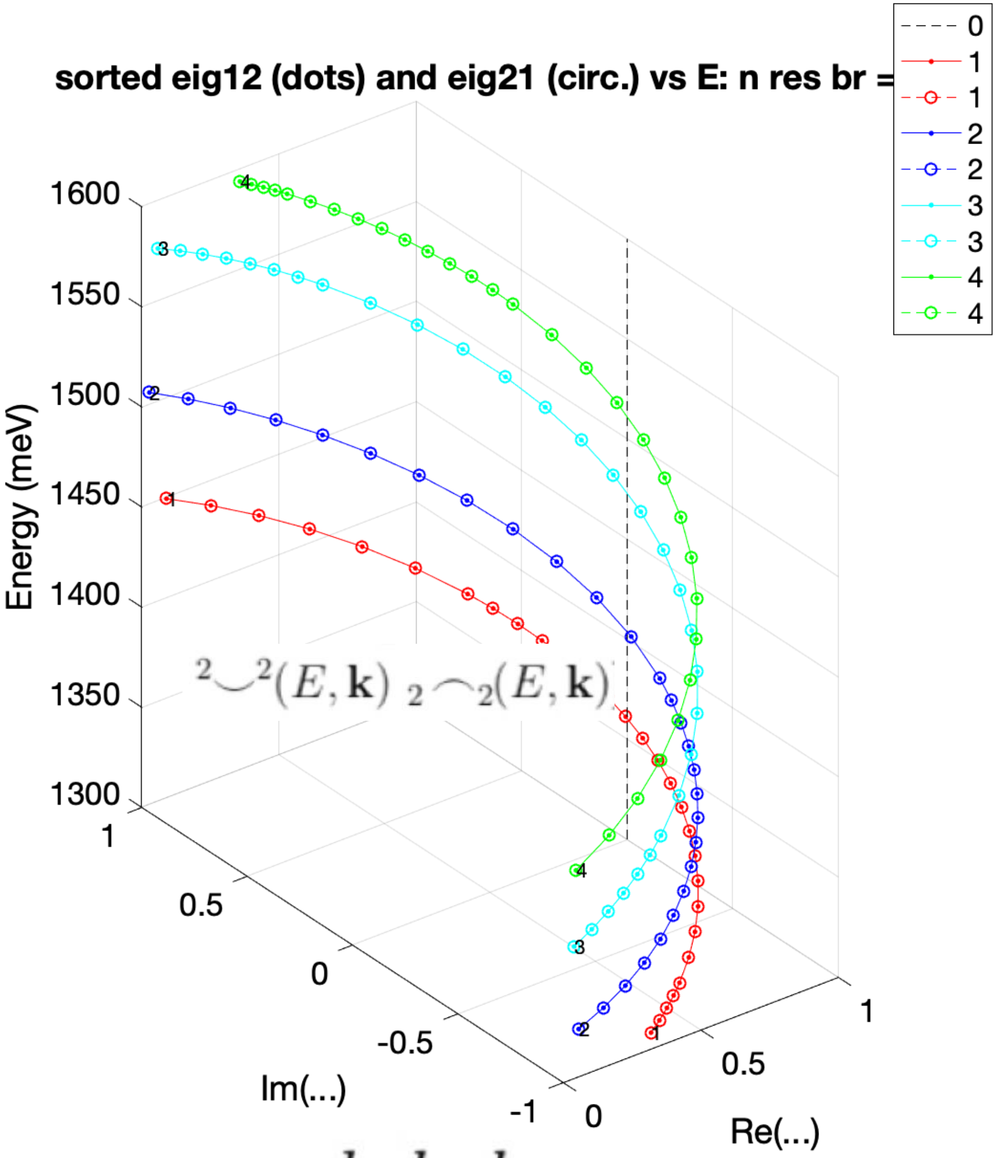

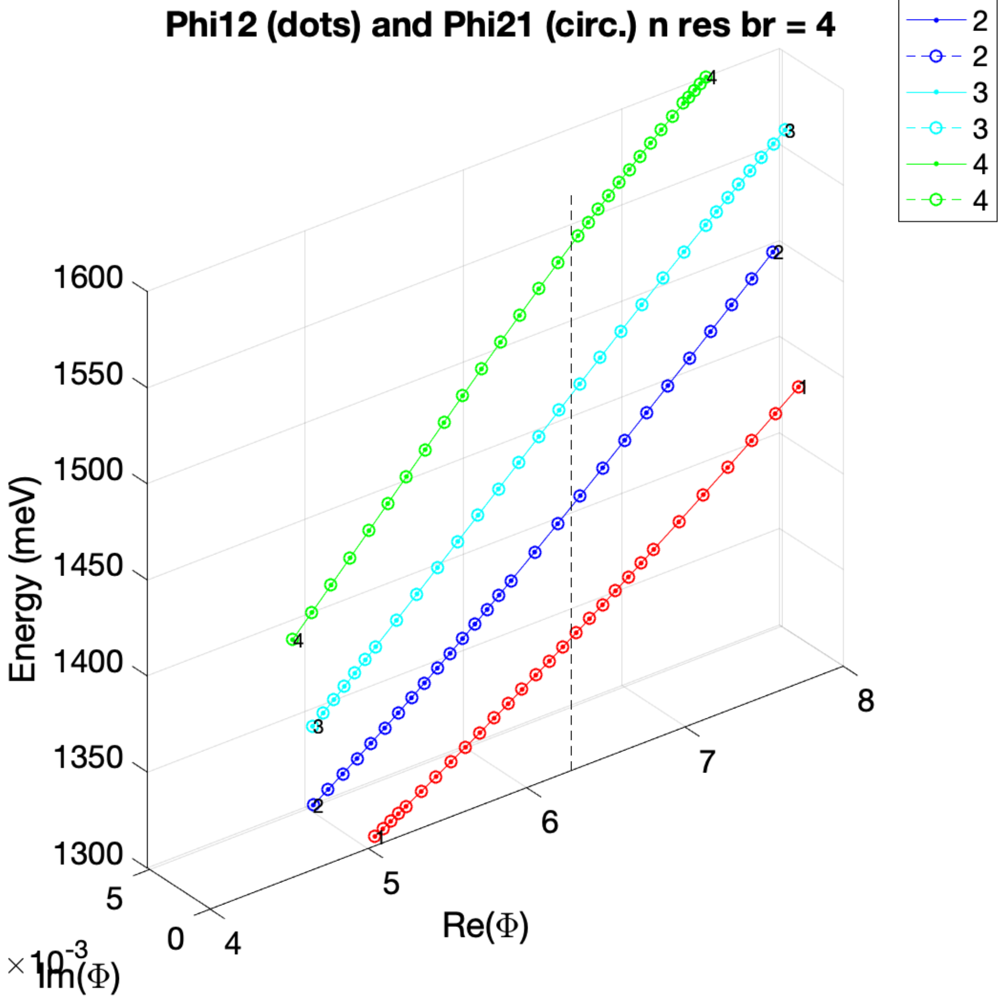

$S_1^{ab} t^b s_2^{ba} t^a$ = 1. Resonanance $\Phi(k_0, k_{||})$ = 2*pi*n

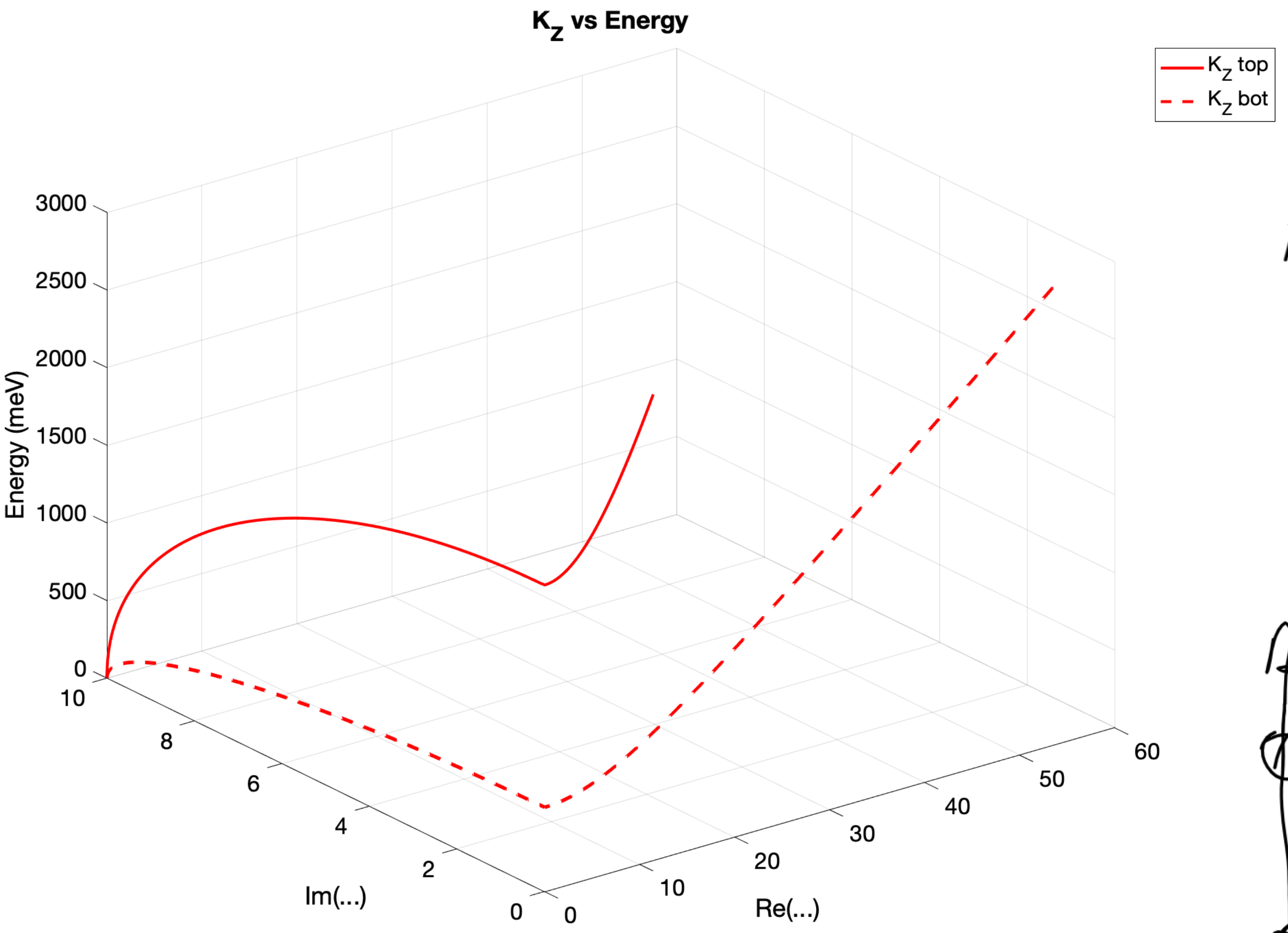

$$k_0 = \frac{\omega}{c}, \quad k_z = \sqrt{k_0^2 \varepsilon - k_{||}^2}, \quad k_y = 0$$

$$r_s^w = \frac{k_z^w - k_z^i}{k_z^w + k_z^i} \quad r_p^w = \frac{k_z^i \varepsilon^w - k_z^w \varepsilon^i}{k_z^i \varepsilon^w + k_z^w \varepsilon^i}$$

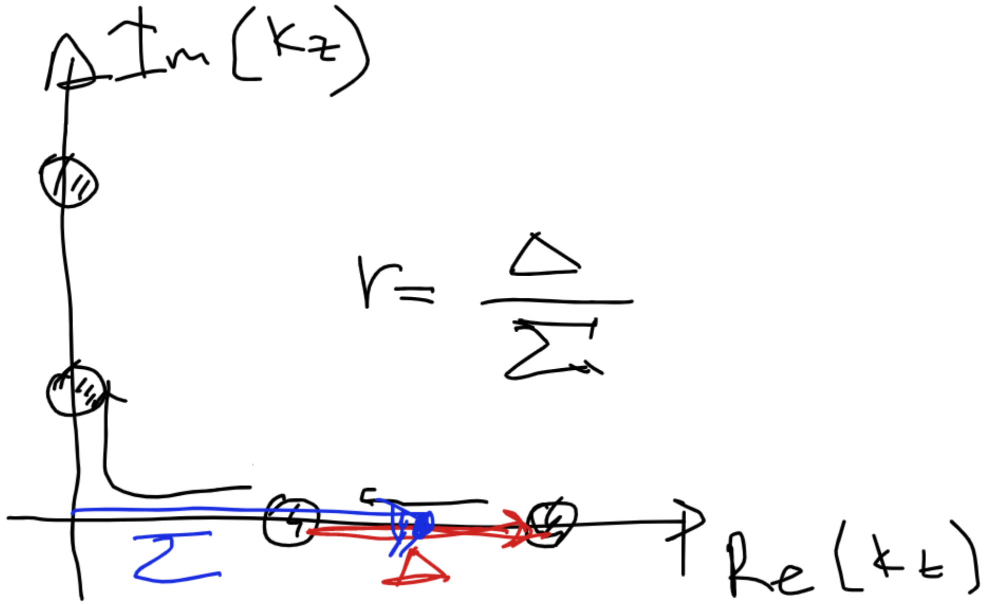

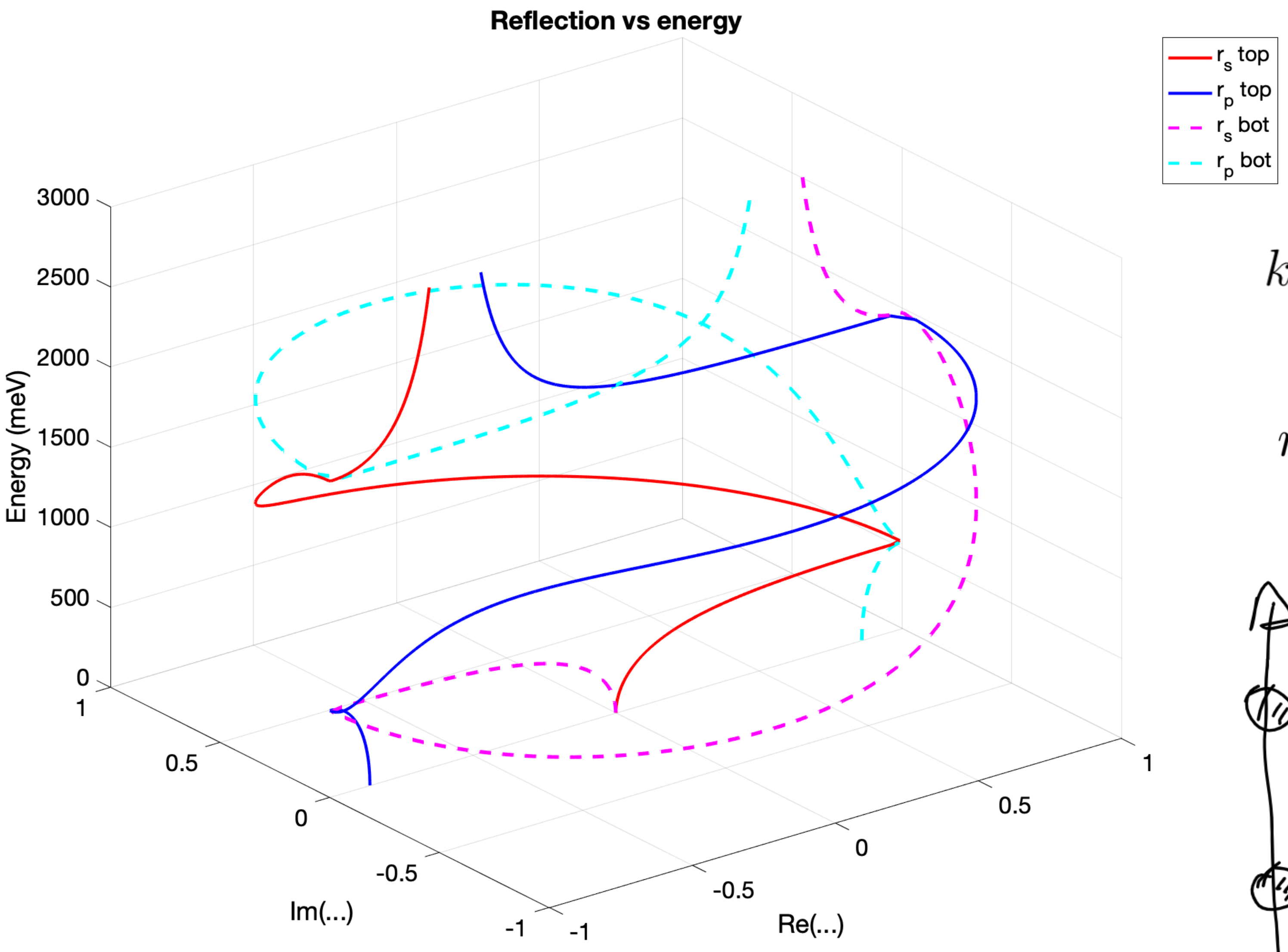

$$k_0 = \frac{\omega}{c}, \quad k_z = \sqrt{k_0^2 \varepsilon - k_{||}^2}, \quad k_y = 0$$

$$r_s^w = \frac{k_z^w - k_z^i}{k_z^w + k_z^i} \quad r_p^w = \frac{k_z^i \varepsilon^w - k_z^w \varepsilon^i}{k_z^i \varepsilon^w + k_z^w \varepsilon^i}$$

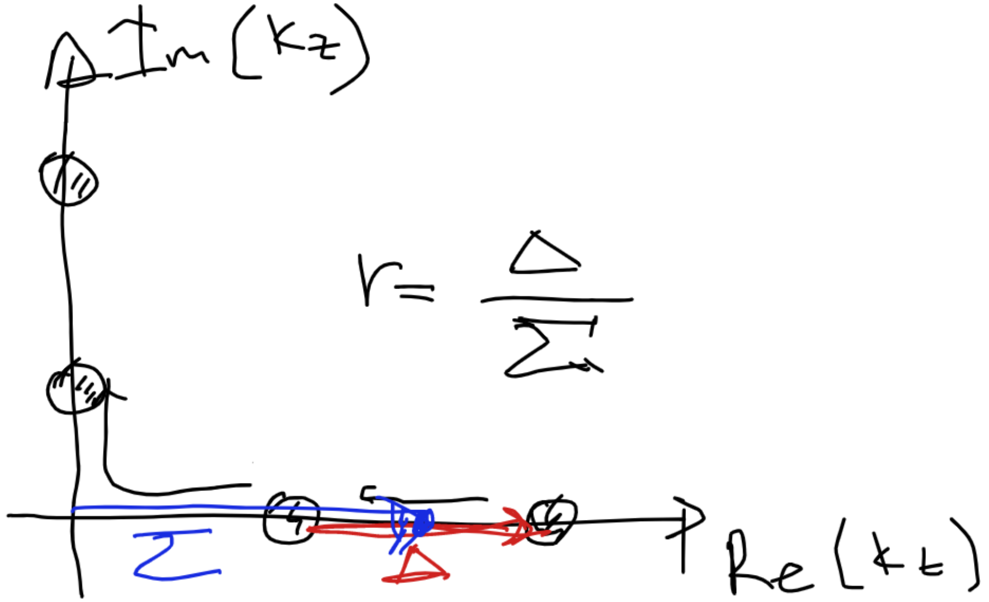

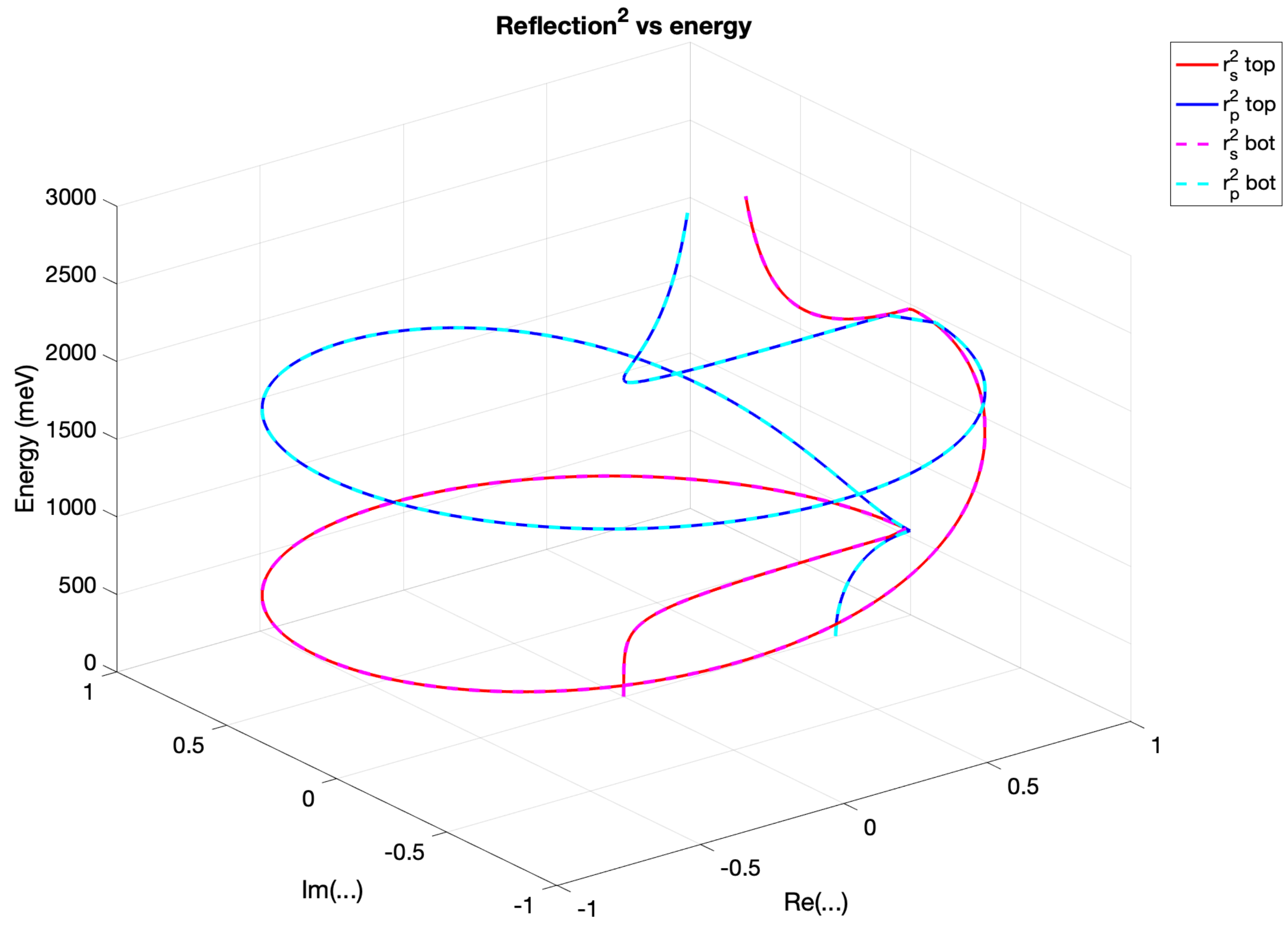

$$k_0 = \frac{\omega}{c}, \quad k_z = \sqrt{k_0^2 \varepsilon - k_{||}^2}, \quad k_y = 0$$

$$r_s^w = \frac{k_z^w - k_z^i}{k_z^w + k_z^i} \quad r_p^w = \frac{k_z^i \varepsilon^w - k_z^w \varepsilon^i}{k_z^i \varepsilon^w + k_z^w \varepsilon^i}$$

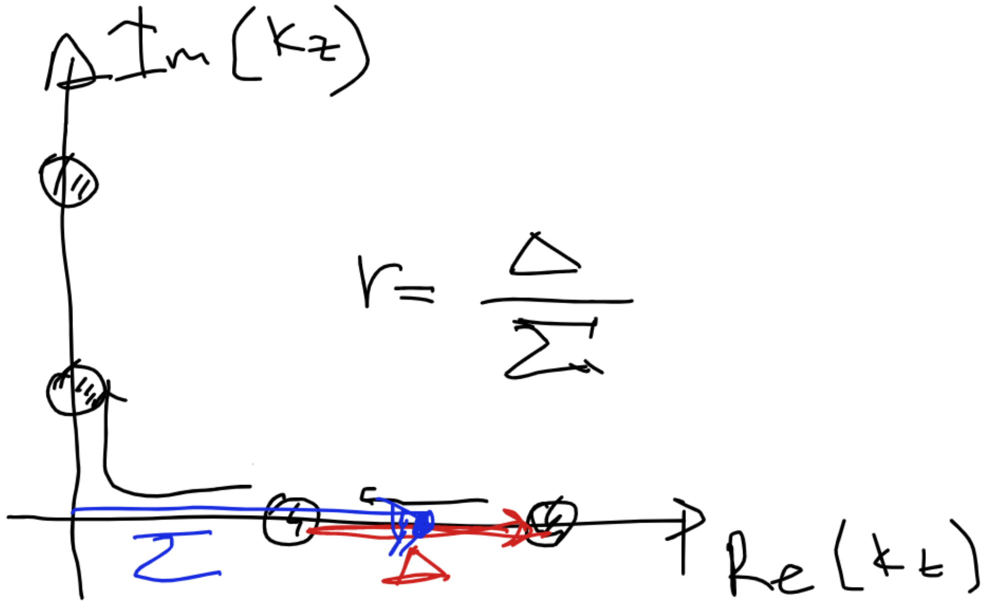

$$S_1^{ab} t^b s_2^{ba} t^a X = X e^{i\Phi}, \quad \Phi = \Phi(k_0, k_{||})$$

Roundtrip phase of resonant mode

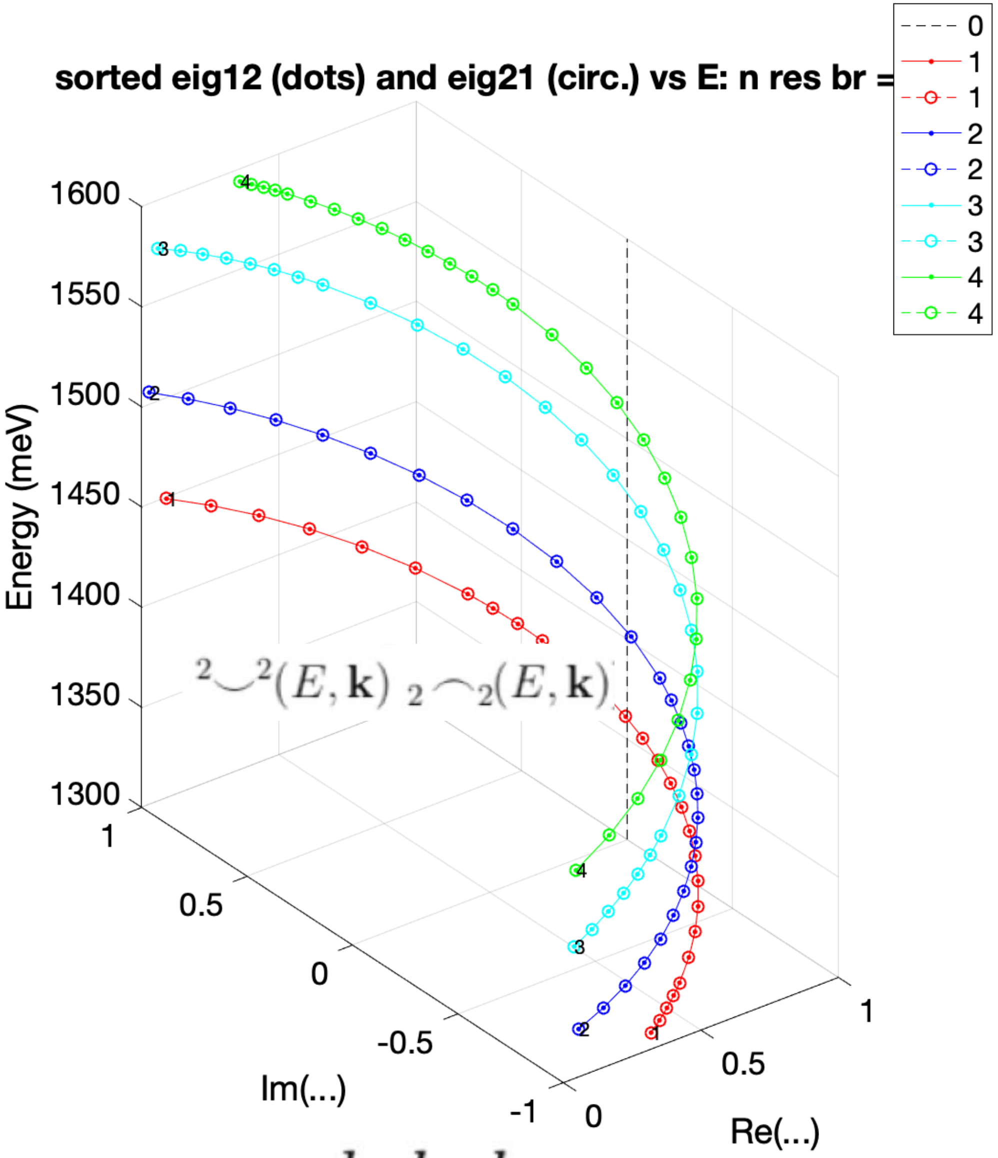

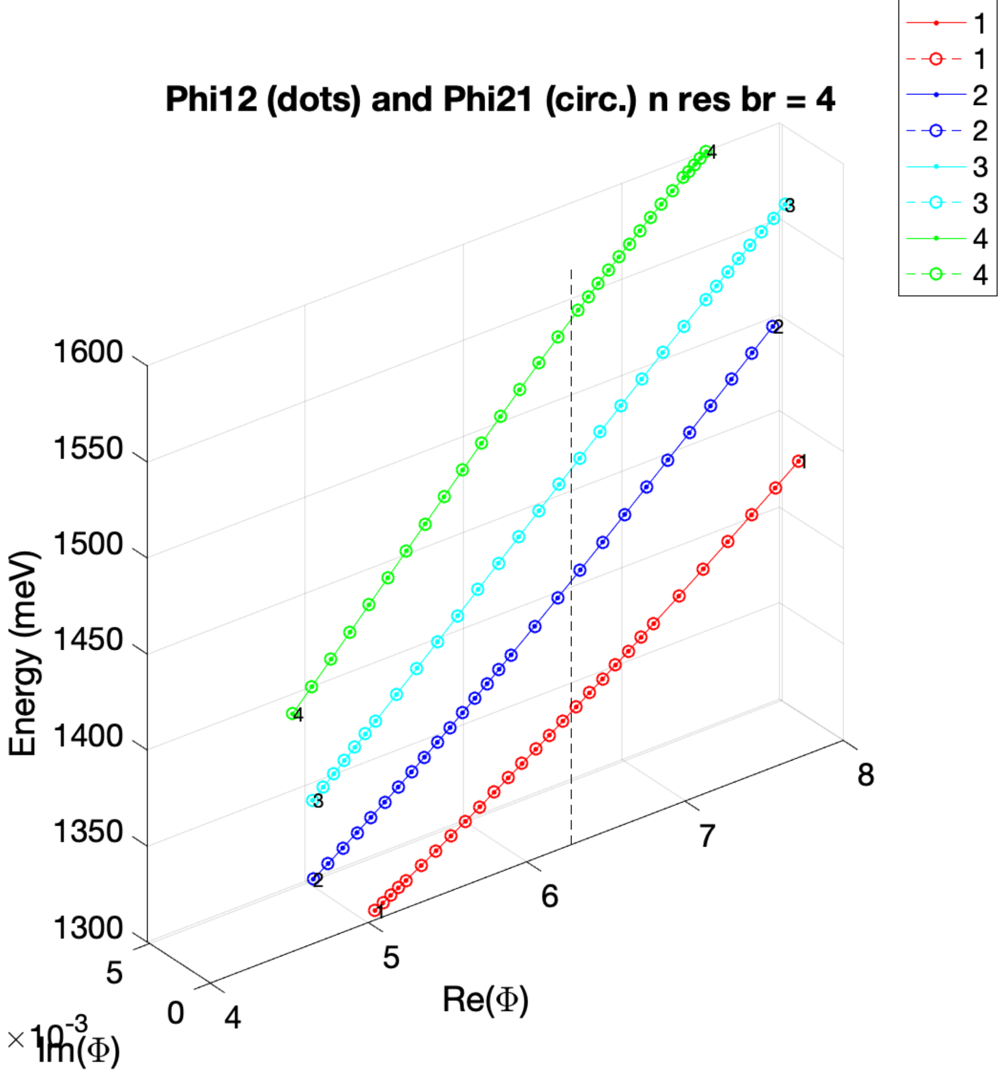

$S_1^{ab} t^b s_2^{ba} t^a$ = 1. Resonanance $\Phi(k_0, k_{||})$ = 2*pi*n

Roundtrip phase of resonant mode is smooth function of energy

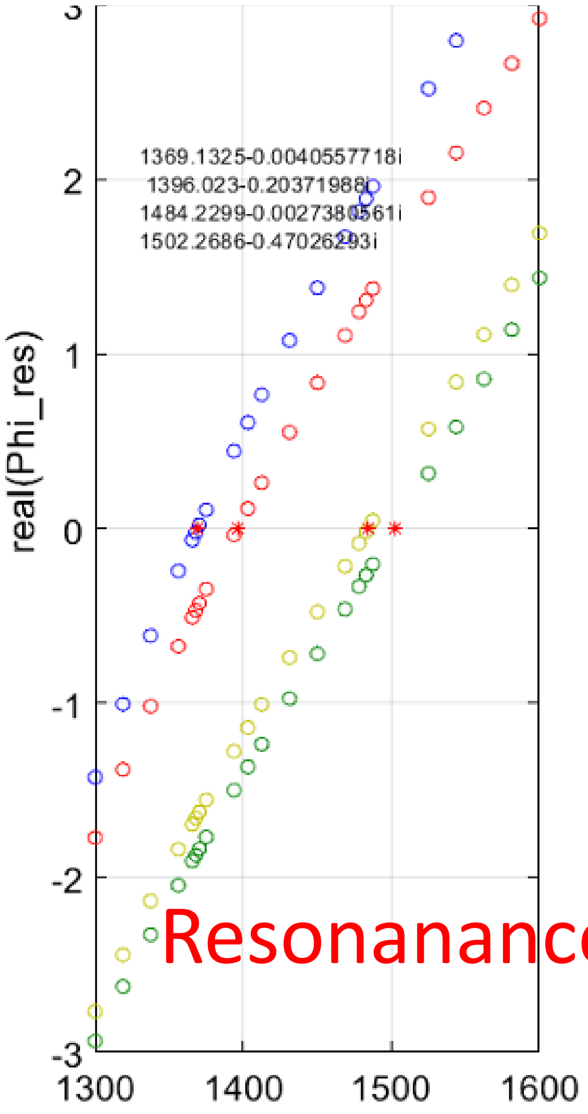

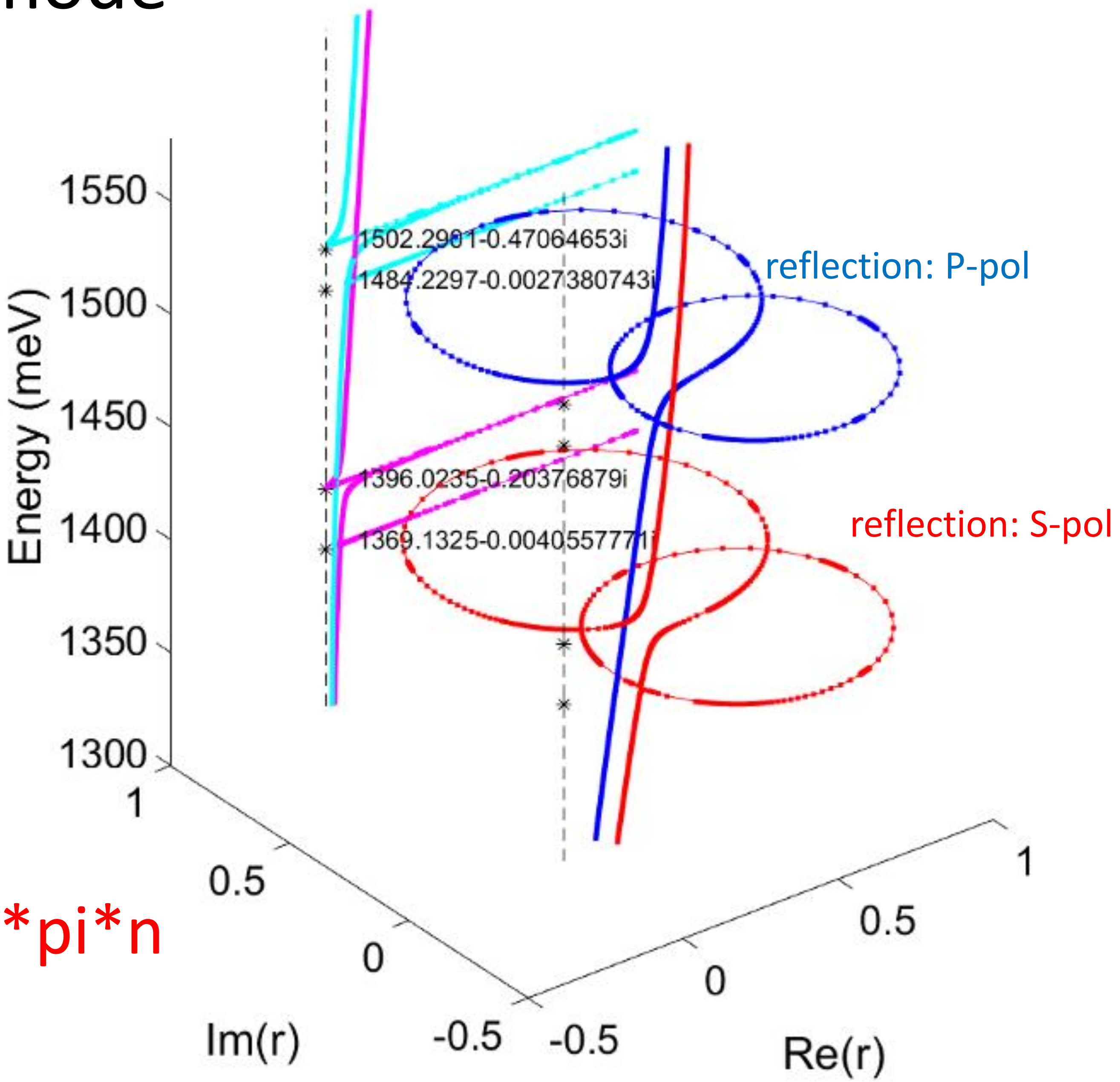

Resonanance : Phase = 2*pi*n

Reflection near resonances is well described

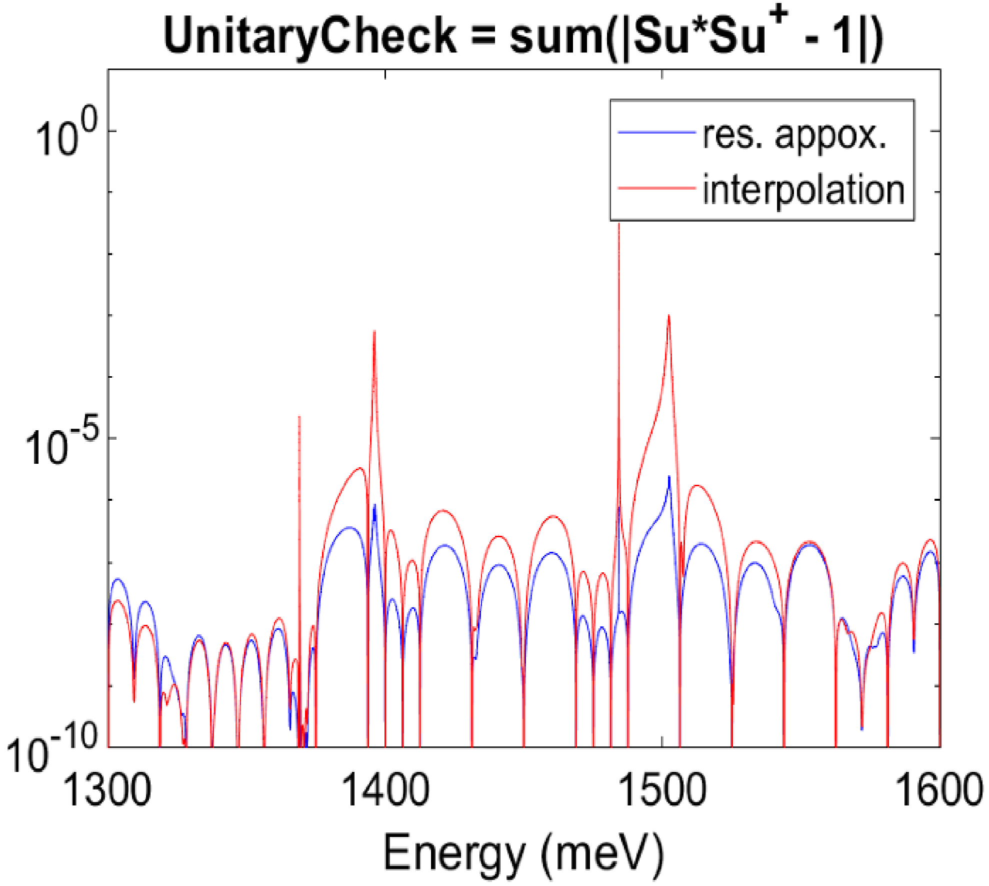

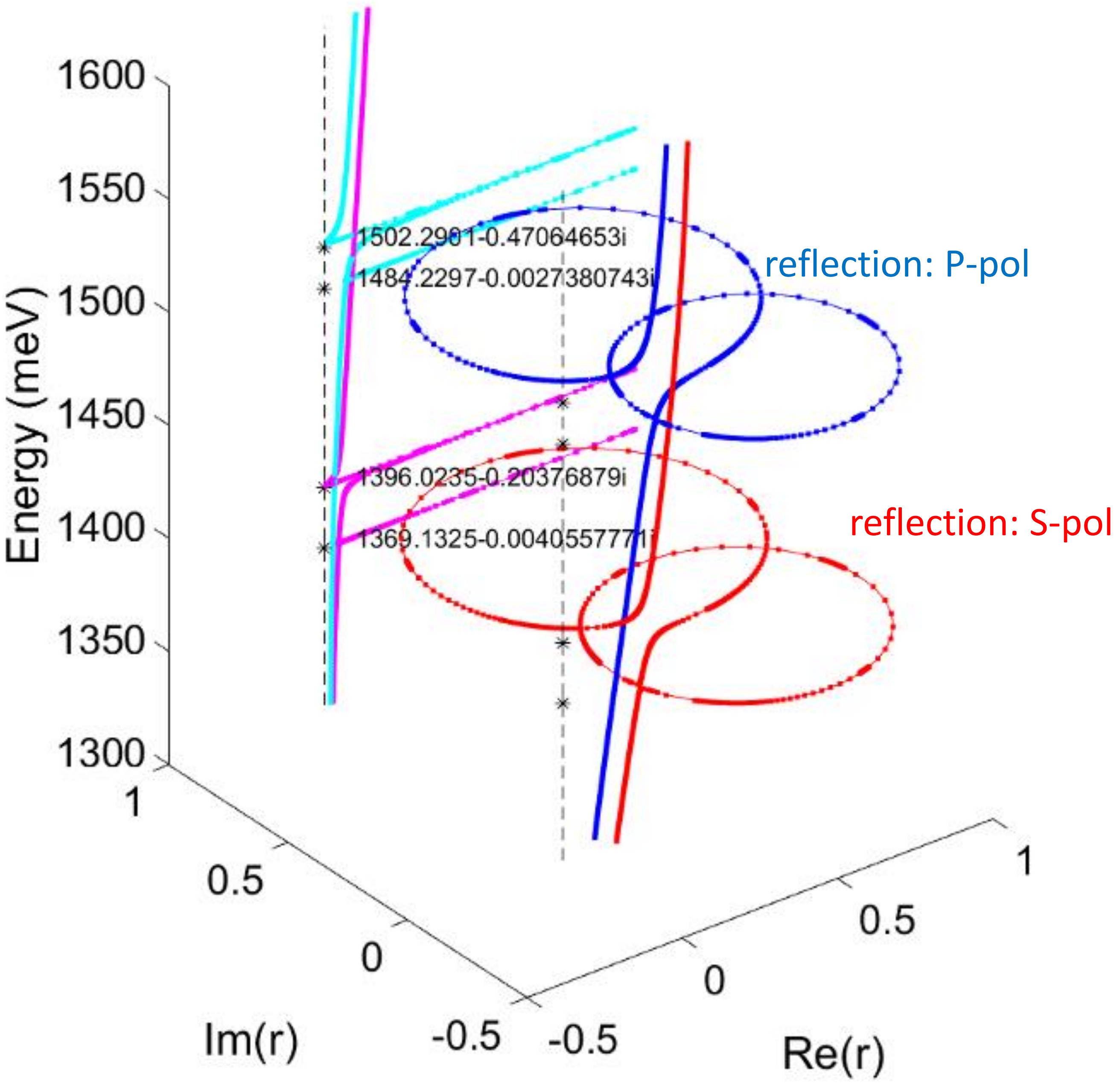

3. Как раскалываются резонансы ?

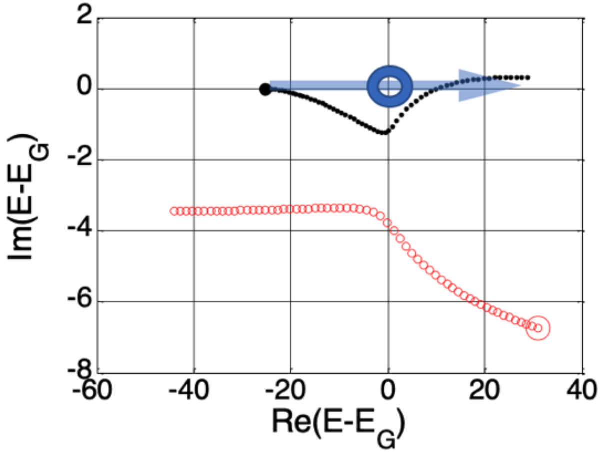

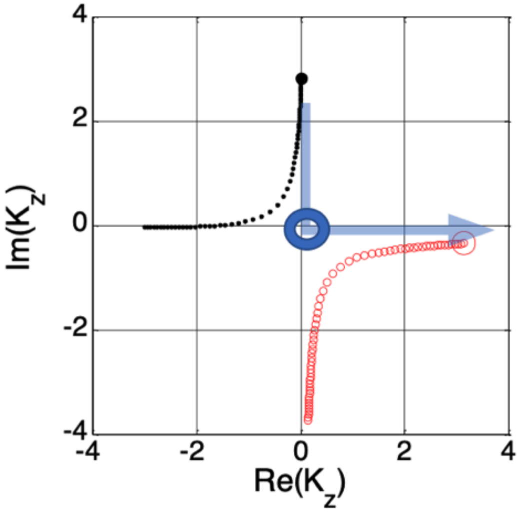

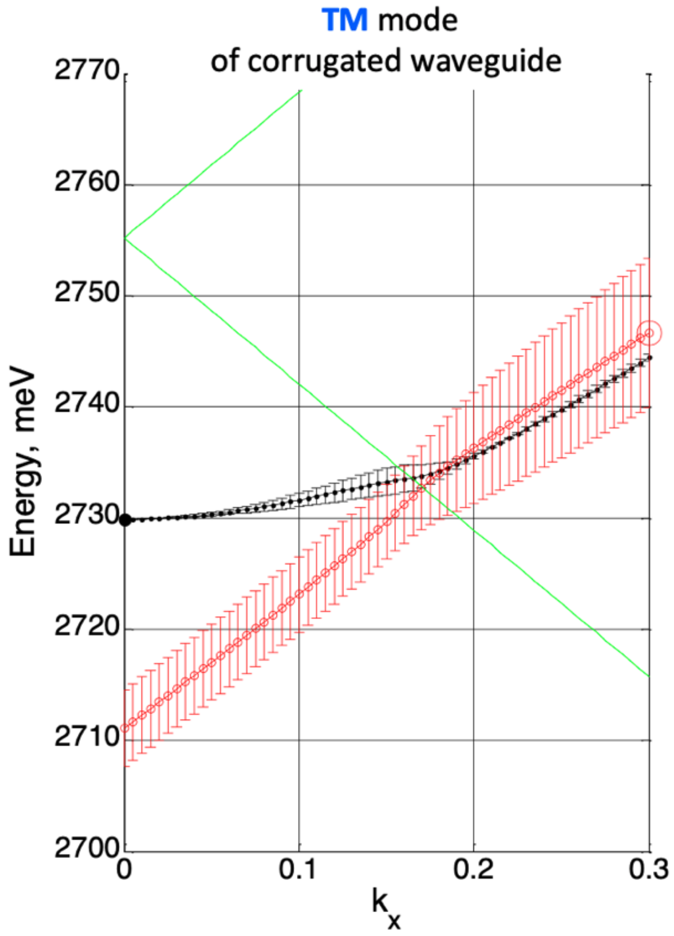

SOVIET PHYSICS JETP VOLUME 26, NUMBER 4 APRIL, 1968

ON THRESHOLD PHENOMENA IN CLASSICAL ELECTRODYNAMICS

B. M. BOLOTOVSKIĬ and A. N. LEBEDEV

P. N. Lebedev Physical Institute, Academy of Sciences, U.S.S.R.

Submitted April 21, 1967

Zh. Eksp. Teor. Fiz. 53, 1349–1352 (October, 1967)

It is shown that for a wide class of problems in electrodynamics, the behavior of the amplitudes and phases at the threshold for the production of new proper waves can be determined from the conservation laws. The method proposed, which is analogous to the quantum theory of many-channel nuclear reactions, is employed for an explanation of the Wood anomalies.

$$\psi_n^{\pm} = \exp\left[iy\left(k_y - \frac{2\pi n}{d}\right) \pm iz\left[\frac{\omega^2}{c^2} - \left(k_y - \frac{2\pi n}{d}\right)^2\right]^{1/2}\right],$$

$$n = 0, \pm 1, \pm 2\ldots$$

$$\varkappa_j = \left[\frac{\omega^2}{c^2} - \left(k_y - \frac{2\pi j}{d}\right)^2\right]^{1/2}$$

SOVIET PHYSICS JETP VOLUME 30, NUMBER 1 JANUARY 1970

CONTRIBUTION TO THE THEORY OF THRESHOLD PHENOMENA IN DIFFRACTION OF ELECTROMAGNETIC WAVES

B. M. BOLOTOVSKIĬ and K. I. KUGEL'

P. N. Lebedev Physics Institute, U.S.S.R. Academy of Sciences

Submitted November 11, 1968

Zh. Eksp. Teor. Fiz. 57, 165–174 (July, 1969)

The behavior of the amplitudes and phases of electromagnetic waves at the threshold of appearance of a new electromagnetic wave (a spectrum of a new order) is considered for the case of scattering by a transparent diffraction lattice or by the open end of a cylindrical waveguide.

Diffraction anomalies

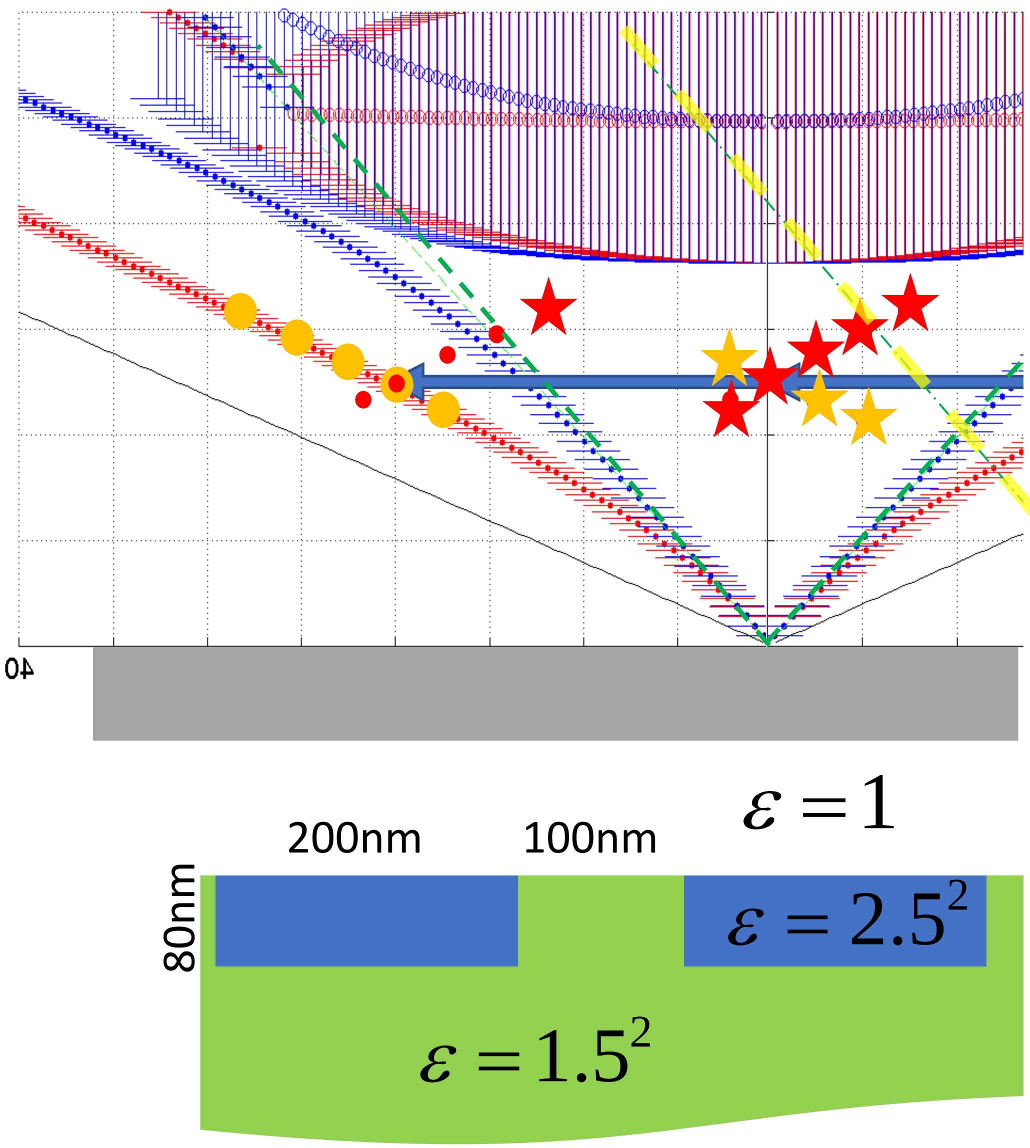

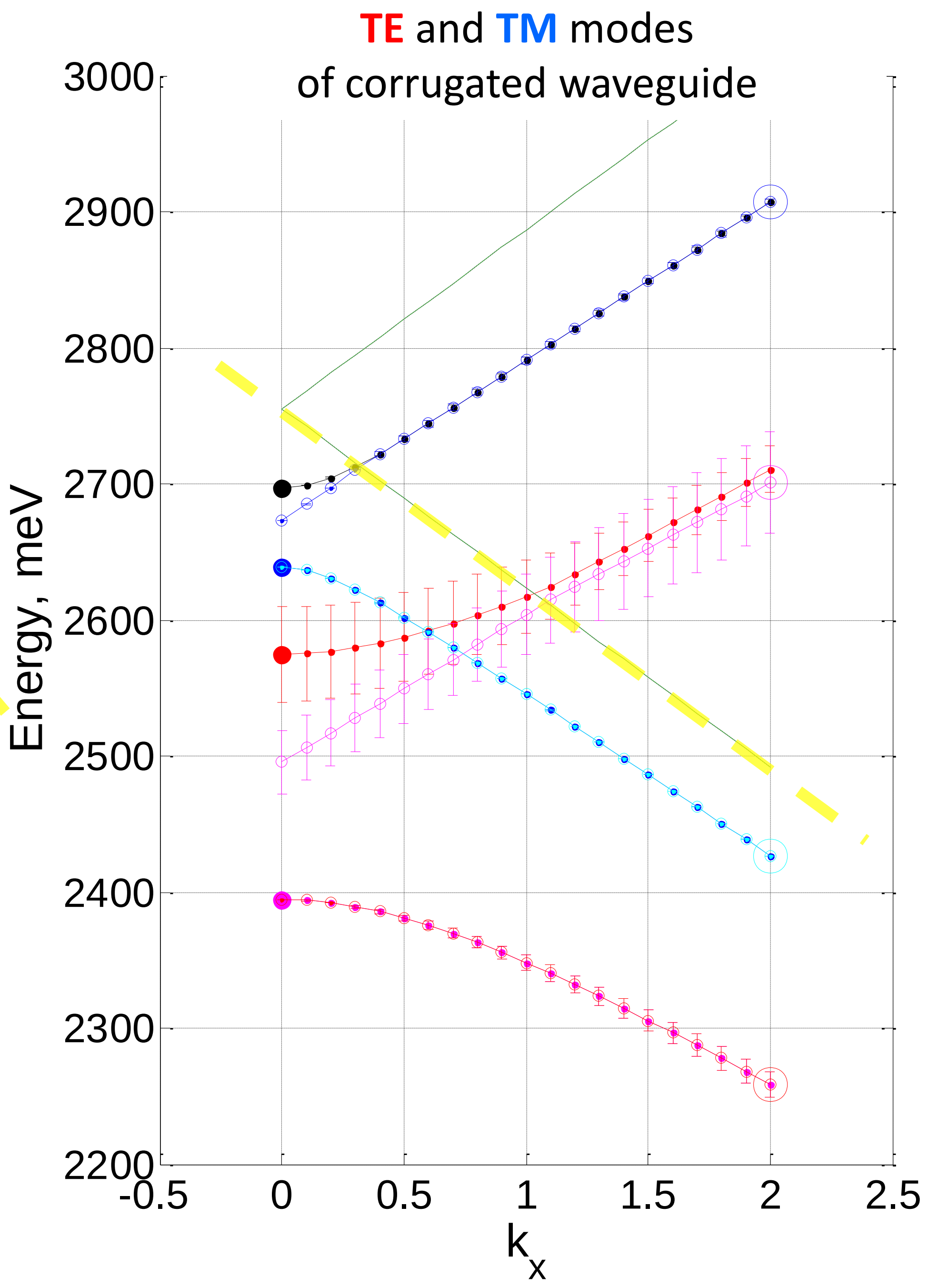

$$k_z\left(G_x^n\right)=\sqrt{\frac{\varepsilon_i}{c^2}\omega^2-\left(k_x+G_x^n\right)^2}$$

$$k_z\left(G_x^n\right)\sim\sqrt{E-E_G}$$

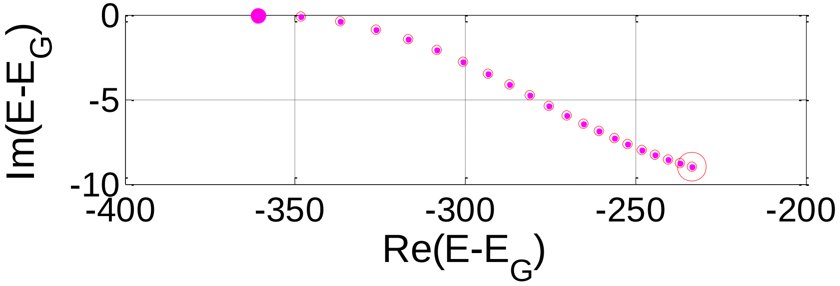

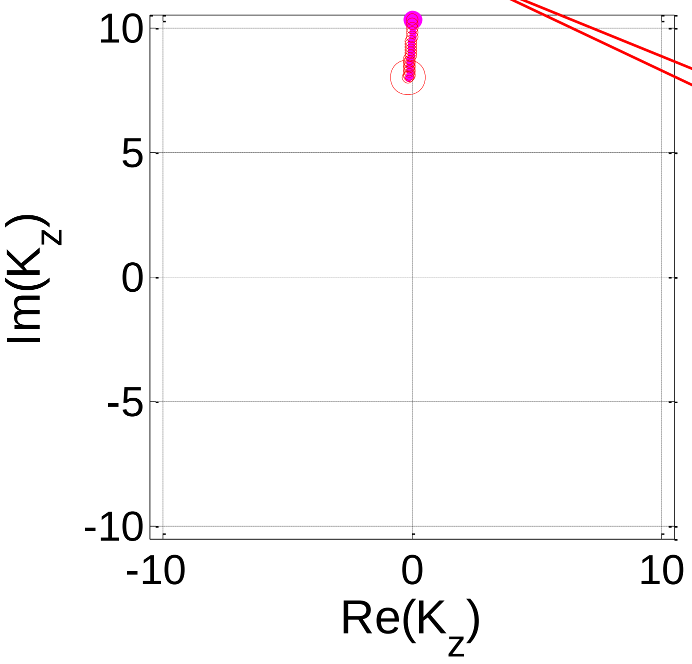

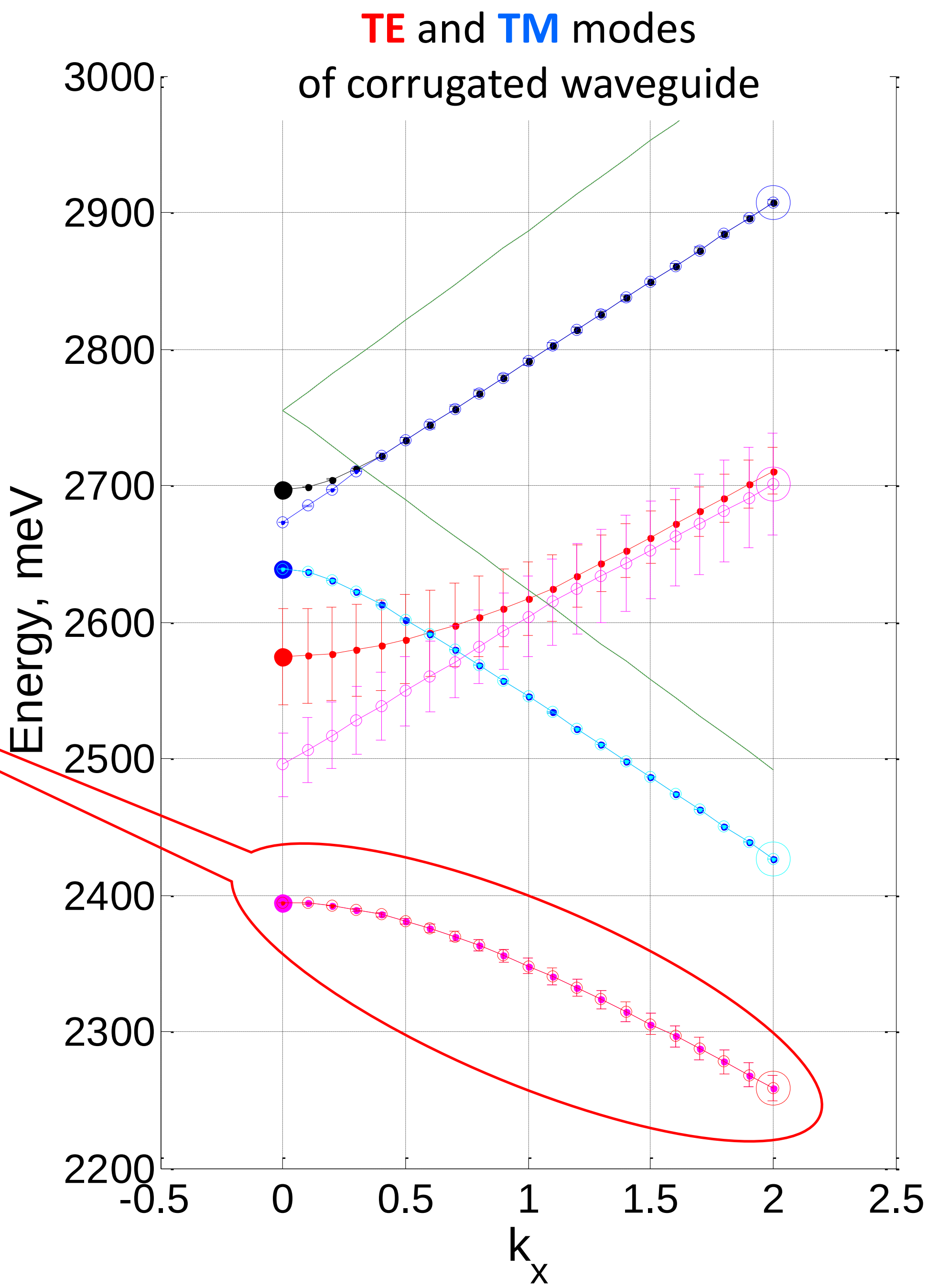

$$k_z\left(G_x^n\right) \sim \sqrt{E - E_G}$$

$$E - E_G \sim k_z^2(G)$$

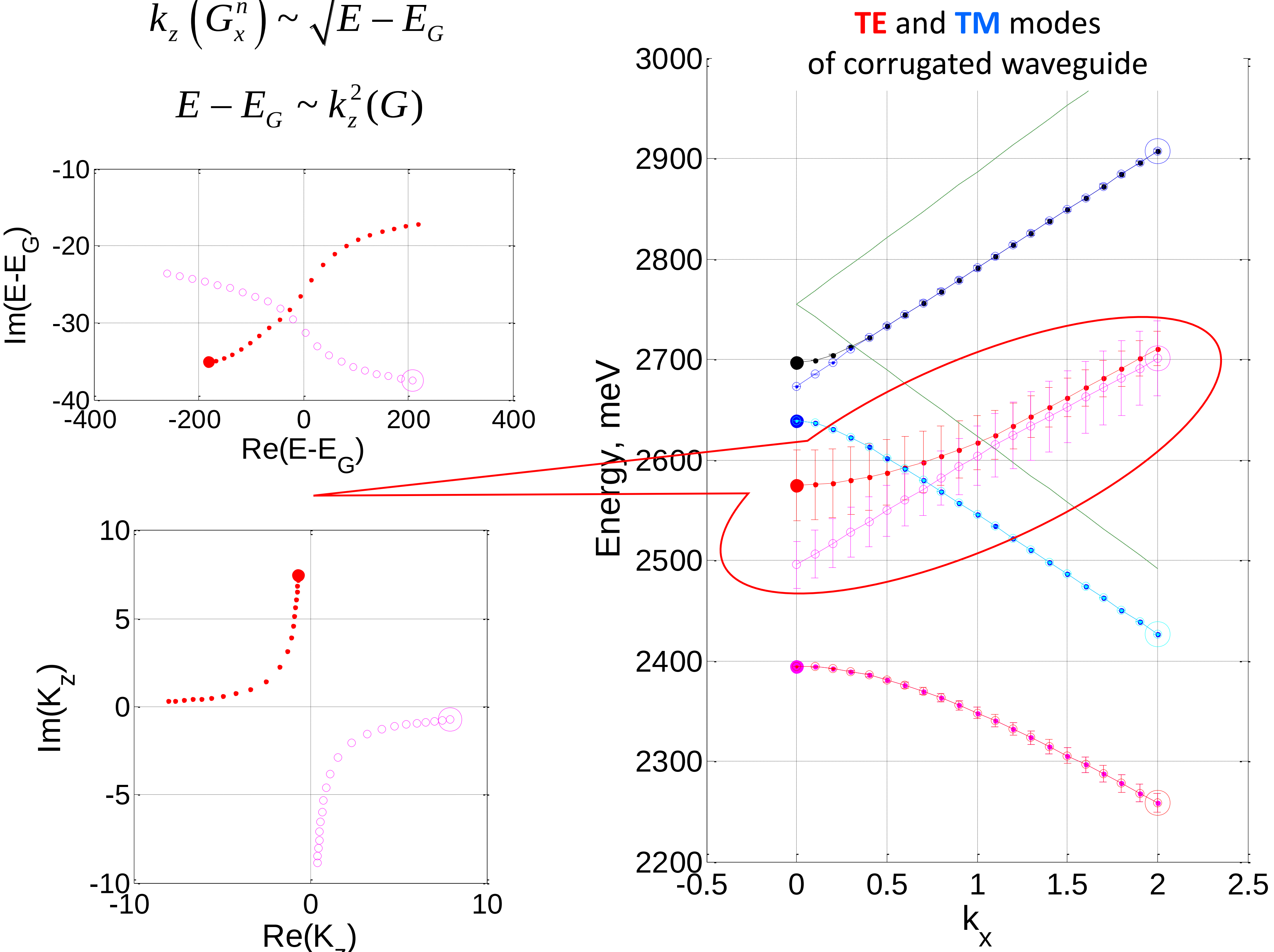

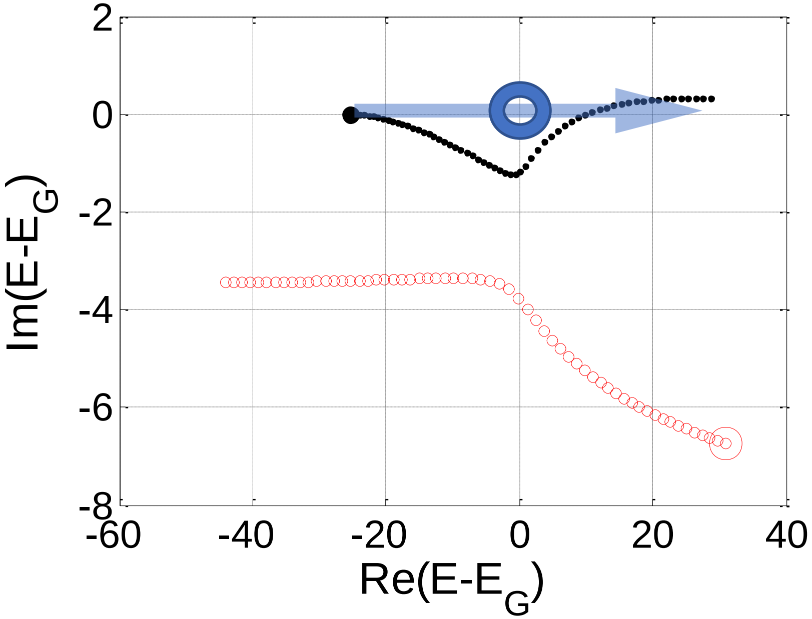

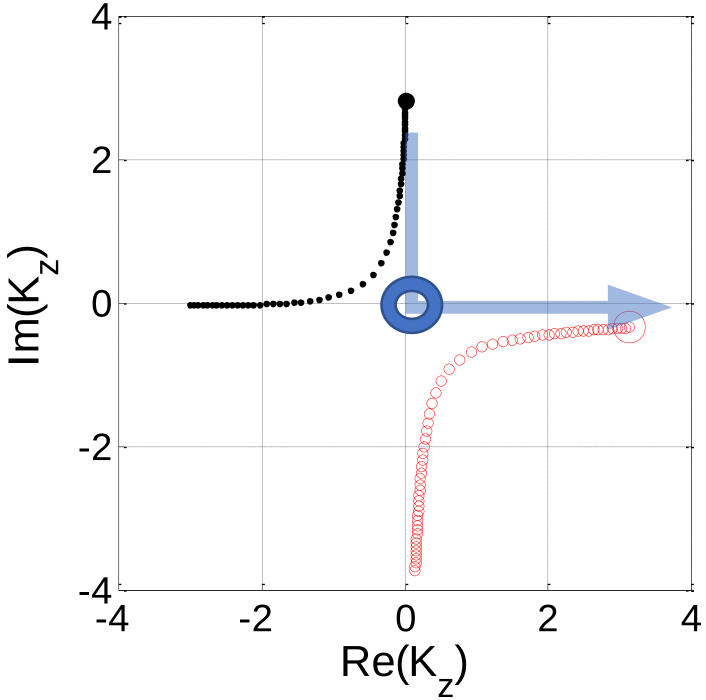

TM mode
of corrugated waveguide

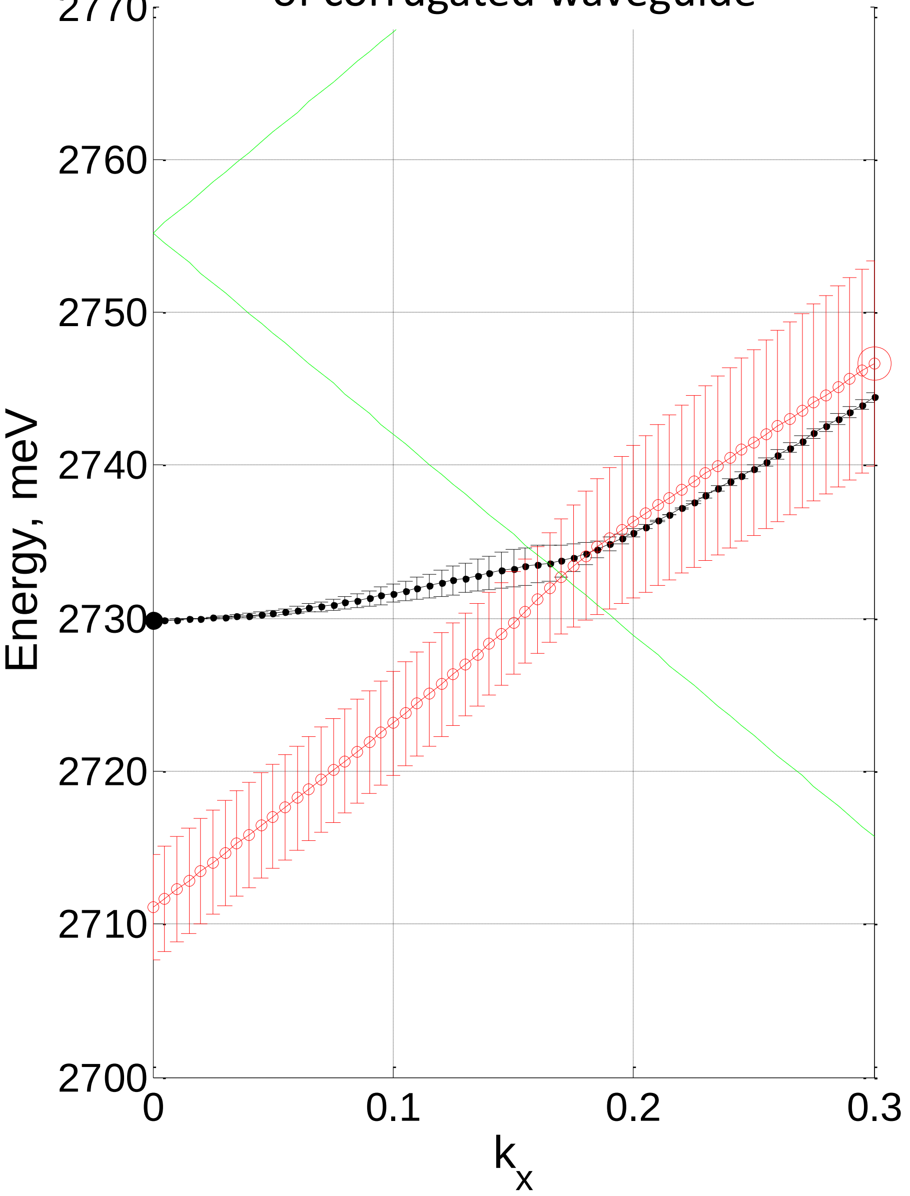

Reflection near **TM** mode
of corrugated waveguide

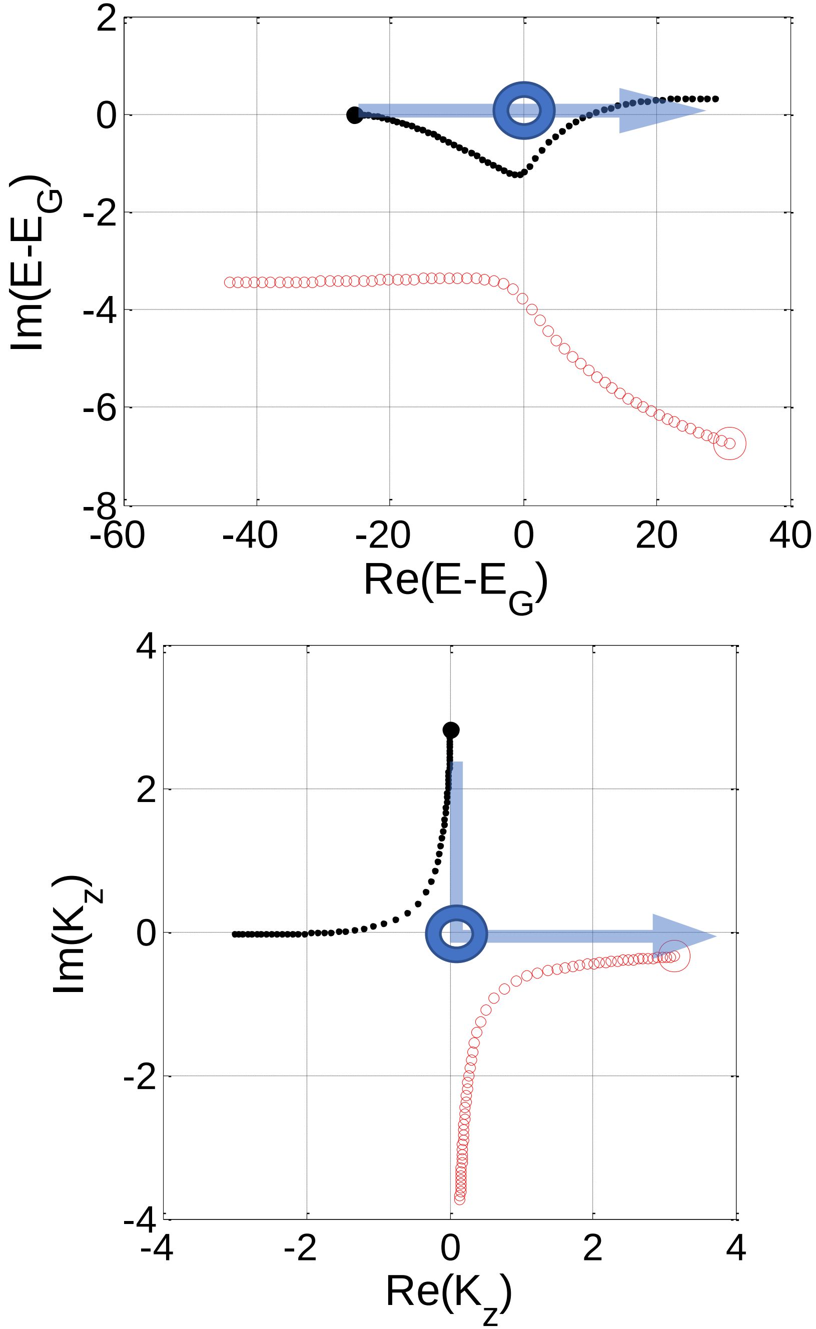

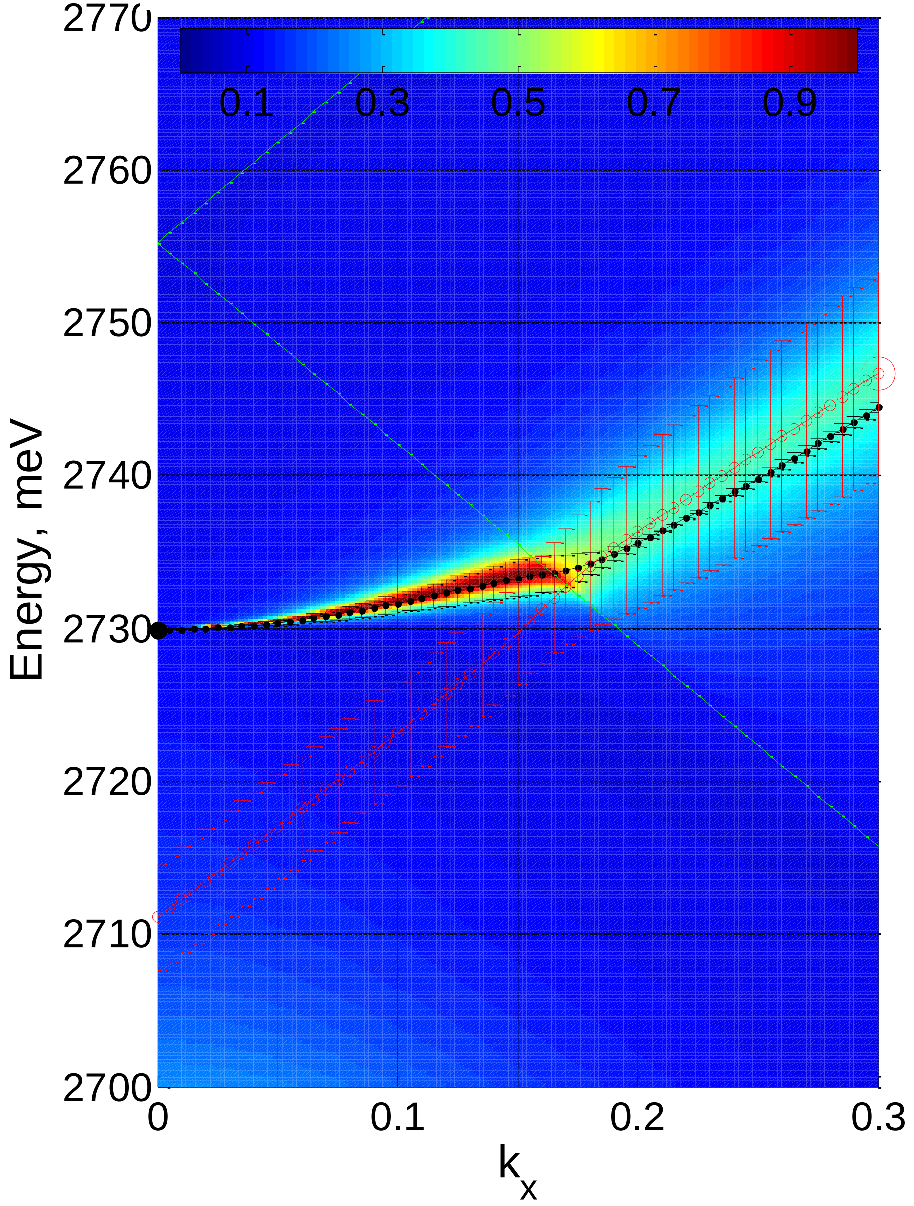

Reflection near **TM** mode of corrugated waveguide

$$E = \hbar\omega$$

$$k_z\left(G_x^n\right) = \sqrt{\frac{e_i}{c^2} w^2 - \left(k_x + G_x^n\right)^2}$$

$$k_z^2 \propto \left(E - E_G\right)$$

$$E = E_G + A k_z^2$$

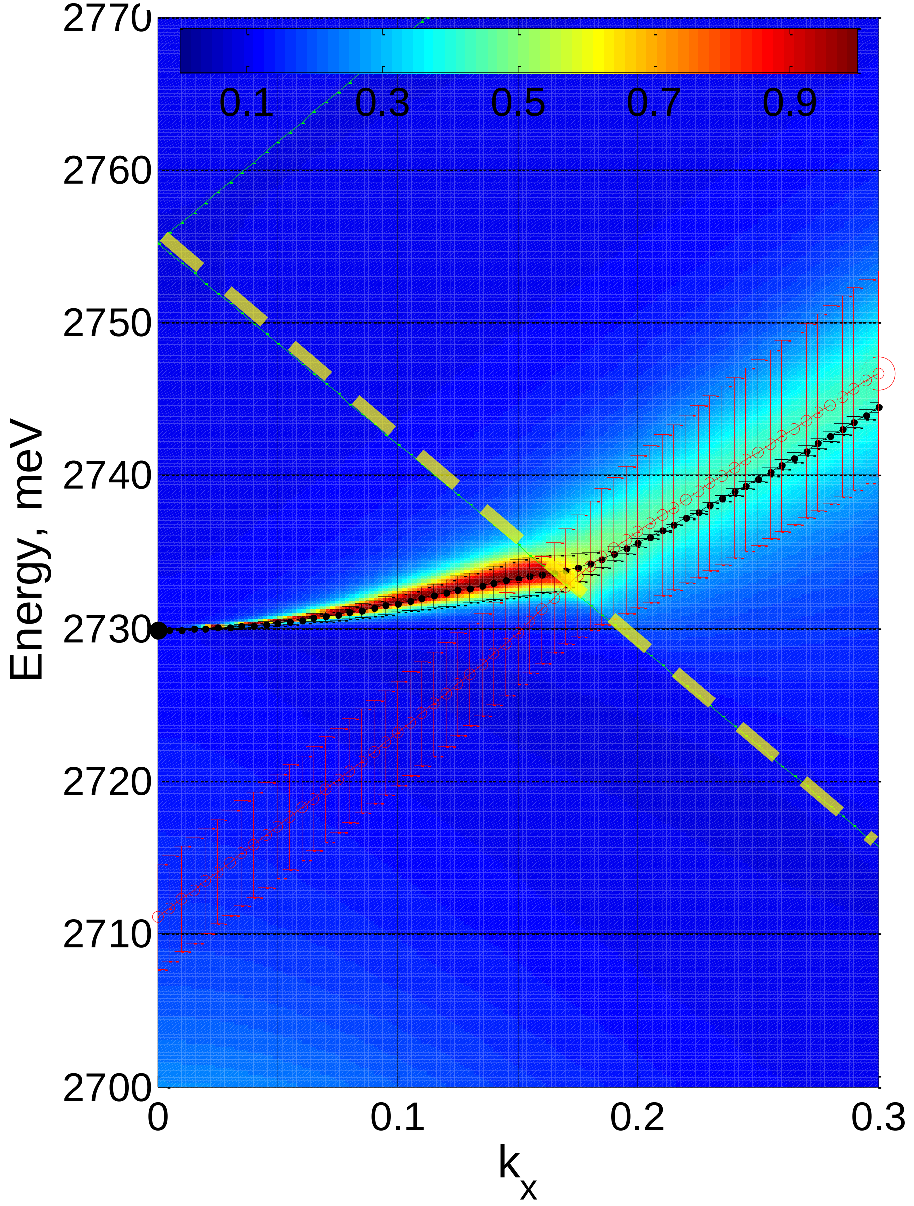

Akimov AB, Gippius NA, Tikhodeev SG.
JETP Letters 93(8):427 (2011)

$$\tilde{S} + \sum_r |O_r\rangle \frac{1}{E - E_r} \langle I_r|$$

$$\tilde{S} + \sum_r |o_r\rangle \frac{1}{k_z - k_z^r} \langle i_r|$$

Akimov AB, Gippius NA, Tikhodeev SG.
JETP Letters 93(8):427 (2011)

Reflection near **TM** mode
of corrugated waveguide

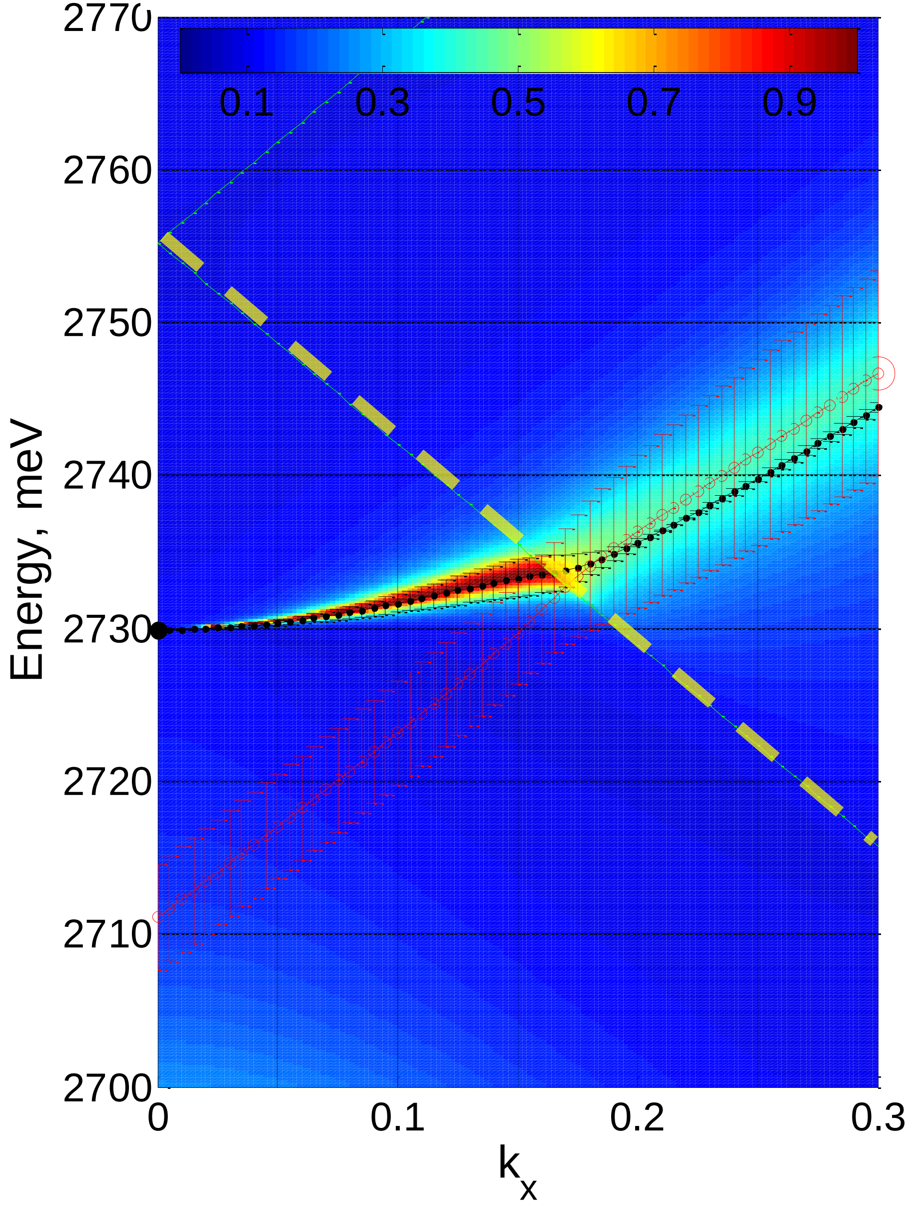

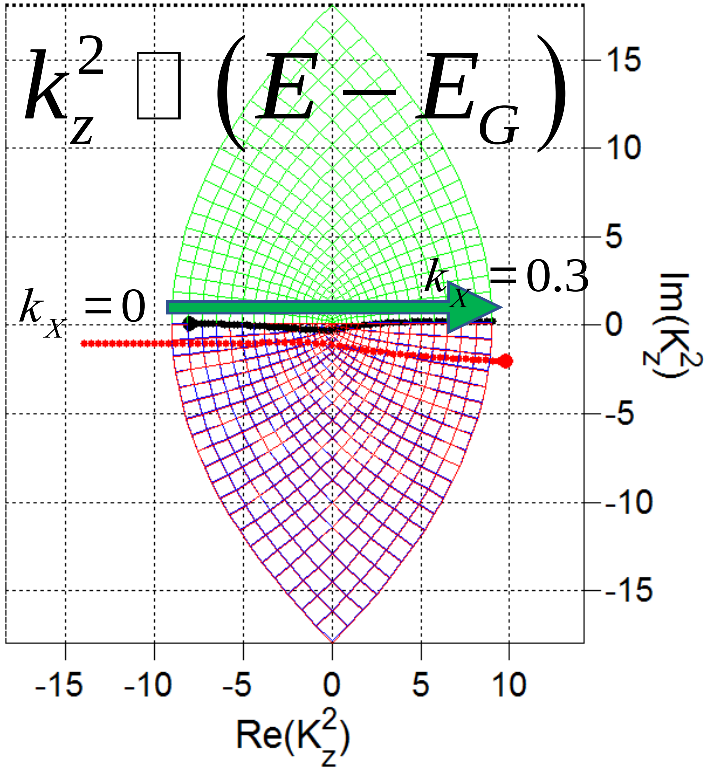

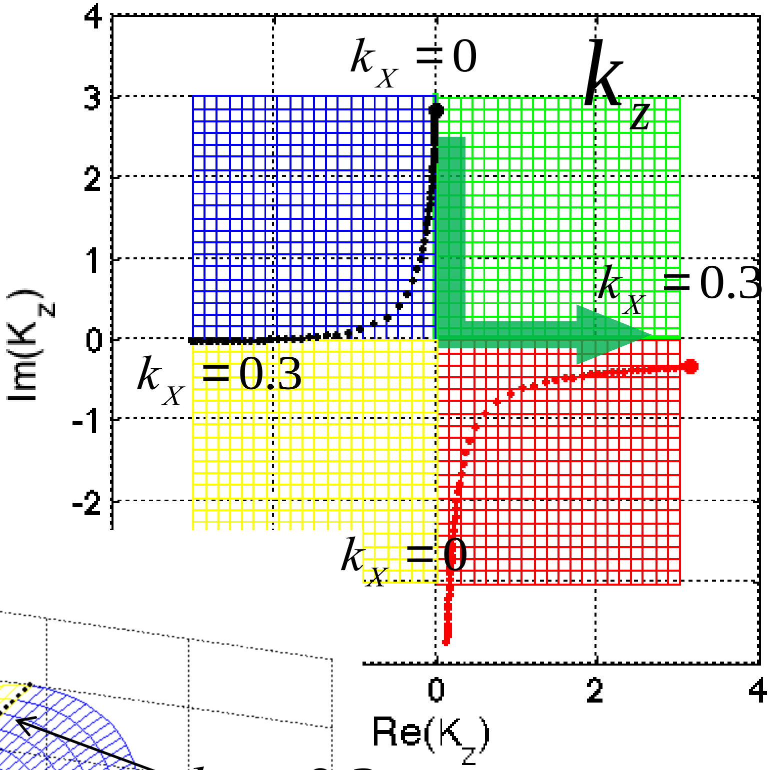

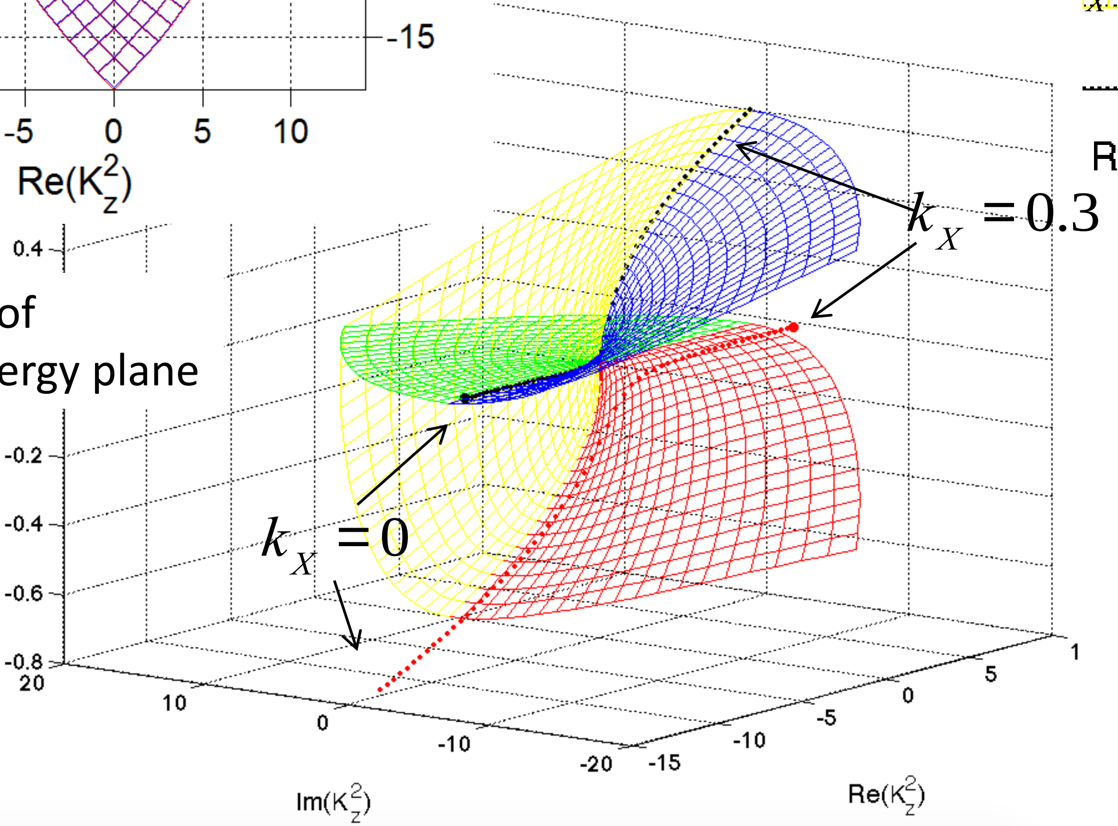

Two leaves of complex energy plane

Reflection of corrugated waveguide (green line) and
the approximations with
two poles (red dashed line)
and one pole (thin lines)

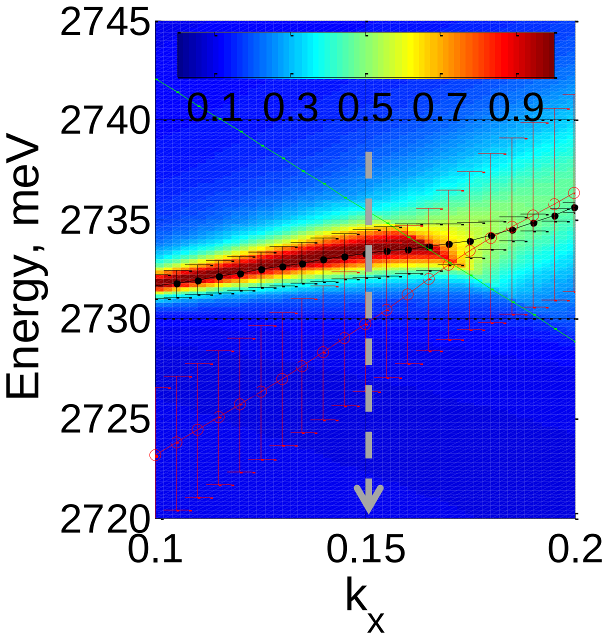

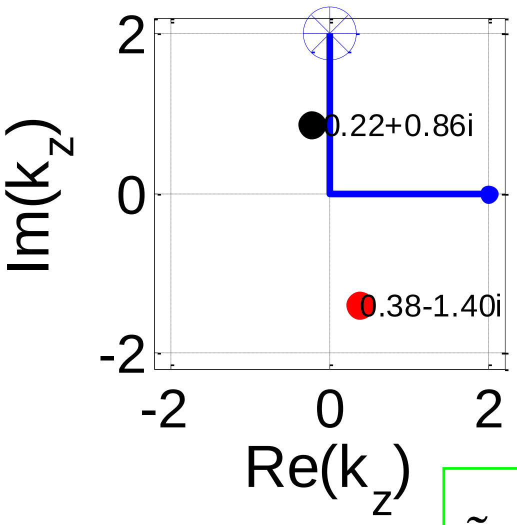

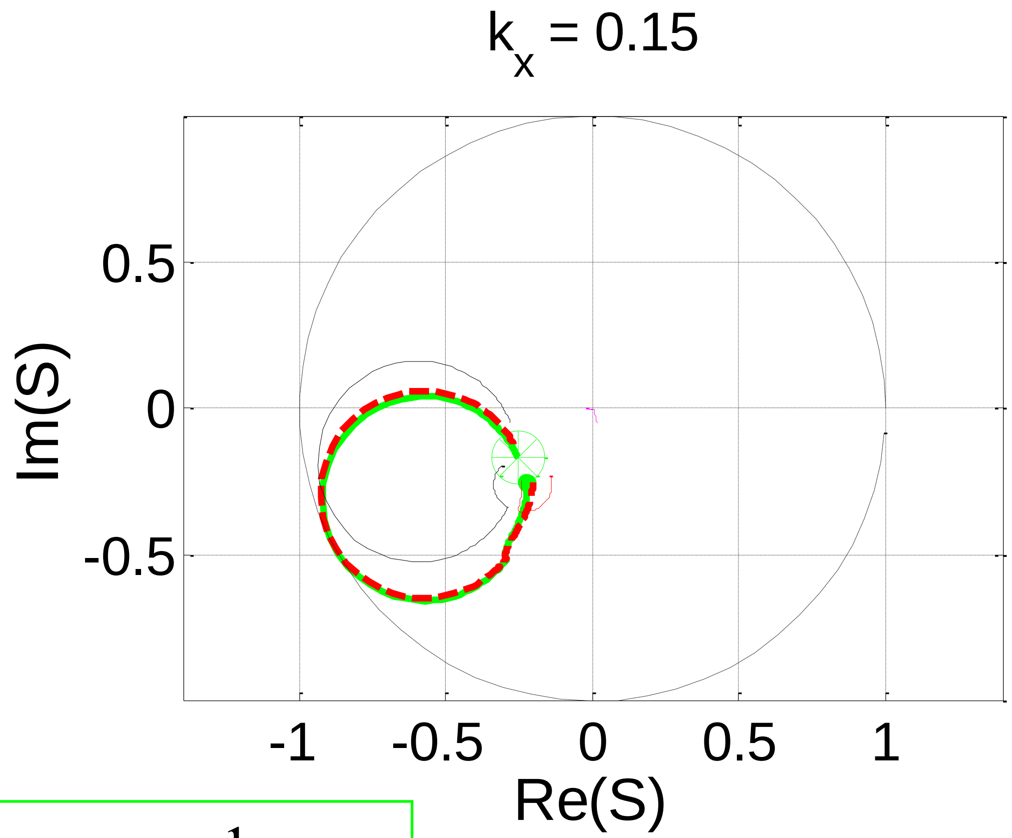

$$\tilde{S} + \sum_r |o_r\rangle \frac{1}{k_z - k_z^r} \langle i_r|$$

Reflection of corrugated waveguide (green line) and
the approximations with
two poles (red dashed line)
and one pole (thin lines)

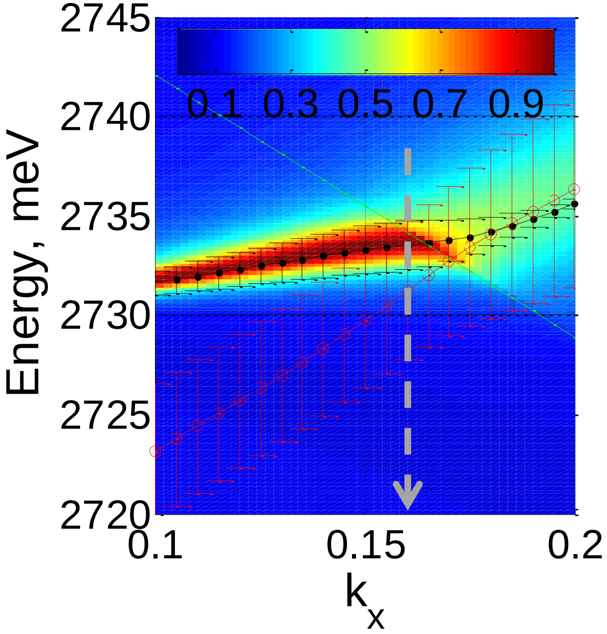

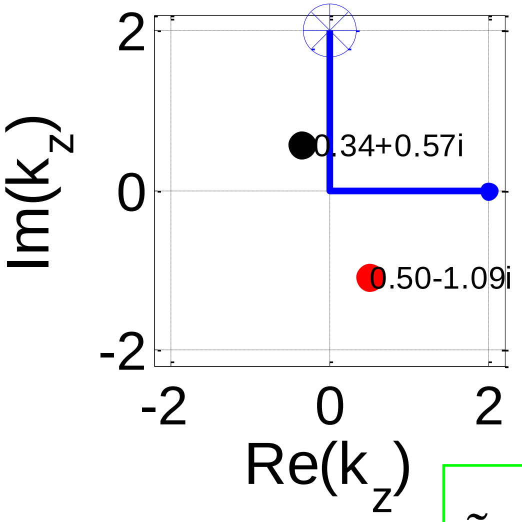

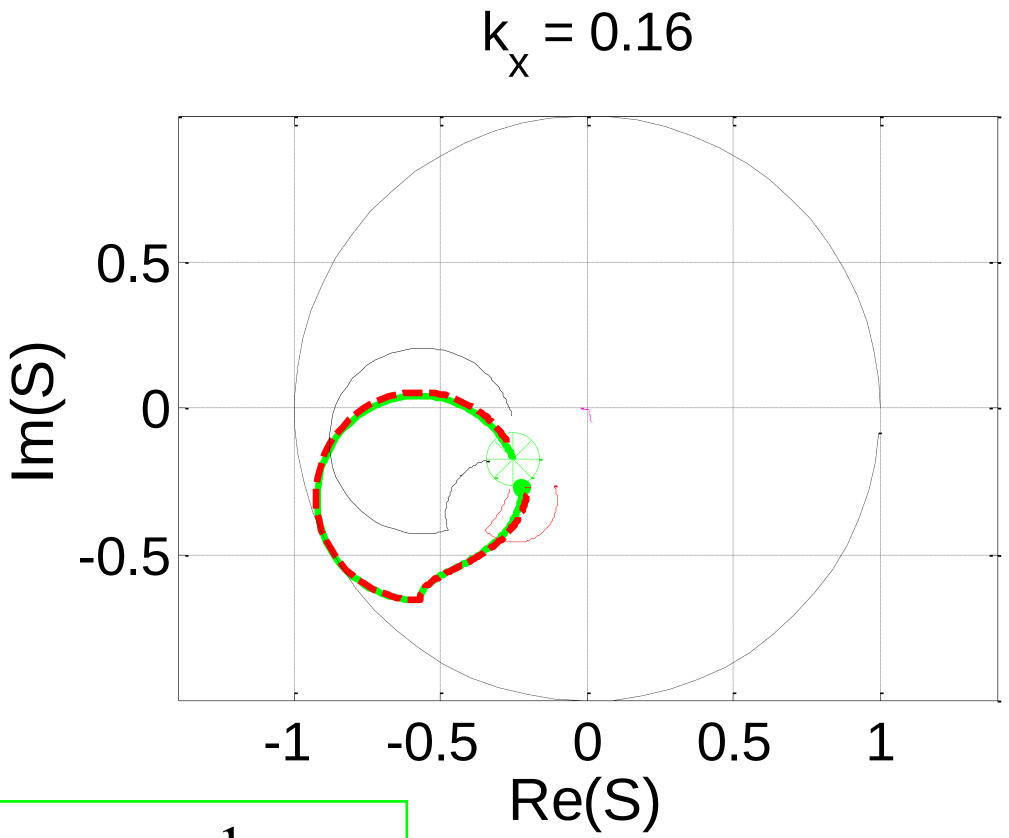

$$\tilde{S}+\sum_{r}\left|o_{r}\right\rangle \frac{1}{k_{z}-k_{z}^{r}}\left\langle i_{r}\right|$$

Reflection of corrugated waveguide (green line) and
the approximations with
two poles (red dashed line)
and one pole (thin lines)

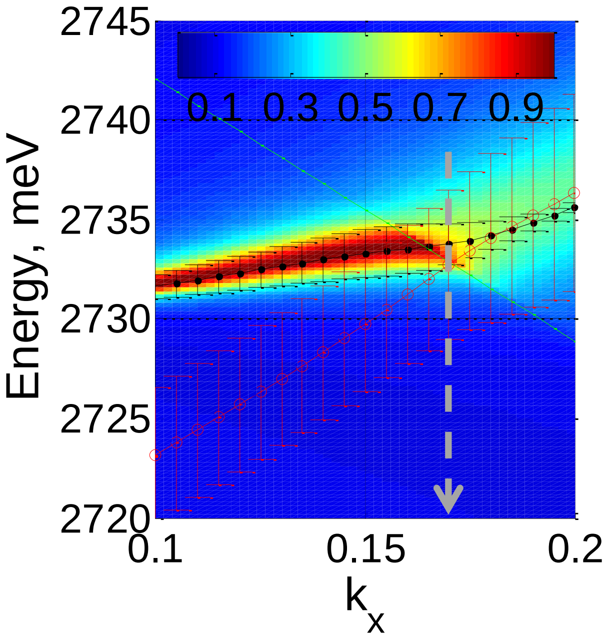

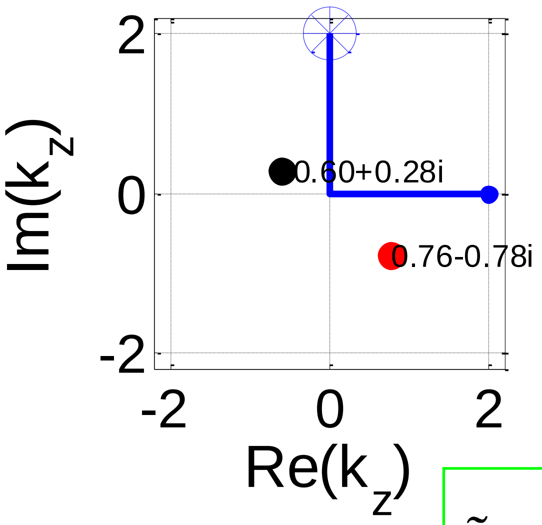

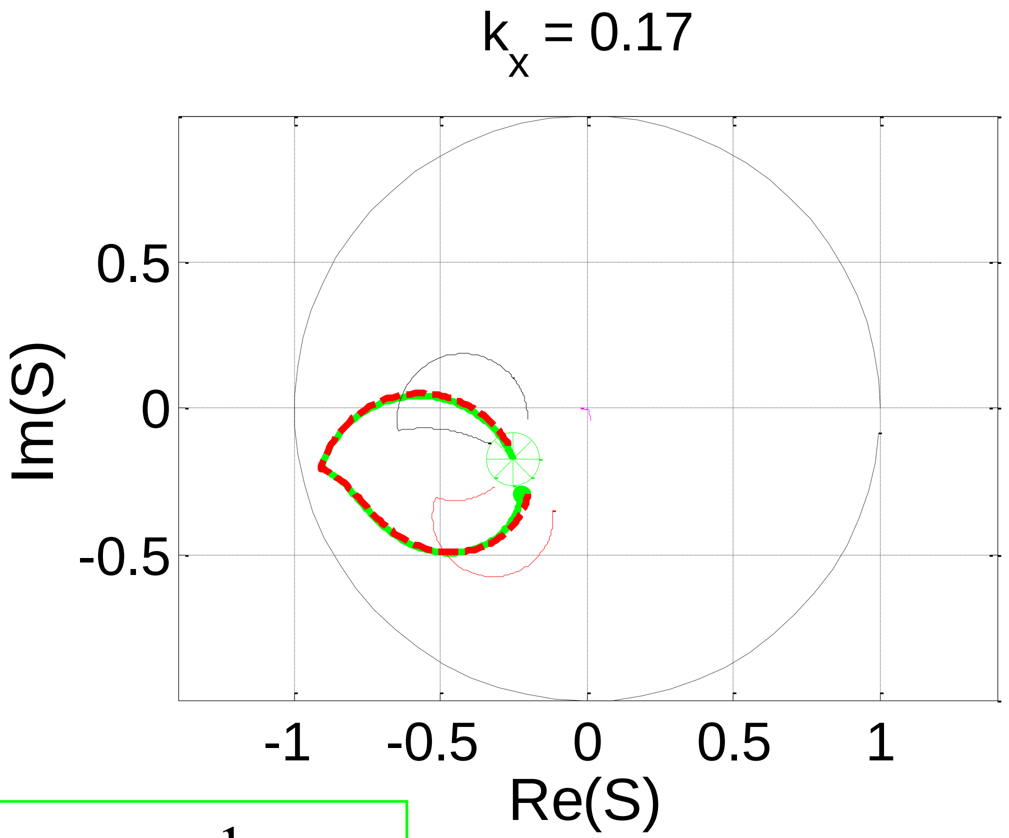

$$\tilde{S} + \sum_r \left|o_r\right\rangle \frac{1}{k_z - k_z^r} \left\langle i_r\right|$$

Reflection of corrugated waveguide (green line) and
the approximations with
two poles (red dashed line)
and one pole (thin lines)

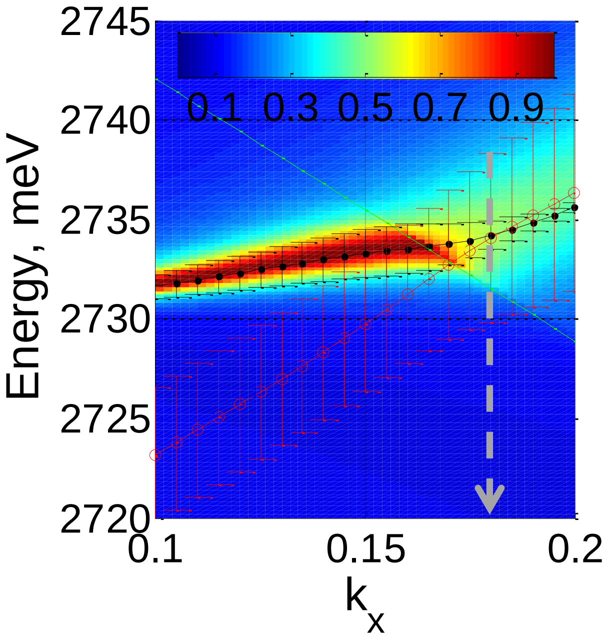

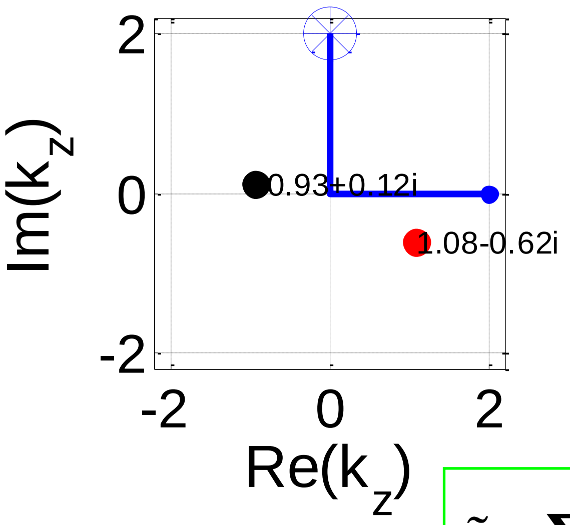

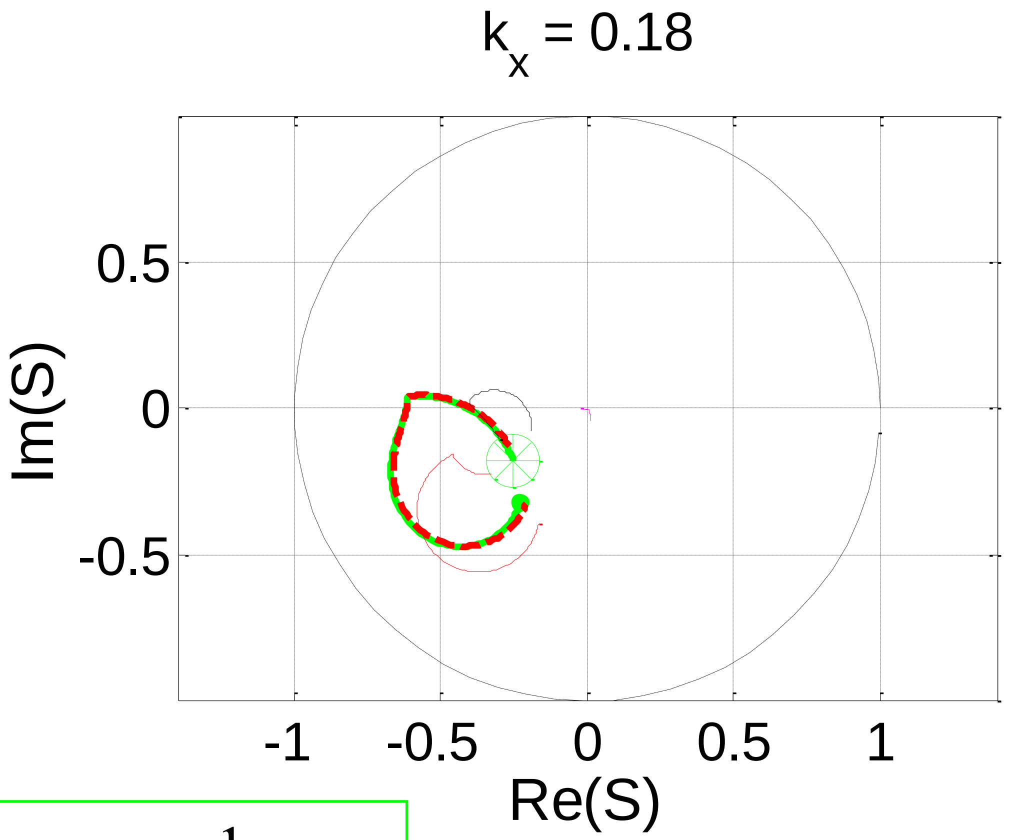

$$\tilde{S} + \sum_r |o_r\rangle \frac{1}{k_z - k_z^r} \langle i_r|$$

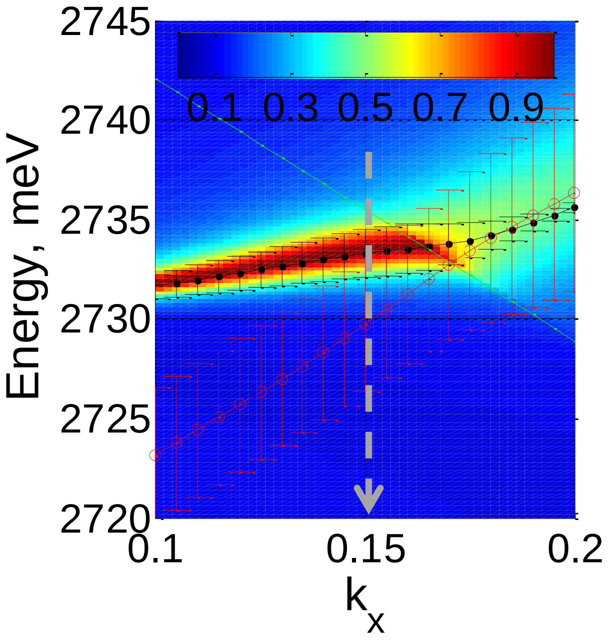

Reflection of corrugated waveguide (green line) and
the approximations with
two poles (red dashed line)
and one pole (thin lines)

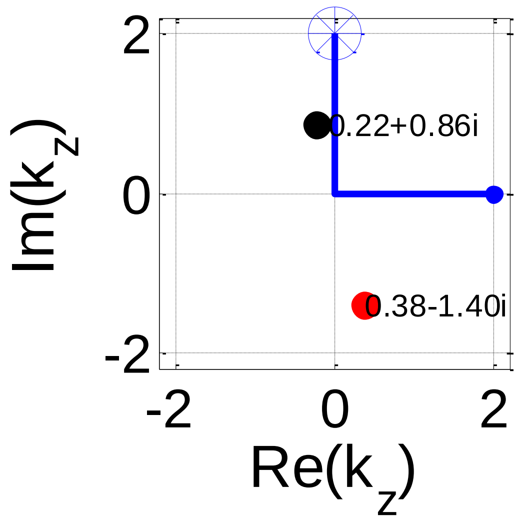

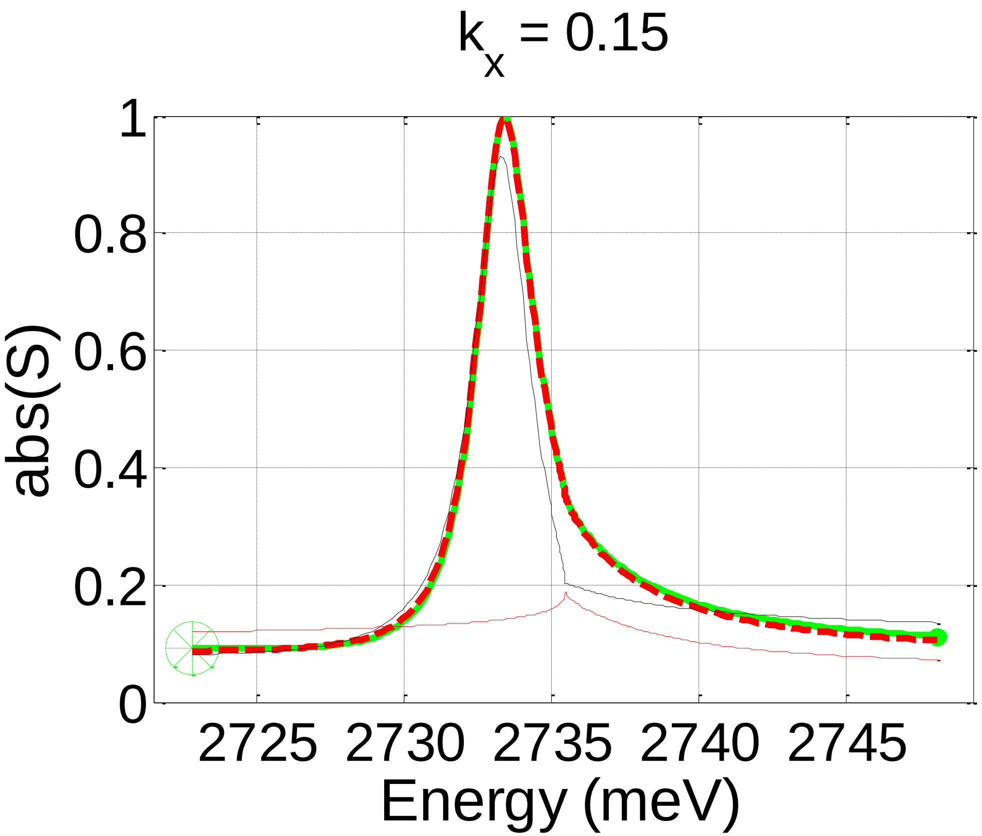

$$E - E_G(k_x) \sim k_z^2(G)$$

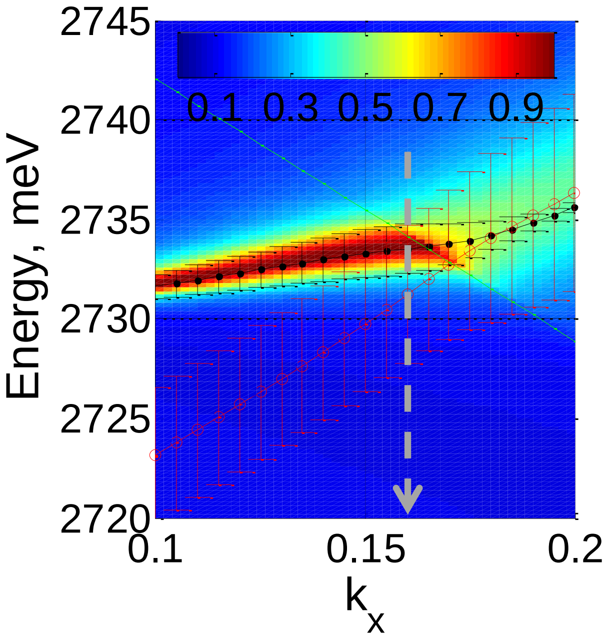

Reflection of corrugated waveguide (green line) and the approximations with two poles (red dashed line) and one pole (thin lines)

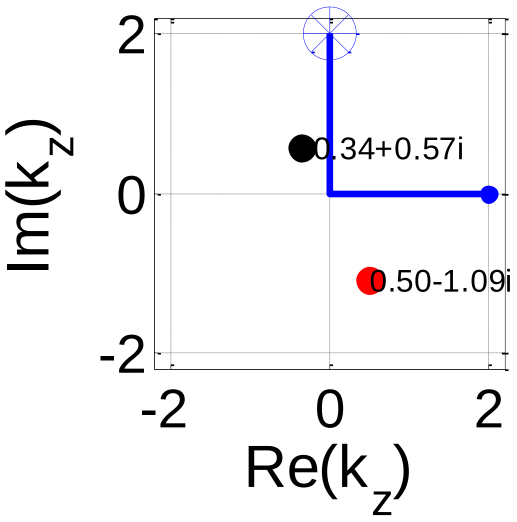

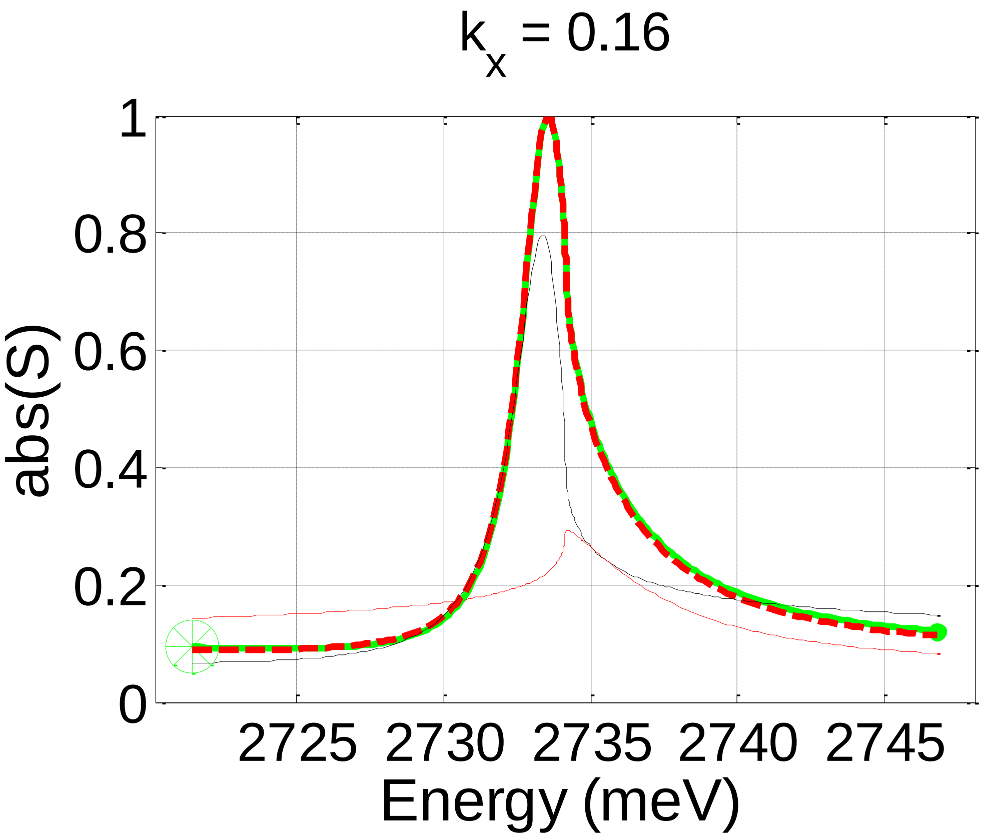

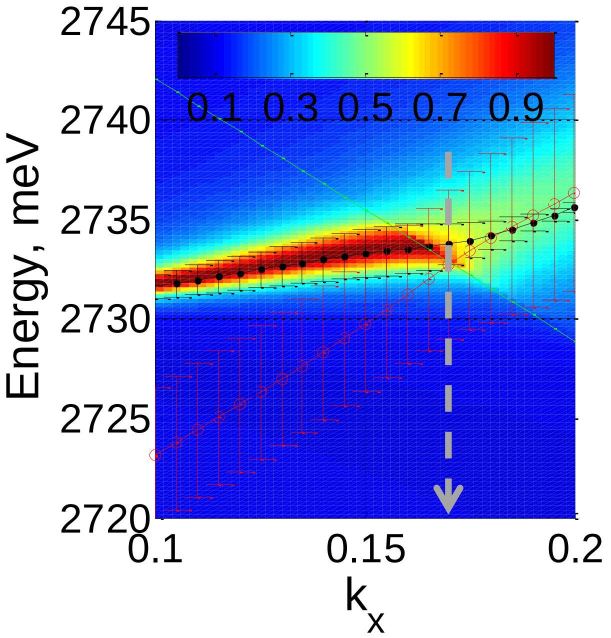

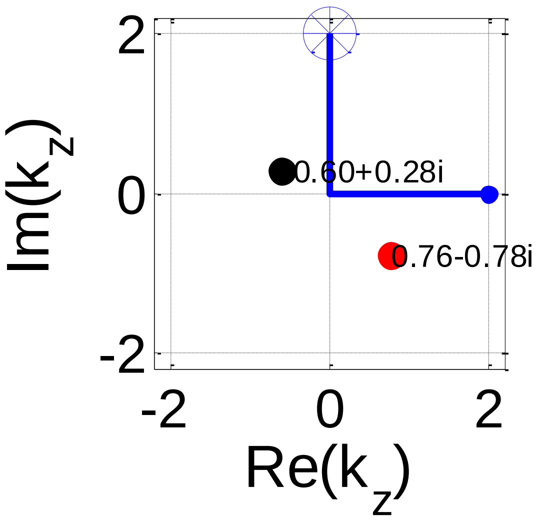

Reflection of corrugated waveguide (green line) and
the approximations with
two poles (red dashed line)
and one pole (thin lines)

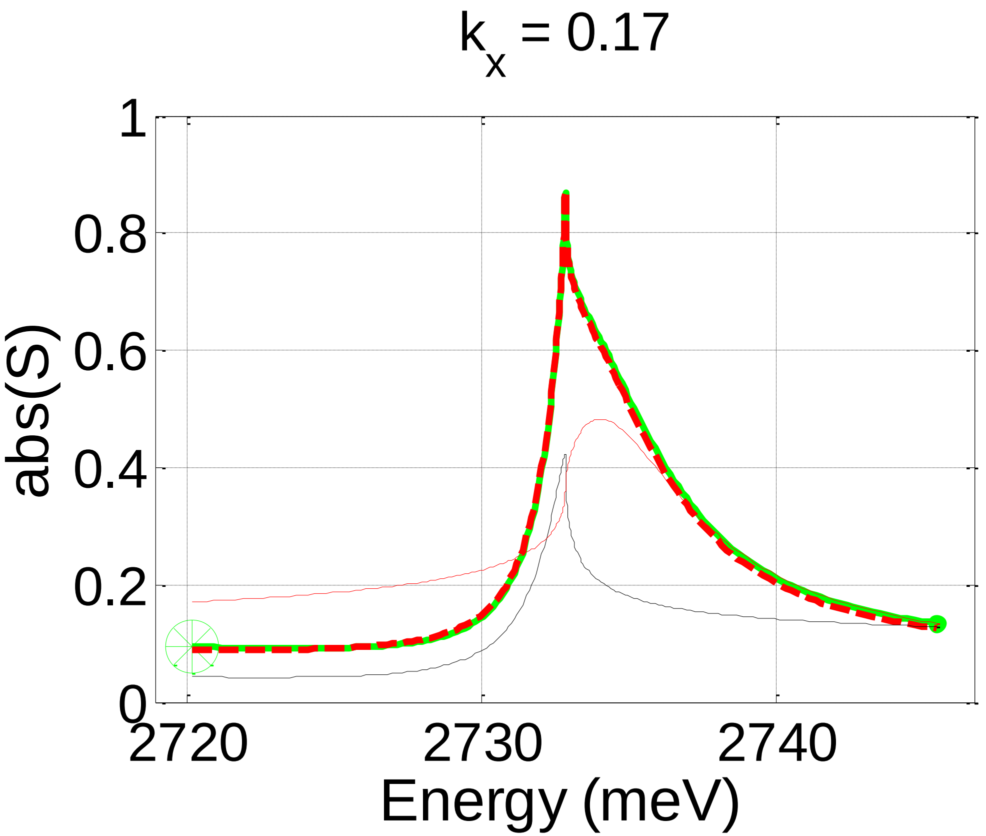

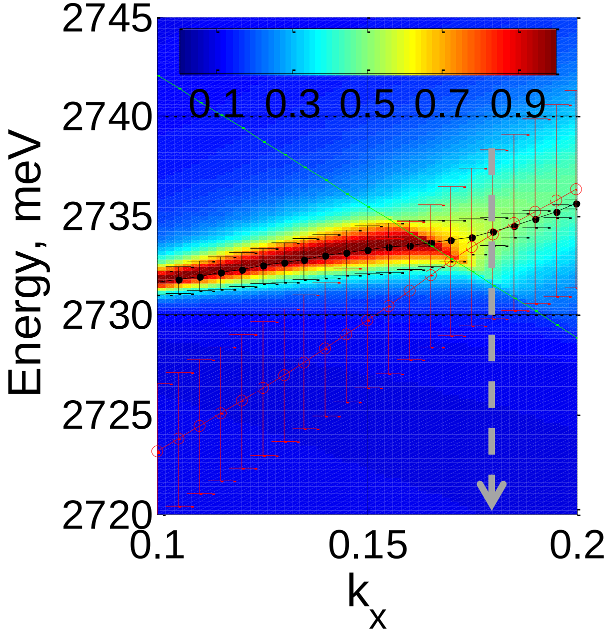

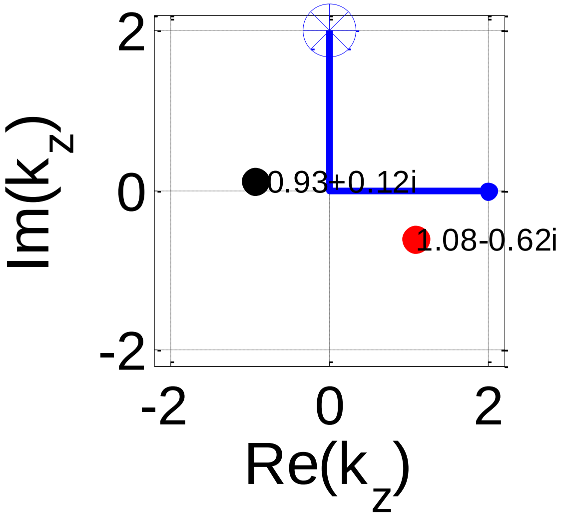

Reflection of corrugated waveguide (green line) and
the approximations with
two poles (red dashed line)
and one pole (thin lines)

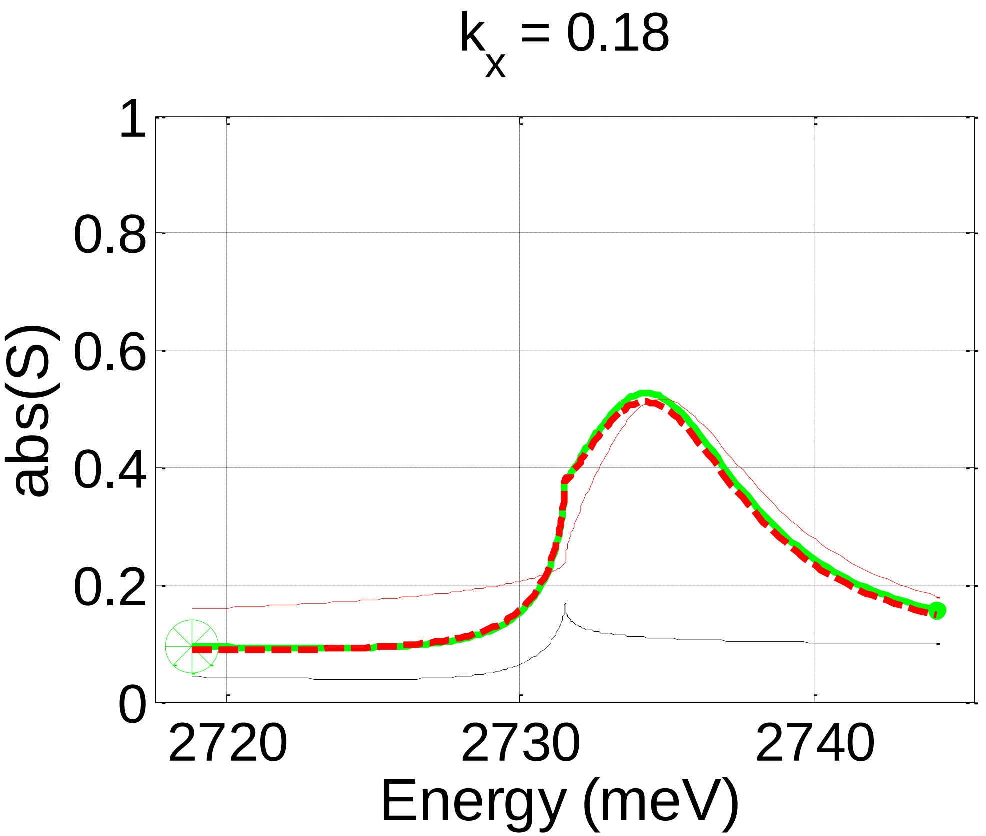

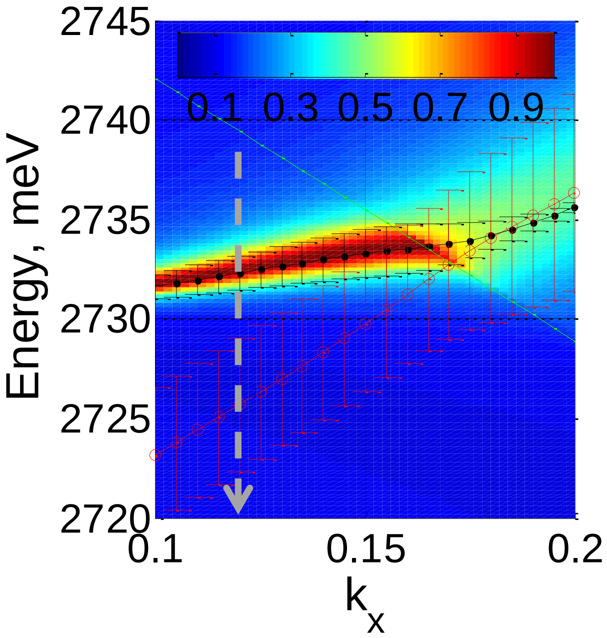

Reflection as function of
K_z - the 'sunrise'-harmonic
propagation constant in vertical direction

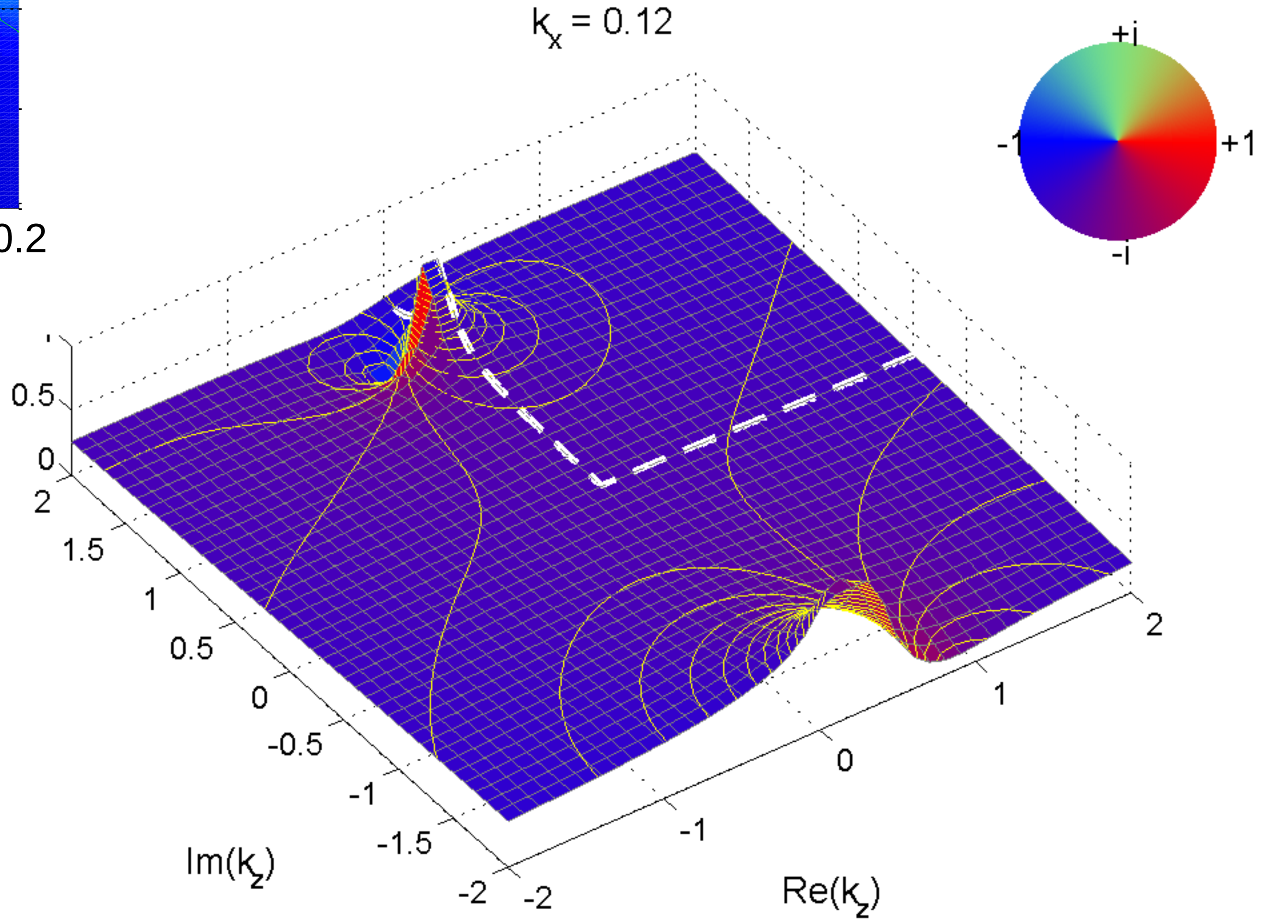

Resonantly enhanced Wood-Rayleigh anomaly

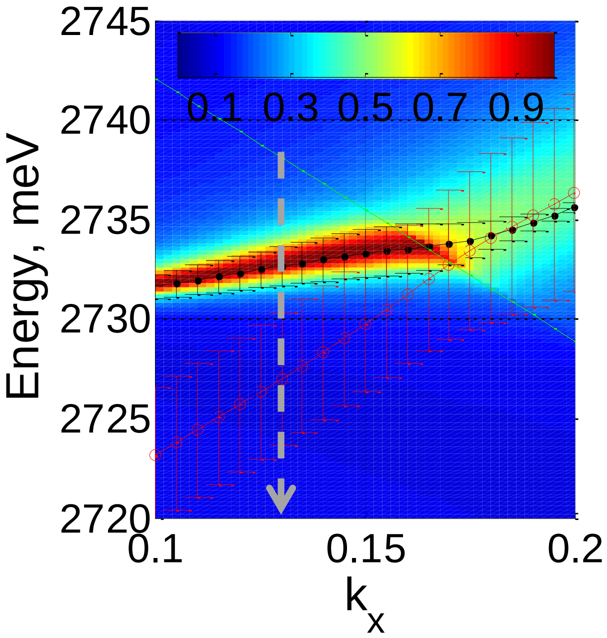

Reflection as function of
K_z - the 'sunrise'-harmonic
propagation constant in vertical direction

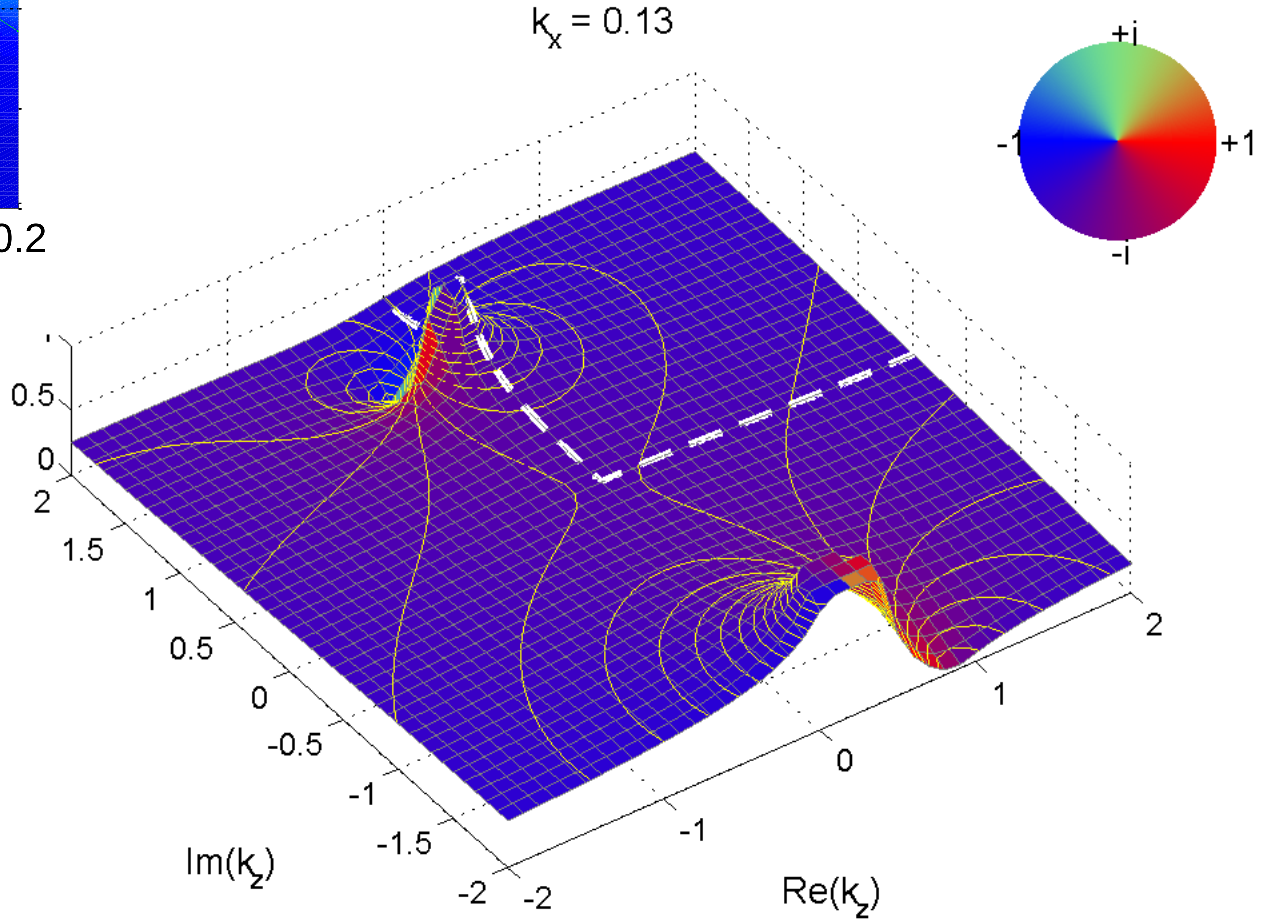

Resonantly enhanced Wood-Rayleigh anomaly

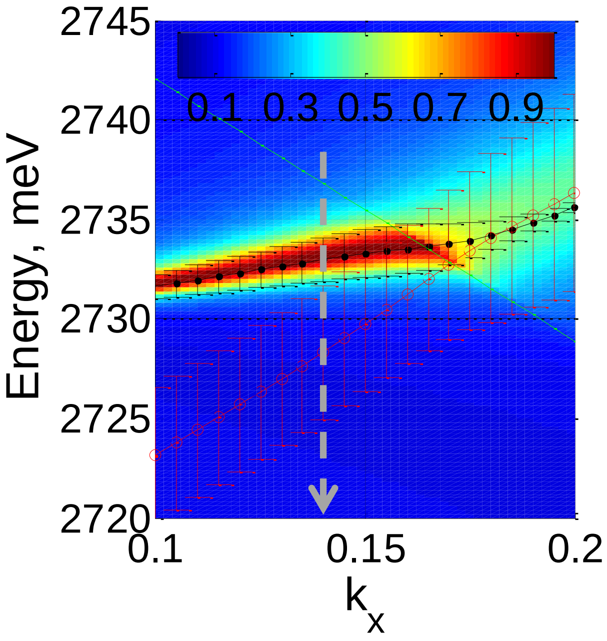

Reflection as function of
K_z - the 'sunrise'-harmonic
propagation constant in vertical direction

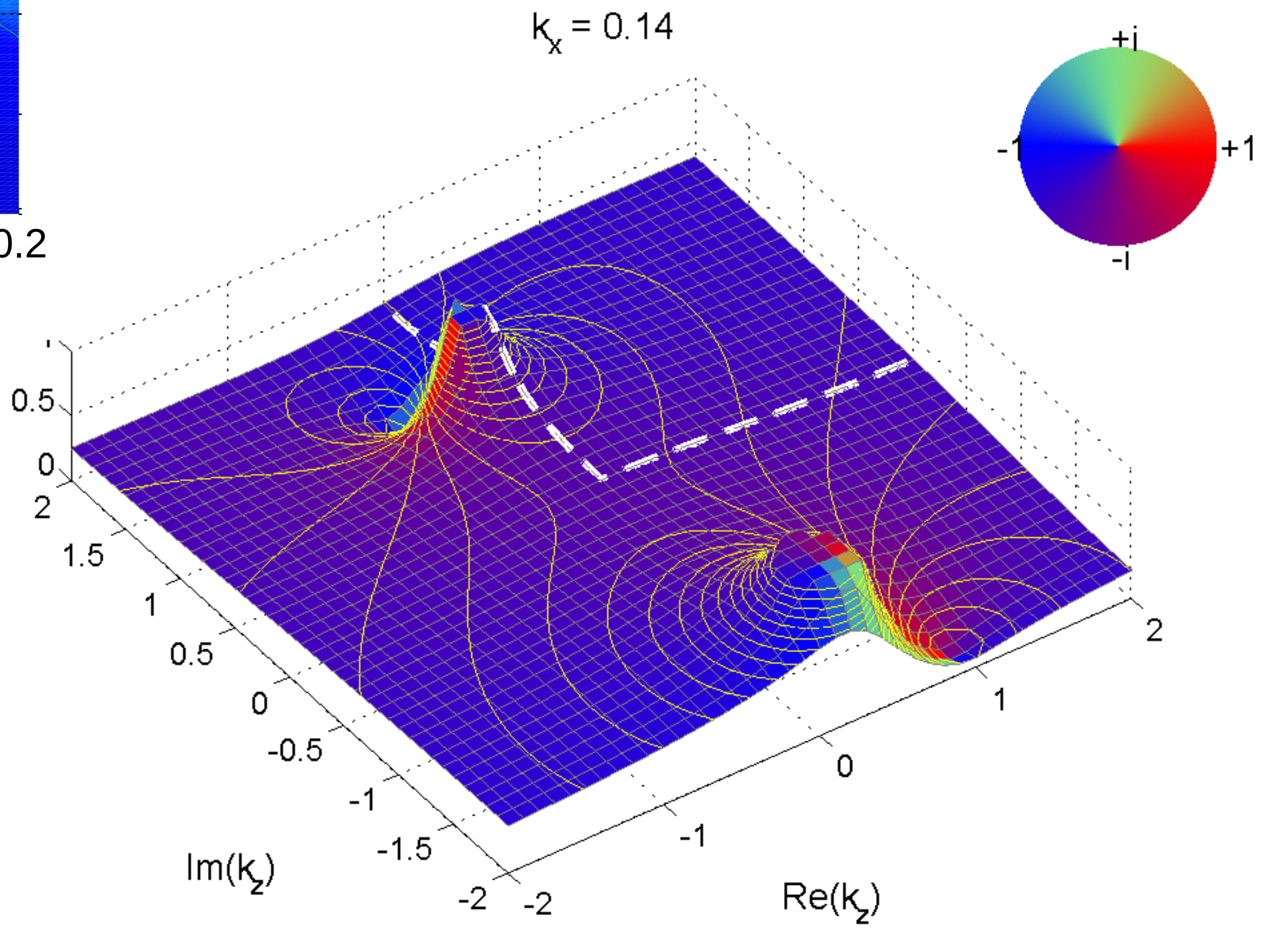

Resonantly enhanced Wood-Rayleigh anomaly

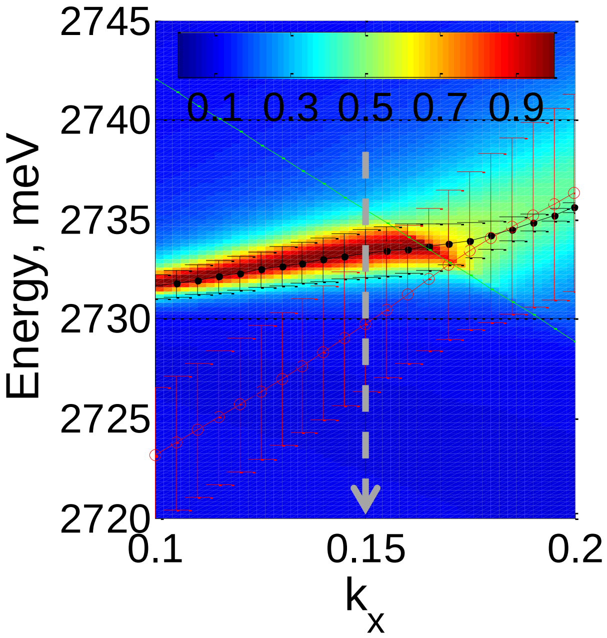

Reflection as function of
K_z - the 'sunrise'-harmonic
propagation constant in vertical direction

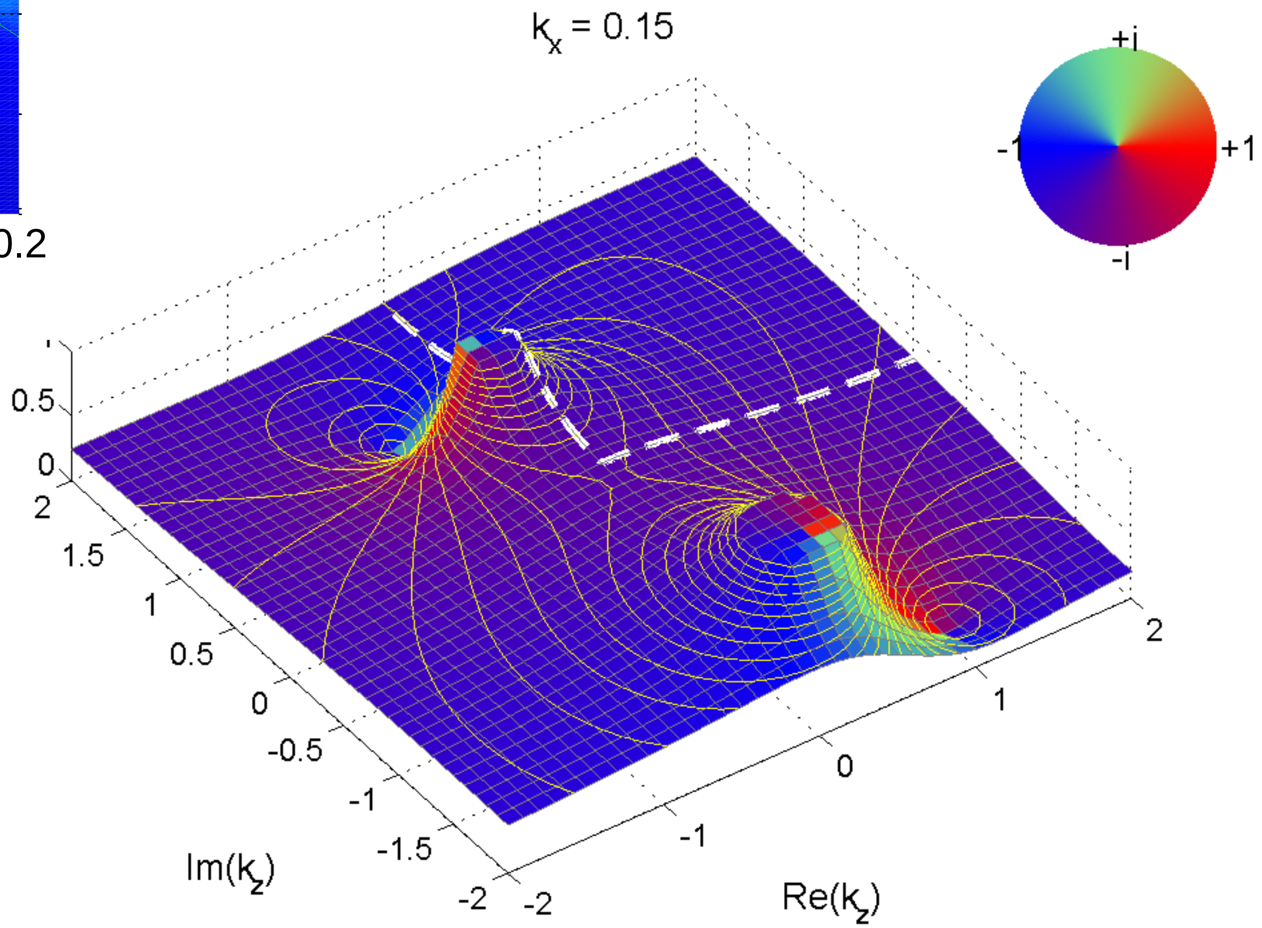

Resonantly enhanced Wood-Rayleigh anomaly

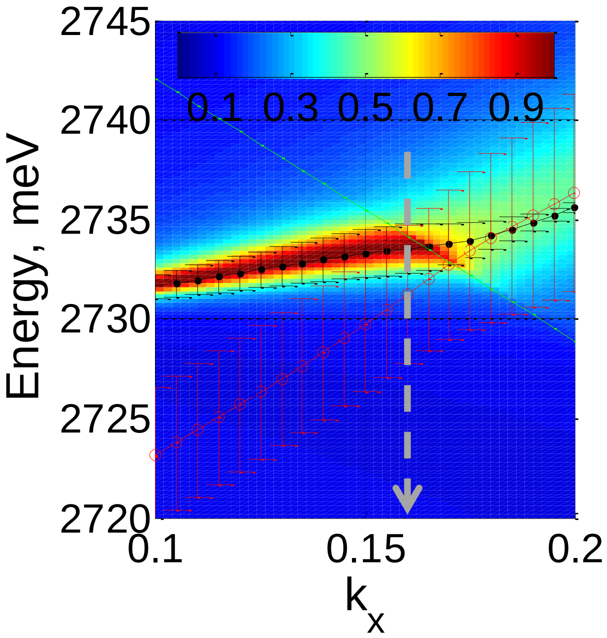

Reflection as function of
K_z - the 'sunrise'-harmonic
propagation constant in vertical direction

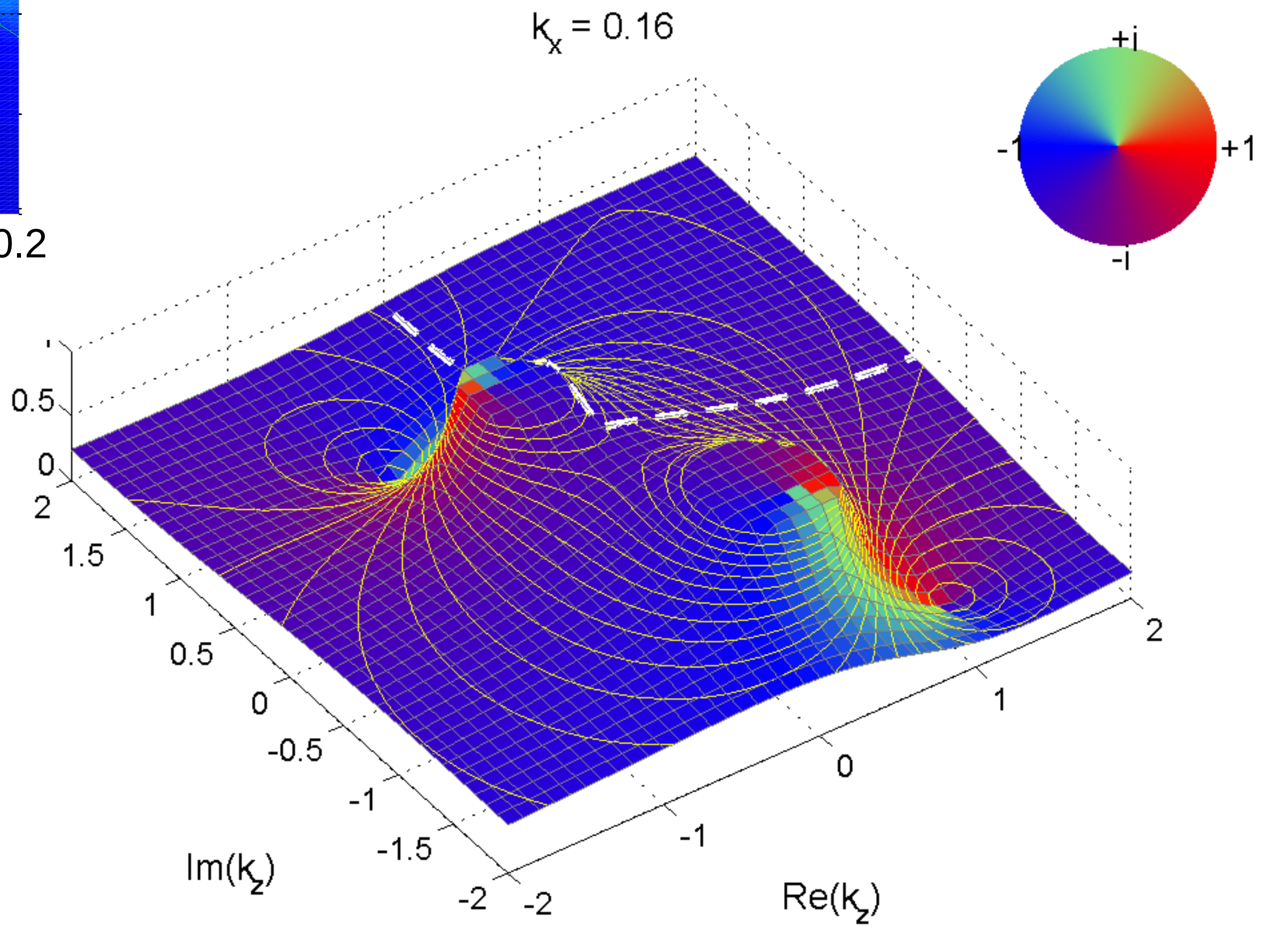

Resonantly enhanced Wood-Rayleigh anomaly

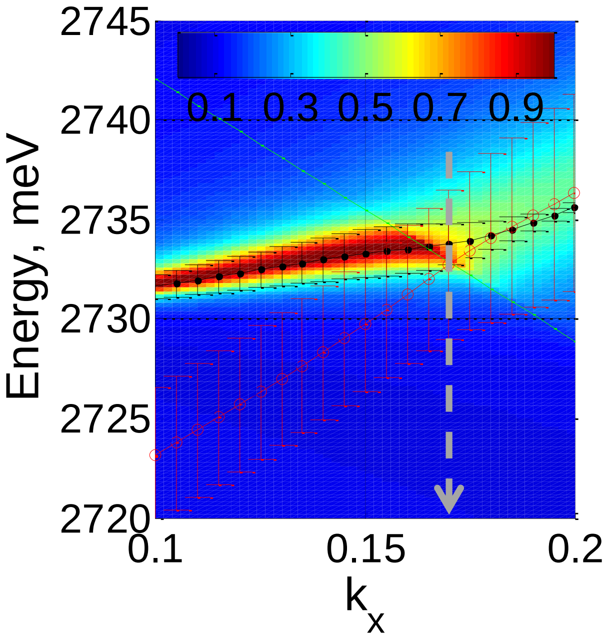

Reflection as function of
K_Z - the 'sunrise'-harmonic
propagation constant in vertical direction

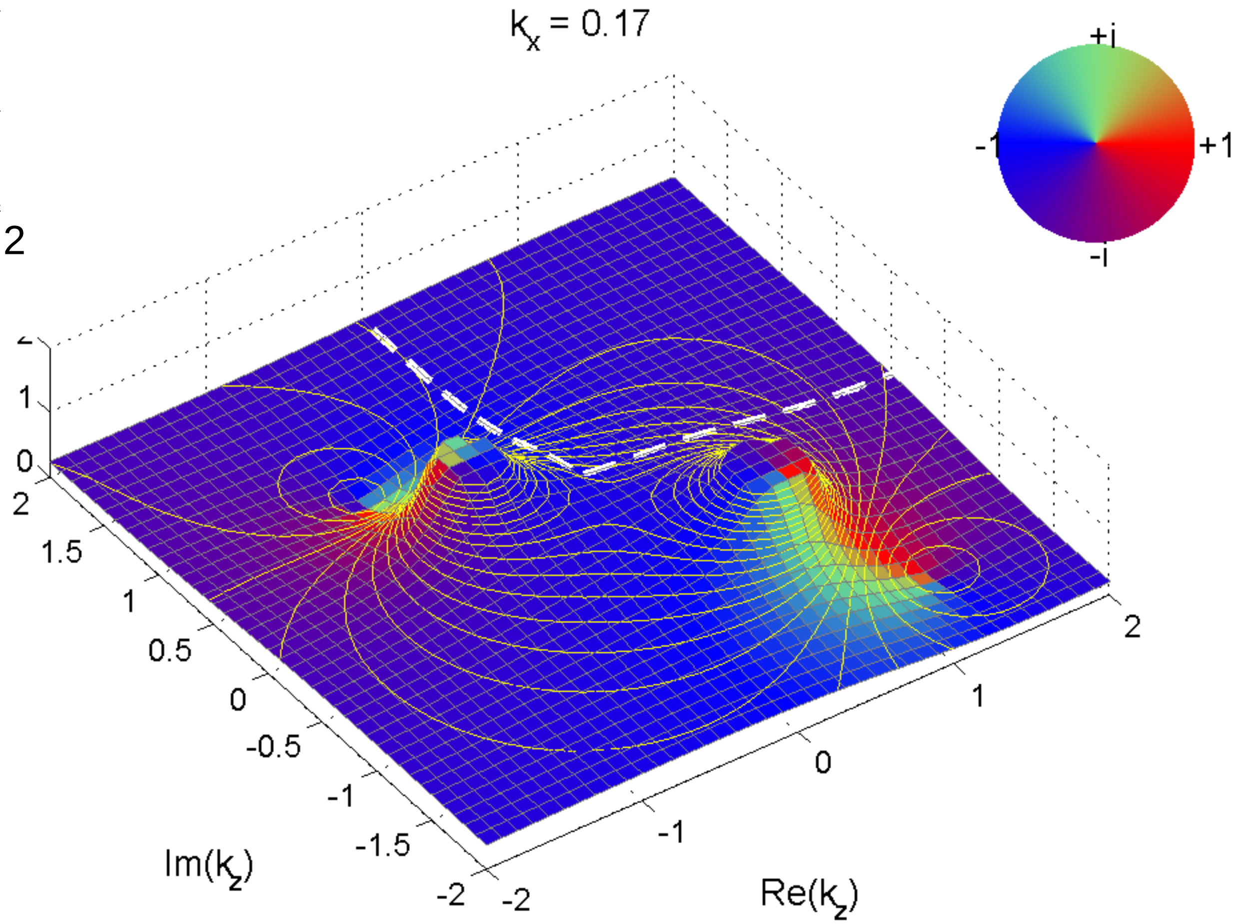

Resonantly enhanced Wood-Rayleigh anomaly

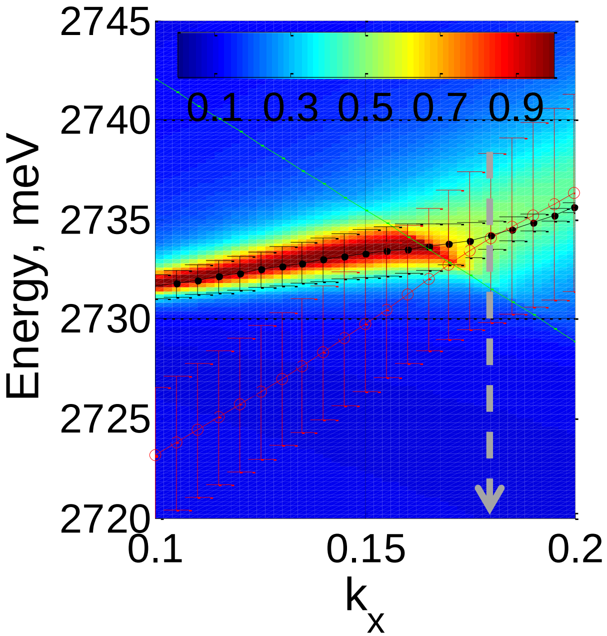

Reflection as function of
K_Z - the 'sunrise'-harmonic
propagation constant in vertical direction

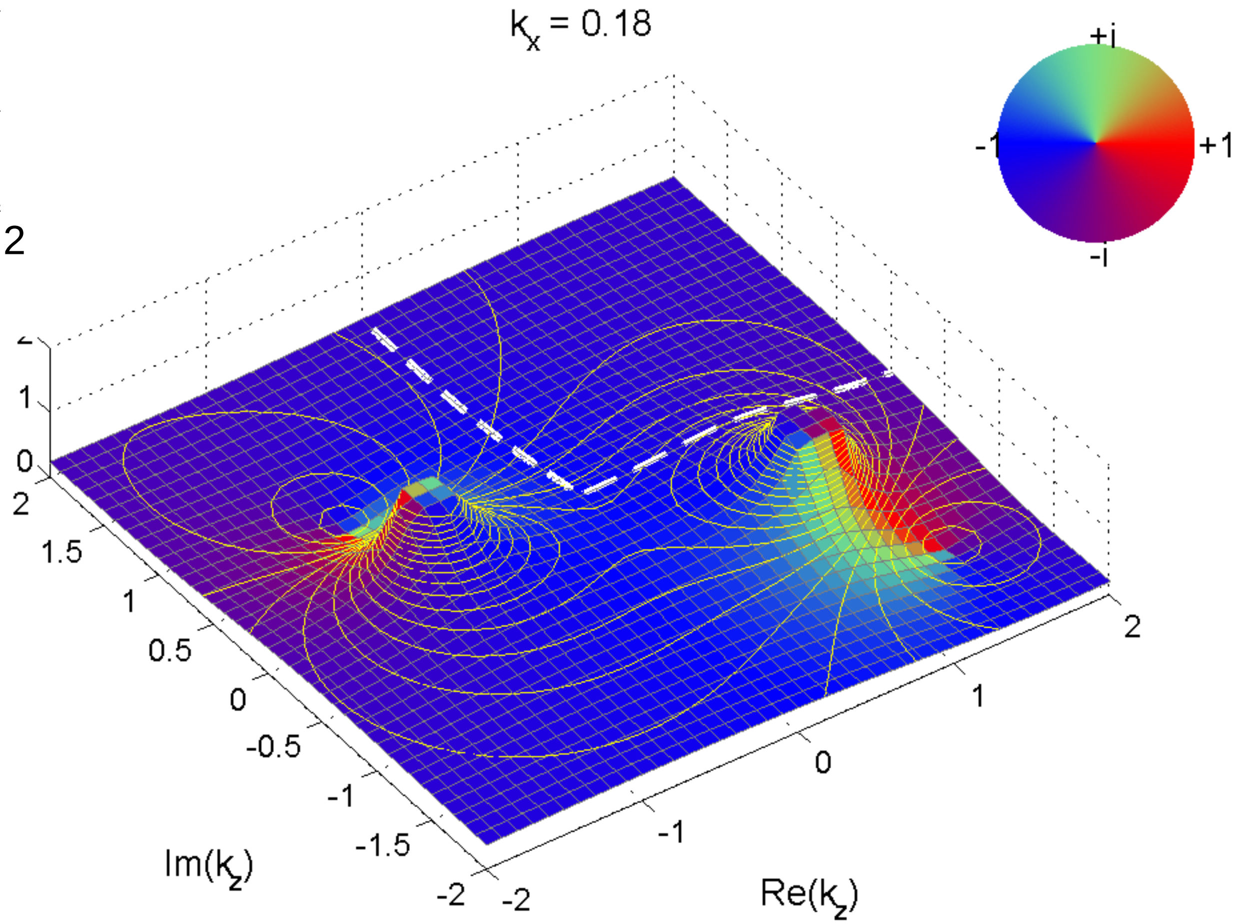

Resonantly enhanced Wood-Rayleigh anomaly

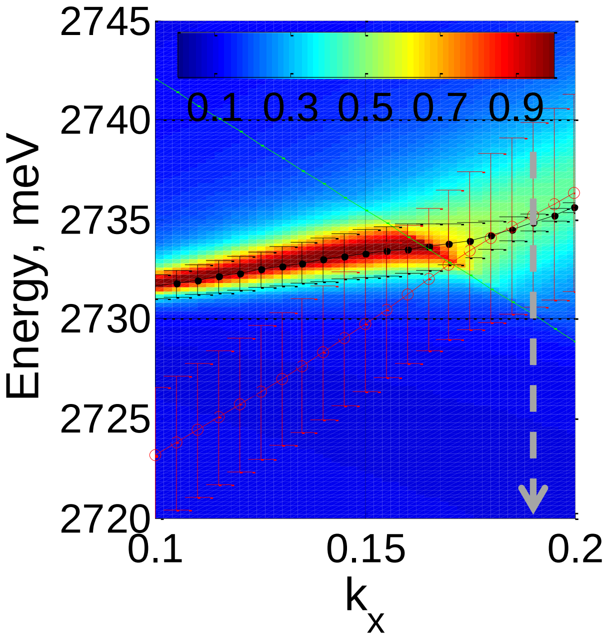

Reflection as function of
K_z - the ’sunrise’-harmonic
propagation constant in vertical direction

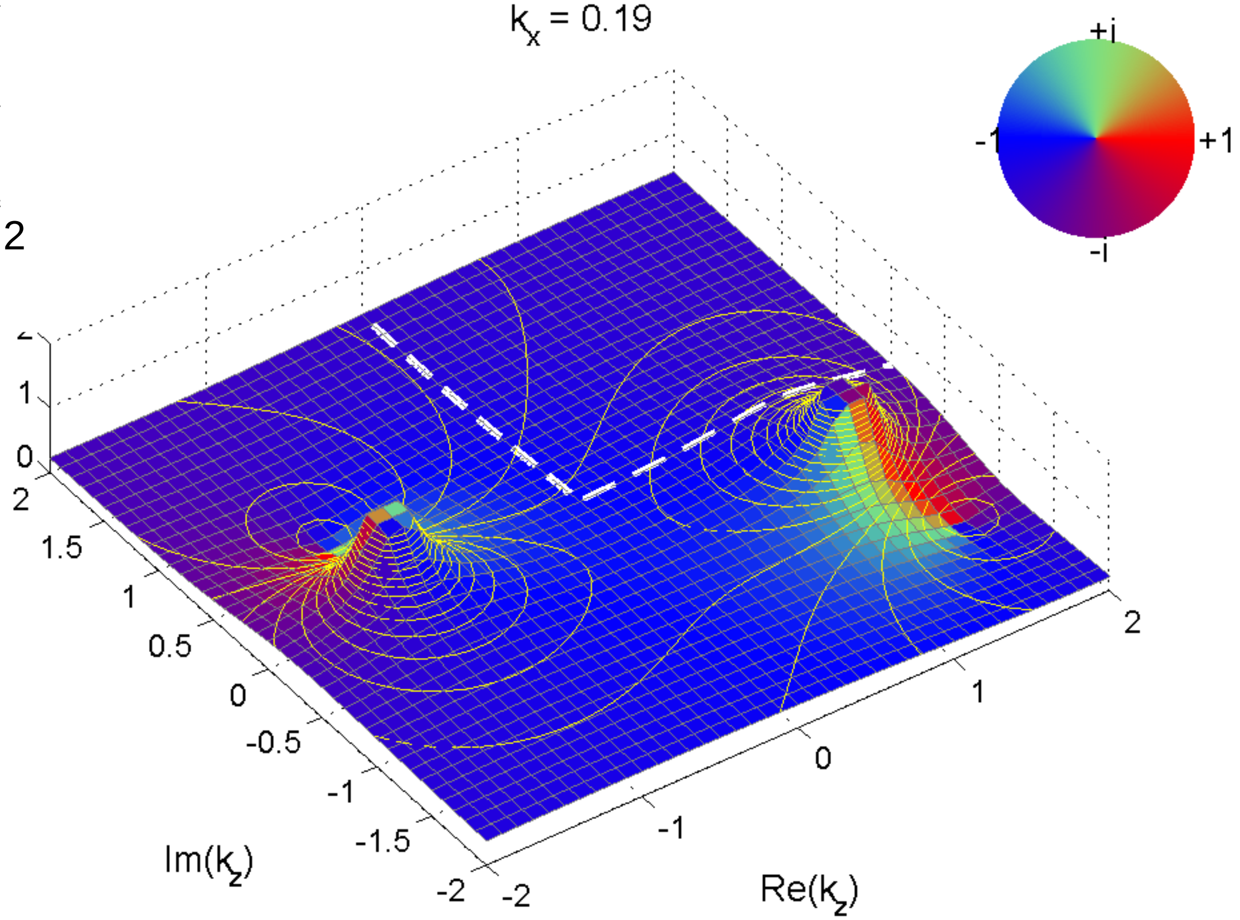

Resonantly enhanced Wood-Rayleigh anomaly

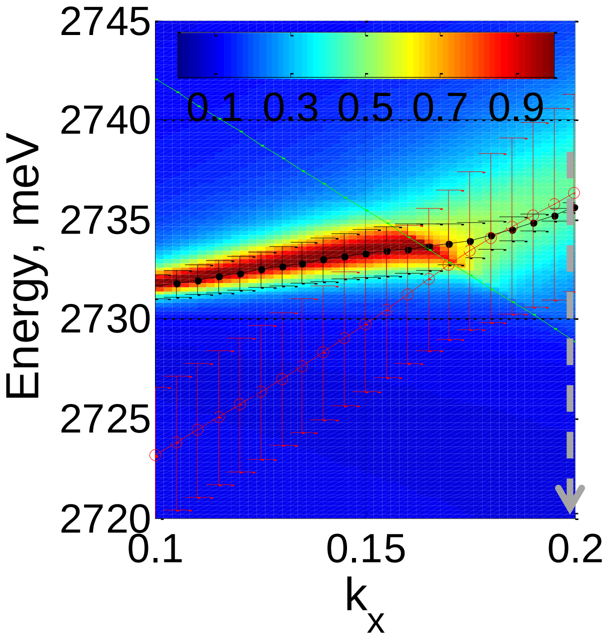

Reflection as function of
K_z - the ’sunrise’-harmonic
propagation constant in vertical direction

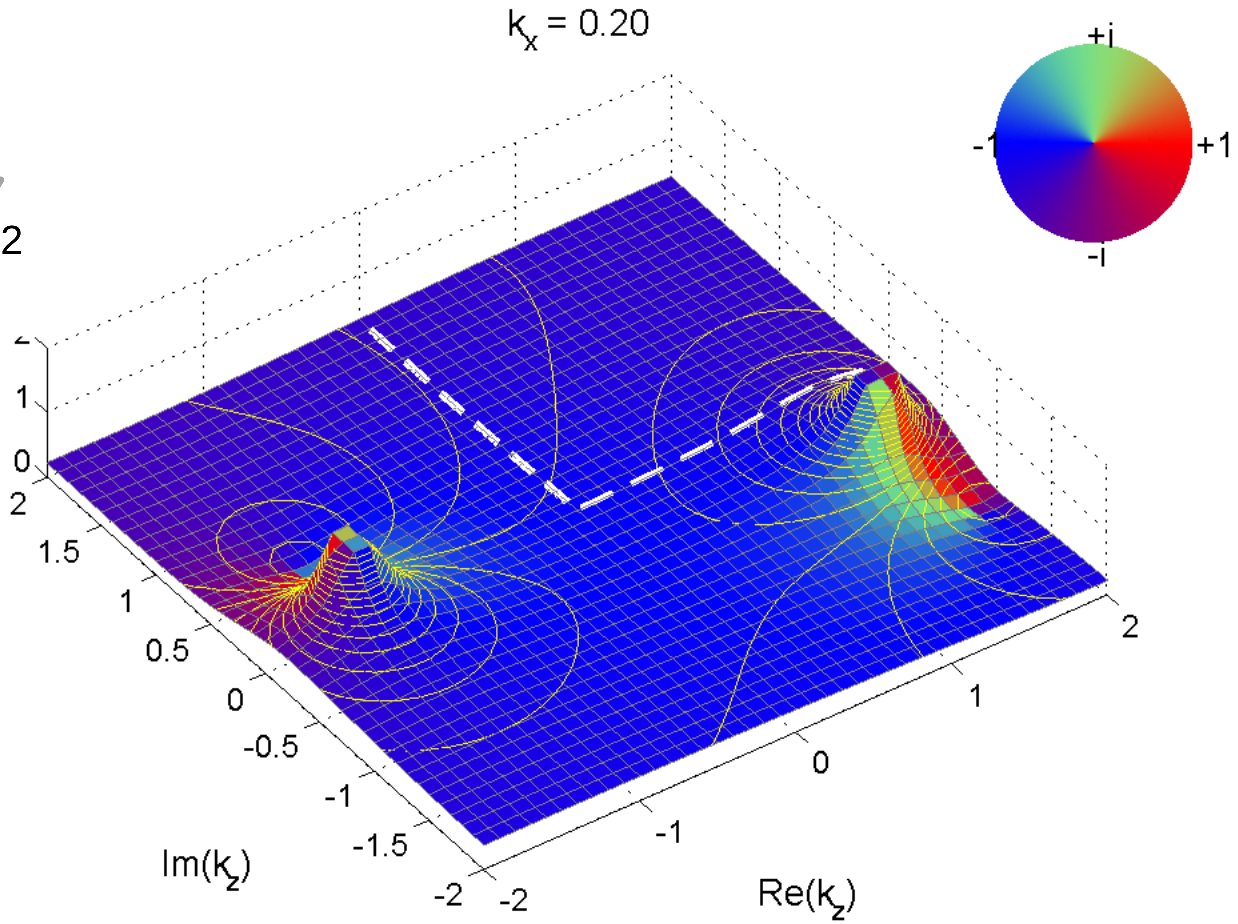

Resonantly enhanced Wood-Rayleigh anomaly

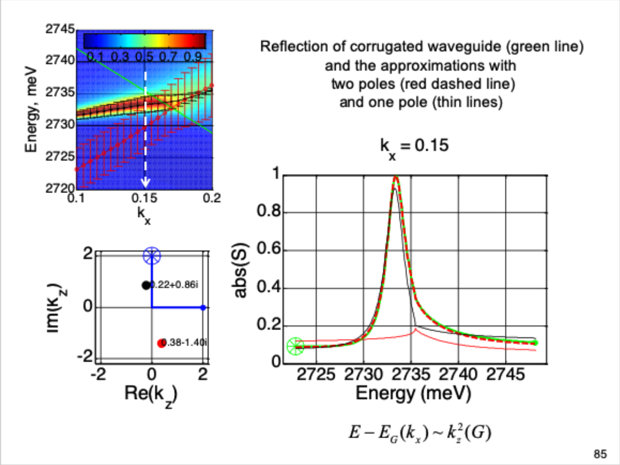

85

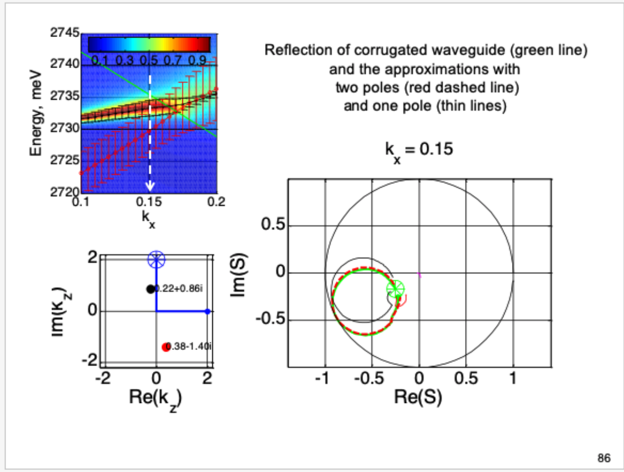

86

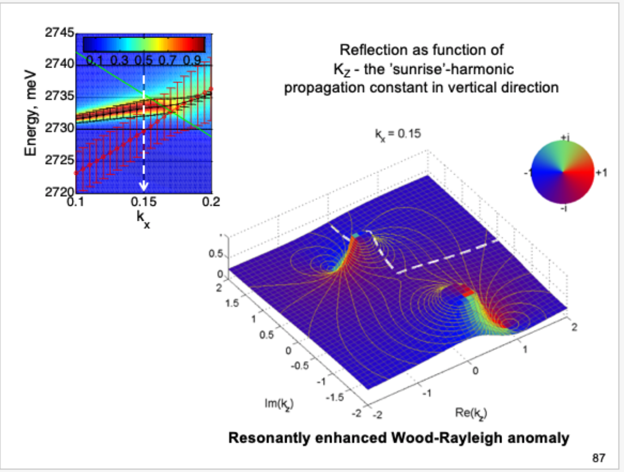

87

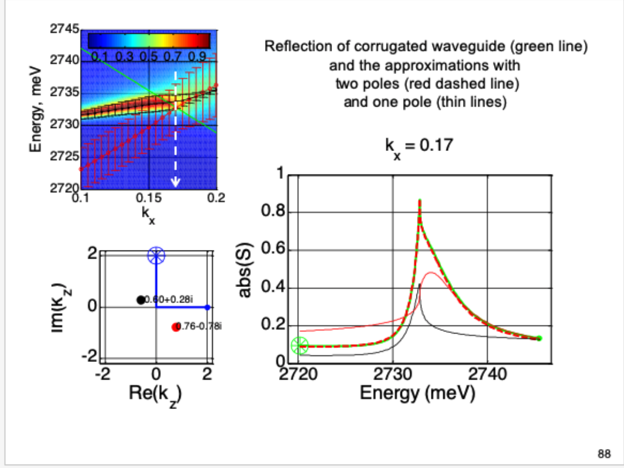

88

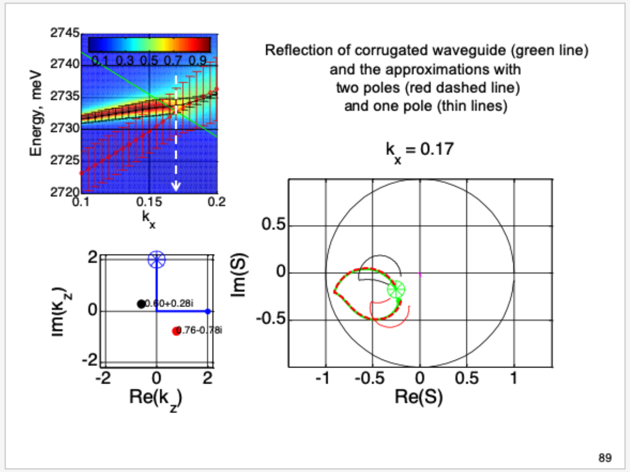

89

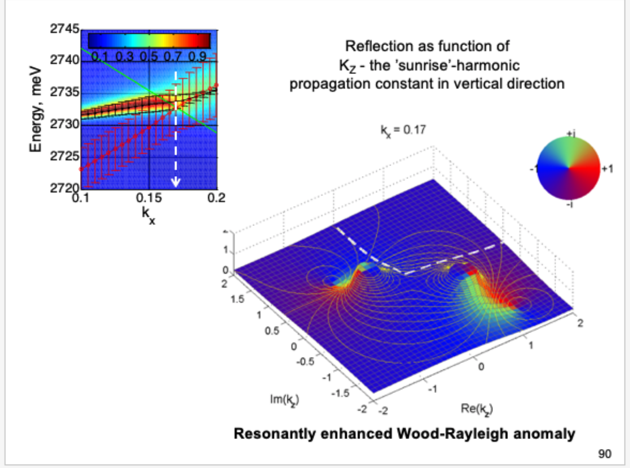

90

Выводы -1

интерполяция парциальных матриц рассеяния и линеаризация резонансной фазы позволяет достаточно точно описывать резонансы в составных системах

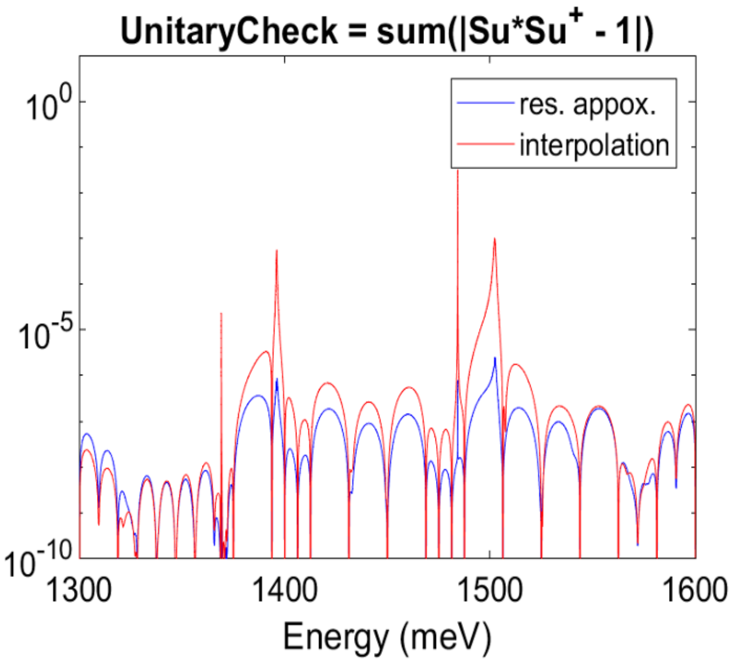

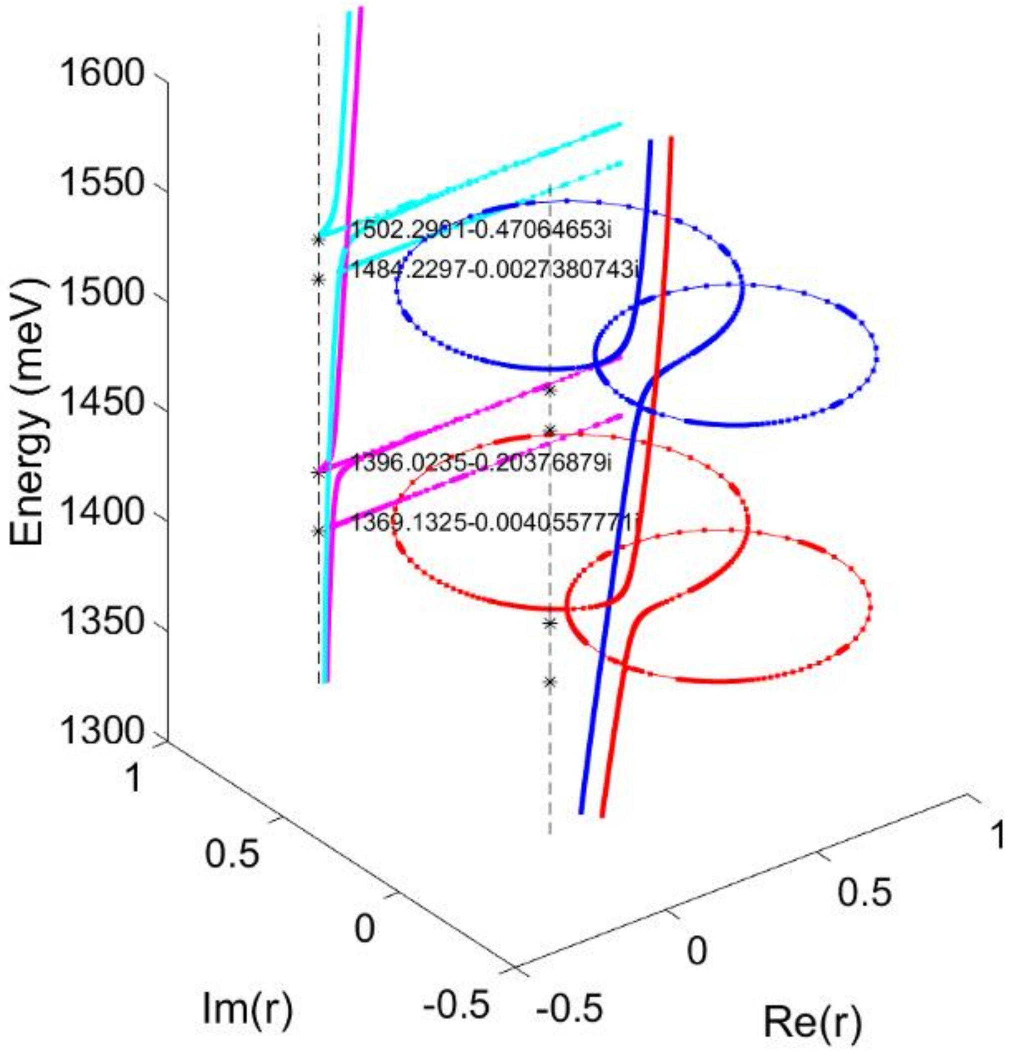

Выводы - 2: Спасибо за внимание !!

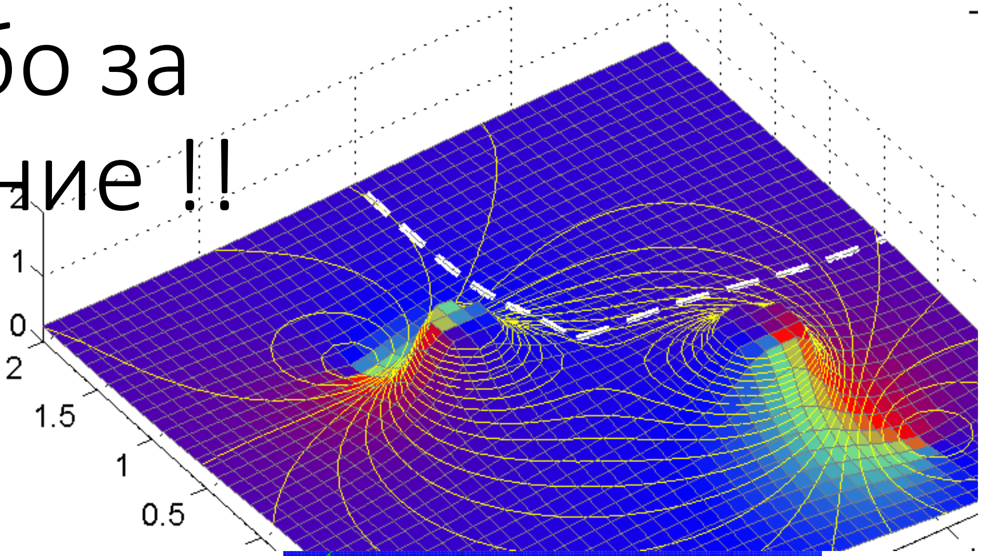

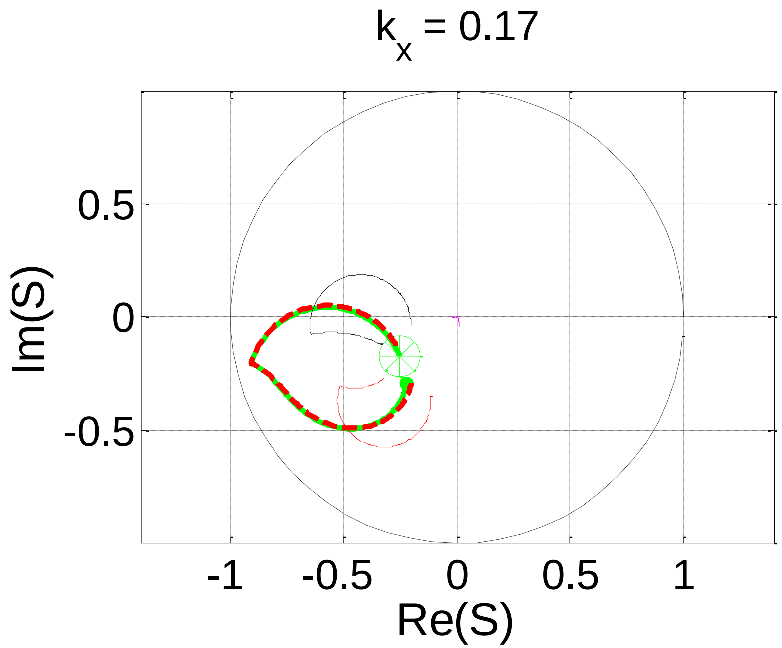

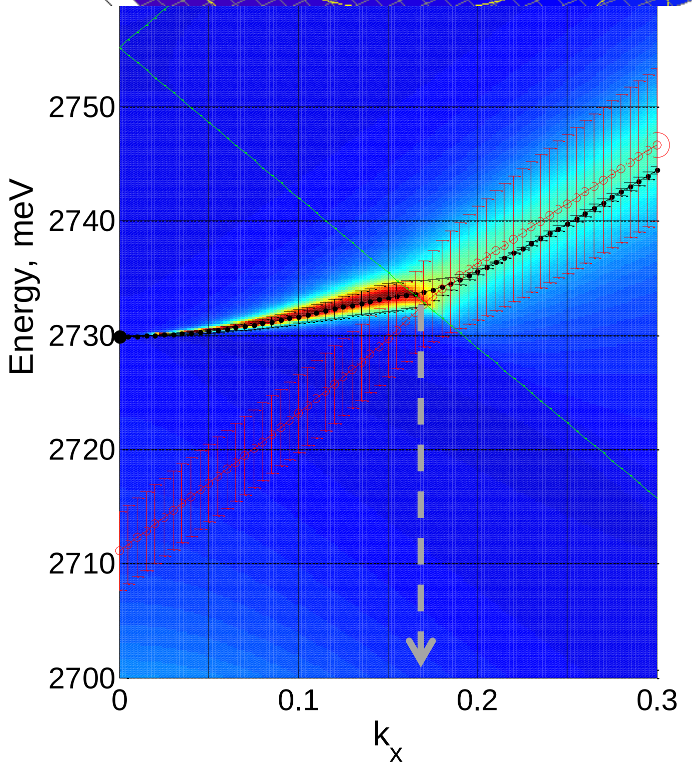

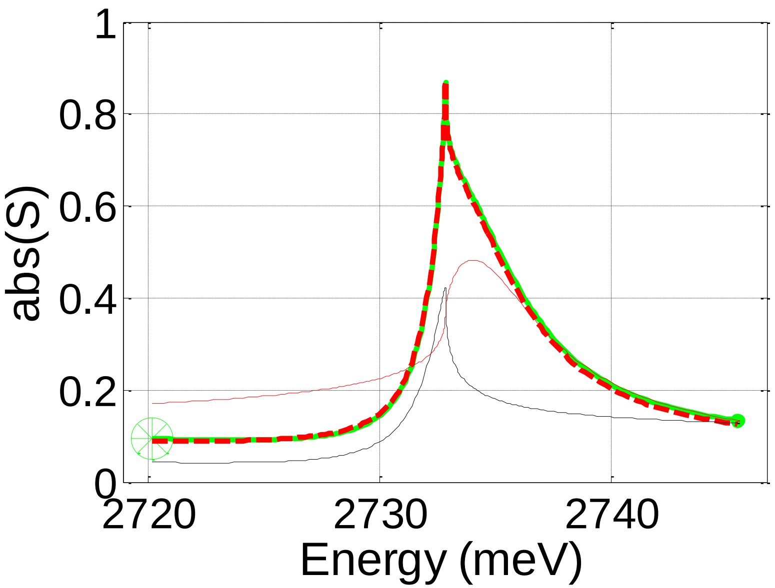

4. Как скрутить свет винтом?

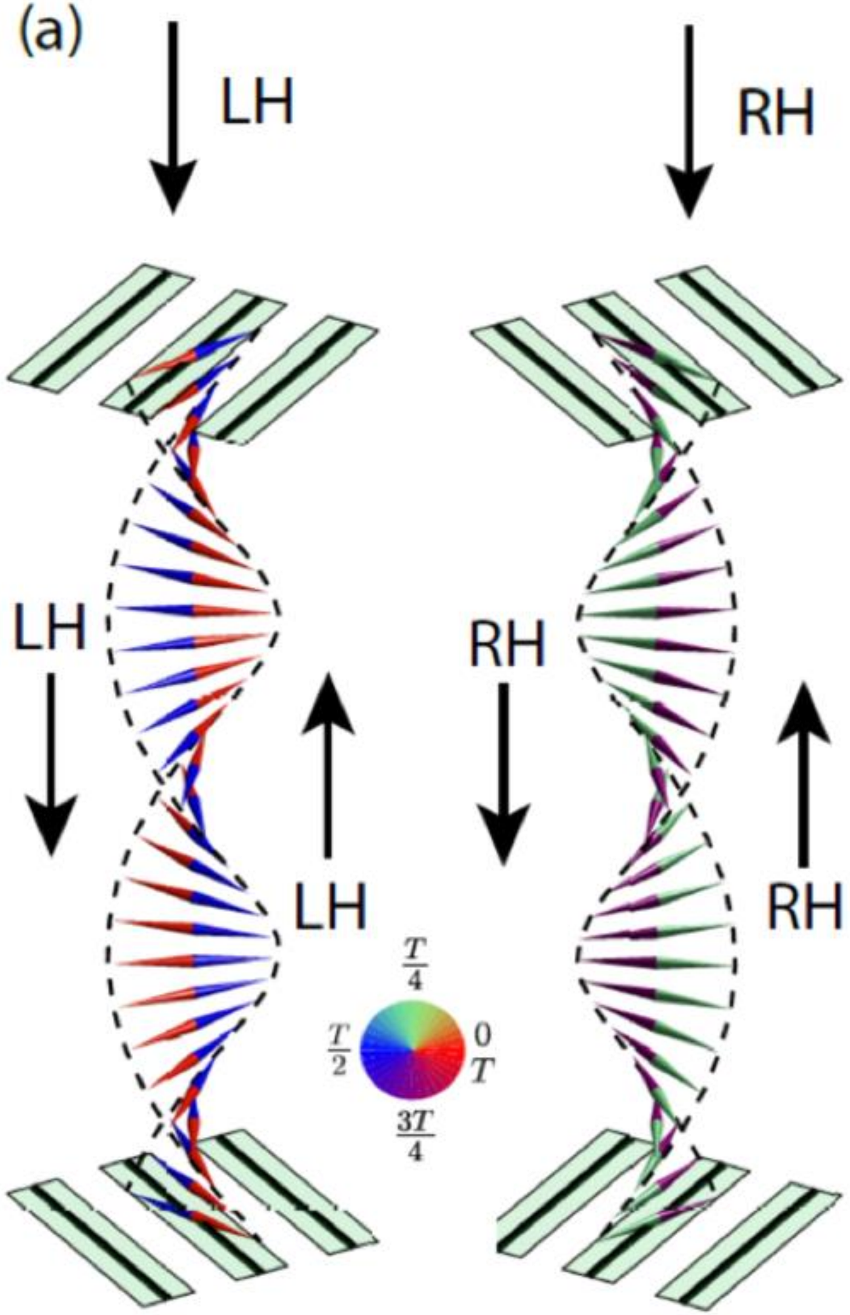

"Chiral light in twisted Fabry-Pérot cavities"

Sergey A. Dyakov, Natalia S. Salakhova,
Alexey V. Ignatov, Ilia M. Fradkin,
Vitaly P. Panov, Jang-Kun Song,
Nikolay A. Gippius

Accepted to
Advanced Optical Materials.

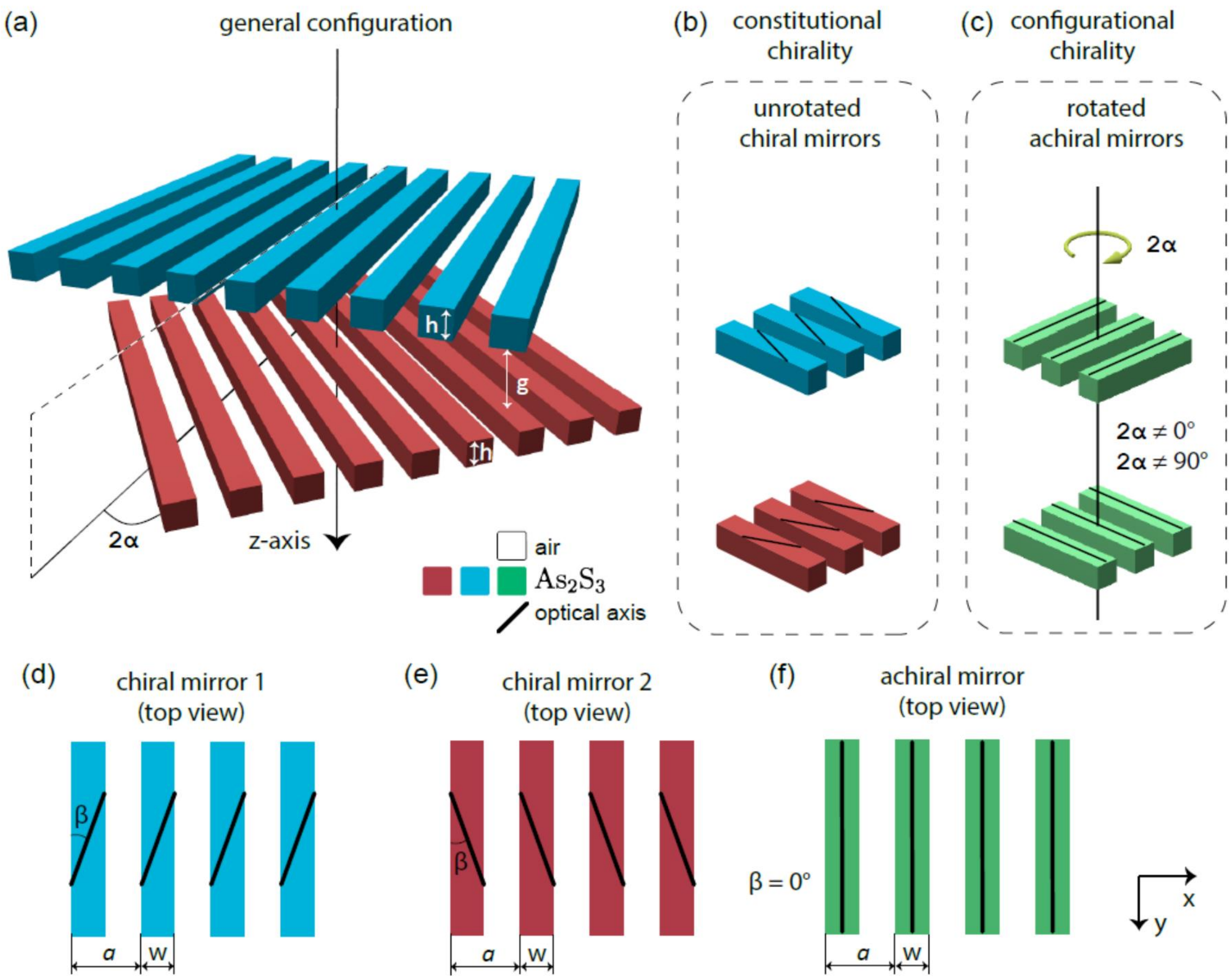

Cavity with
configurational chirality,
constructed
from non-chiral mirrors
twisted into
a chiral configuration

(a)

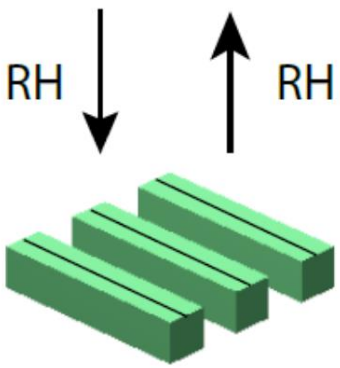

(f)

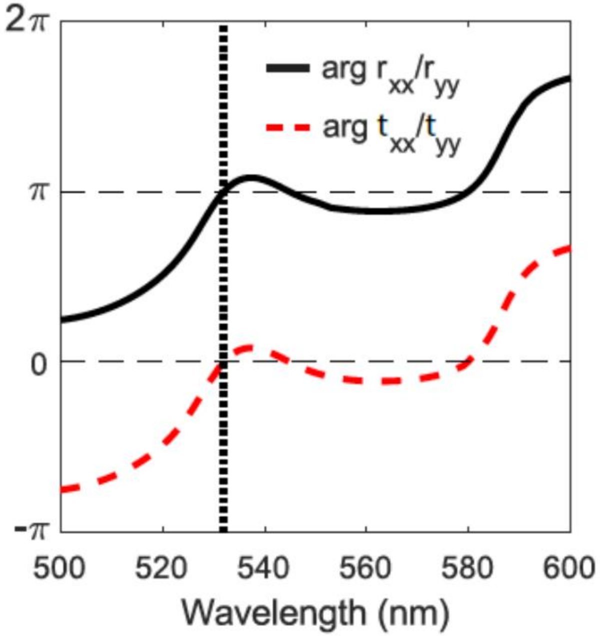

(a)

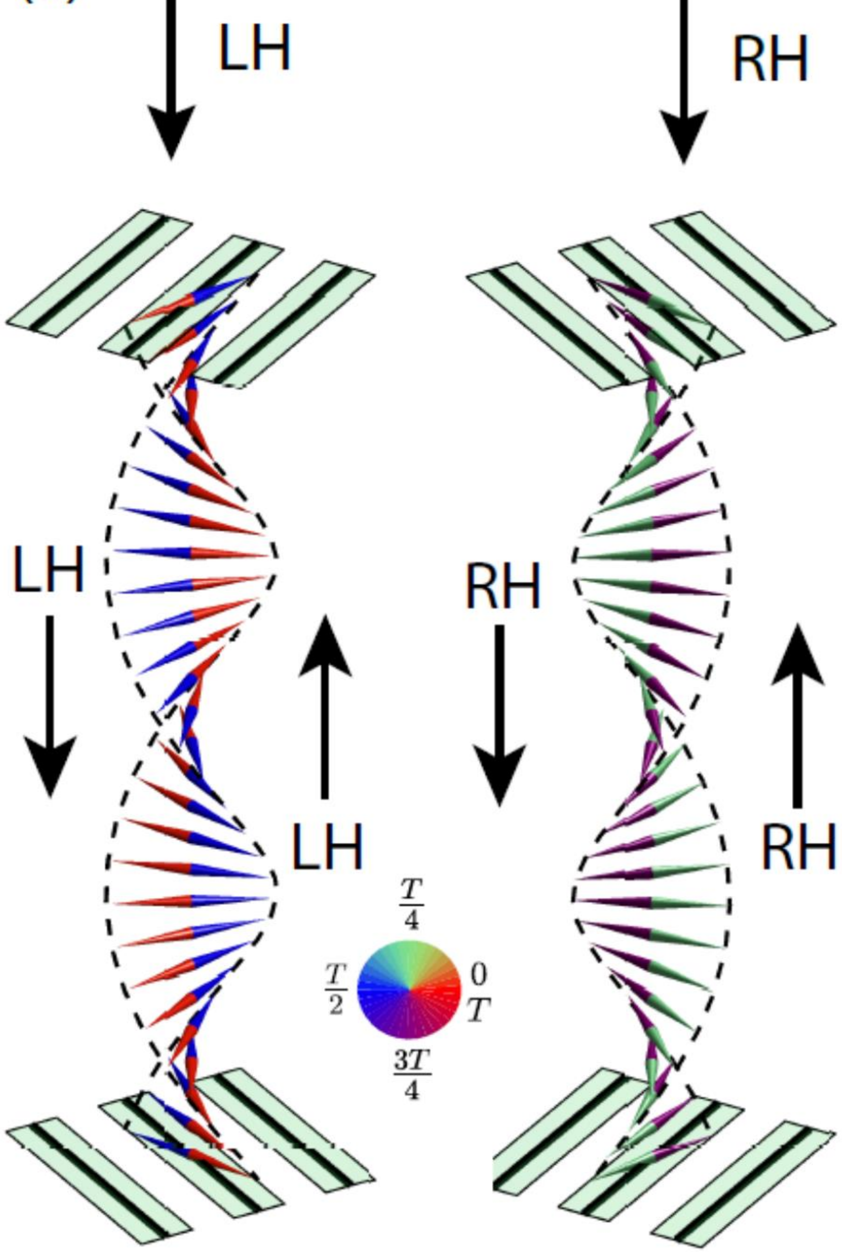

Conclusions

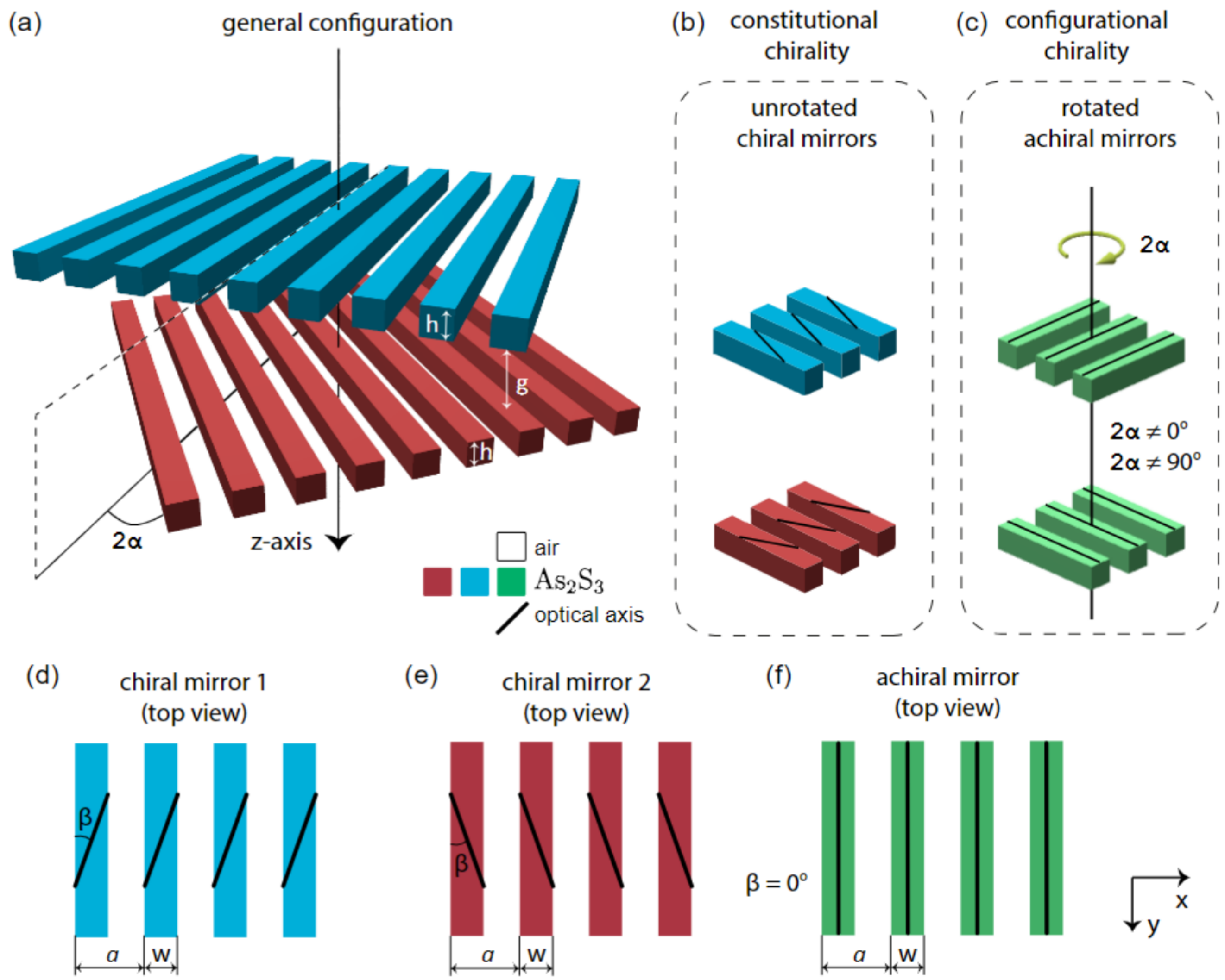

By exploiting the anisotropy of As_2S_3, we have designed cavities with both constitutional and configurational chiralities.

For both types of cavities, we simulated the field distribution of left-handed and right-handed incident waves within the region between the mirrors. At resonant gap sizes, we observed a linearly polarized standing wave with a polarization direction twisted in a helical shape, resulting from the interference between counter-propagating circularly polarized waves of the same handedness.

These chiral Fabry-Pérot cavities can be adjusted to match the technologically available distance between the mirrors by appropriately tuning their twist angle.